



This is to certify that the

dissertation entitled

- I. α -Epoxyalkyl Radical Fragmentation: A Computational Study
- II. Experimental and Computational Studies of Carbene Processes: Homologation, Oxygen, atom-transfer, and Alkene Cycloaddition

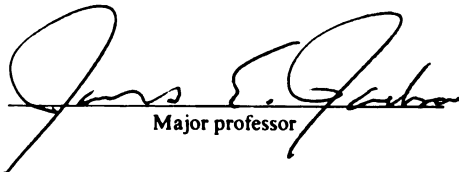
MingShi Lee

has been accepted towards fulfillment
of the requirements for

Ph.D. degree in Chemistry

Date

11/8/93


Major professor

LIBRARY

Michigan State University

PLACE IN RETURN BOX to remove this checkout from your record.
TO AVOID FINES return on or before date due.

| DATE DUE | DATE DUE | DATE DUE |
|----------|----------|----------|
| _____ | _____ | _____ |
| _____ | _____ | _____ |
| _____ | _____ | _____ |
| _____ | _____ | _____ |
| _____ | _____ | _____ |
| _____ | _____ | _____ |
| _____ | _____ | _____ |

I. α -Epoxyalkyl Radical Fragmentation: A Computational Study
II. Experimental and Computational Studies of Carbene Processes:
Homologation, Oxygen Atom-Transfer, and Alkene Cycloaddition

By

MingShi Lee

A DISSERTATION

Submitted to
Michigan State University
in partial fulfillment of the requirements
for the degree of

DOCTOR OF PHILOSOPHY

Department of Chemistry

1993

ABSTRACT

- I. α -Epoxyalkyl Radical Fragmentation: A Computational Study**
- II. Experimental and Computational Studies of Carbene Processes:
Homologation, Oxygen Atom-Transfer, and Alkene Cycloaddition**

By

MingShi Lee

The unusual regioselectivity of α -epoxymethyl radical ring-opening was studied by ab initio methods. Computational results at the PMP4/6-31G*//UMP2/6-31G* level indicate that the barrier for C-O bond cleavage is lower by ~6-7 kcal/mol than that for C-C bond cleavage. The heat of reaction is ~3 kcal/mol more exothermic C-C than for C-O bond cleavage. Several substituted α -epoxymethyl radical ring-openings were examined at the MP4/6-31G*//UHF/6-31G* level. In general, π electron-withdrawing substituents favor C-C cleavage whereas donating substituents favor C-O opening; substituent effects are stronger on the epoxide ring than on the α -methyl.

Reactions of fluorenylidene with terminal alkynes were studied by ESR and product analysis at 77 K. Due to steric interactions, the vinylcarbene intermediate derived from the addition of triplet fluorenylidene to a monosubstituted acetylene could not be

intramolecularly trapped by its aryl ring, as occurs in the case of its triplet diphenylcarbene analog. Through ESR studies and the observation of a 1,2-chlorine atom shift in the addition of fluorenylidene to propargyl chloride at 77 K, it was shown that triplet fluorenylidene addition to alkynes proceeds through the same type of intermediate.

A new type of carbene reaction has been examined: the oxygen atom-transfer from a carbonyl group to fluorenylidene to produce a more stable secondary carbene, such as dimethoxy or diamino carbene, which is not easily generated by a photolytic process. The relative rate constants for various oxygen atom-transfers have been determined by competitive trapping with methanol.

Transition structures for the cycloadditions of singlet carbenes to various "push-pull" alkenes, $\text{HO(X)C}=\text{C(X)CN}$, were studied using the MNDO method. The calculations show an electronic orientation preference of the reaction paths. Carbenes prefer by 3-5 kcal/mol to "add to" the electron-donor end over the electron-acceptor end of the olefin. Steric effects also make distinctions between rotameric transition structures, where $\text{X} = \text{CH}_3$ or Br, the energy differences are 0.5-0.9 kcal/mol. A parallel experimental effort is described to find evidence for the asymmetric path as opposed to a more symmetrical approach of a singlet carbene.

To my parents

ACKNOWLEDGMENT

Thank God. I am finally done with this after exhausting my English vocabulary. Many people deserve thanks for making my stay at Michigan State University an enjoyable one.

I had always wanted to be a synthetic chemist. However, Dr. James E. Jackson, my advisor, opened my narrow vision of chemistry and taught me how to enjoy chemistry. I do not remember how many nights, or should I say early mornings, we spent together chatting about science until recently he finally has synthesized the best natural product he ever made, the bug, Kelvin Charles Parker Jackson. Here I have to mention another Dr. Jackson, Dr. Evelyn Jackson, who is also my Mrs. Advisor. Her generosity and consideration always made me feel at home.

As a foreigner here, I have to thank my lab-mates Sei-Hum Jang, Theresa Wagner and Scott Stoudt, who made the cultural transition much easier for me. Especially, Scott, my personal English tutor, who put a lot of effort into correcting my "chinglish". Also, Einhard Schmidt, a true friend and big brother, never said no to my asking for help and also a long-time "lunch-mate".

Dr. Peter J. Wagner's group was like my second research group. Bong-Ser Park, Bob Smart, Kevin McMahon, and Kung-Lung Cheng, always shared the entertainment with me, either scientific or recreational.

Finally, I have to thank my family for their spiritual and economic support. Though they still do not know what I am doing, the only question they ask is "what do you need?" I hope I have a chance to repay some of their love in the future.

TABLE OF CONTENTS

ABSTRACT:

LIST OF TABLES: **viii**

LIST OF FIGURES: **xii**

| | |
|---|------------|
| CHAPTER 1: α-Epoxyalkyl Radical Fragmentation: | |
| A Computational Study | 1 |
| PART I. The Parent System | 2 |
| PART II. Substituent Effects | 18 |
| CHAPTER 2: Low Temperature Carbene-to-Carbene Homologations | 58 |
| CHAPTER 3: Carbene-to-Carbene Oxygen Transfer Reactions | 106 |
| CHAPTER 4: On the Symmetry of Carbene-Alkene Cyclopropanations: Computational and Experimental Studies | 128 |

LIST OF TABLES

| | | |
|-------------|---|-----------|
| 1.1 | Total and Relative Energies of Calculated Structures 1.1A-1.5A | 16 |
| 1.2 | Calculated Geometries (UHF/6-31G*) of Initial Substituted Radicals (1.1)..... | 36 |
| 1.3 | Calculated Geometries (UHF/6-31G*) of Transition Structures for CC Bond Cleavage (1.2)..... | 36 |
| 1.4 | Calculated Geometries (UHF/6-31G*) of Transition Structures for CO Bond Cleavage (1.4)..... | 37 |
| 1.5 | Calculated Geometries (UHF/6-31G*) of Substituted Product Radicals 1.3 from CC Bond Cleavage | 37 |
| 1.6 | Calculated Geometries (UHF/6-31G*) of Substituted Product Radicals 1.5 from CO Bond Cleavage..... | 38 |
| 1.7 | Total Energies for 1.1B-1.5B (Amino Group on α-Methyl)..... | 39 |
| 1.8 | Total Energies for 1.1C-1.5C (Cyano Group on α-Methyl)..... | 40 |
| 1.9 | Total Energies for 1.1D-1.5D (Boron Group on α-Methyl)..... | 41 |
| 1.10 | Total Energies for 1.1C'-1.5C' (Cyano Group on Epoxide Ring)..... | 42 |
| 1.11 | Total Energies for 1.1D'-1.5D' (Boron Group on Epoxide Ring)..... | 43 |

| | | |
|------|---|-----|
| 1.12 | Reaction Barriers and Heats of Reactions for Ring-Openings of Substituted α -Epoxymethyl Radicals | 44 |
| 1.13 | Heats of Reaction for Ring-Opening of Various Substituted α -Epoxymethyl Radicals..... | 45 |
| 2.1. | Irradiation of 9-Diazofluorene in Mixtures of Propargyl Chloride and 1,2-Dichloroethane | 76 |
| 3.1 | Rate Constants for Oxygen Transfer to Fluorenylidene | 113 |
| 3.2 | Heats of Formation of X=O and X: Species (AM1 Calculated Values in Parentheses)..... | 115 |
| 4.1 | Selected Geometry Parameters and Activation Energies for Transition Structures for the Addition of Methylene to Hydroxyethylene..... | 138 |
| 4.2 | Selected Geometry Parameters and Activation Energies for Transition Structures for the Addition of Chlorocarbene to Hydroxyethylene | 139 |
| 4.3 | Selected Geometry Parameters and Activation Energies for Transition Structures for the Addition of Methylcarbene to Hydroxyethylene | 140 |
| 4.4 | Selected Geometry Parameters and Activation Energies for Transition Structures for the Addition of Methyl Fluorocarbene to Hydroxyethylene..... | 141 |
| 4.5 | Selected Geometry Parameters and Activation Energies for Transition Structures for the Addition of Methylene to Cyanoethylene | 145 |
| 4.6 | Selected Geometry Parameters and Activation Energies for Transition Structures for the Addition of Chlorocarbene to Cyanoethylene..... | 146 |

| | | |
|------|--|-----|
| 4.7 | Selected Geometry Parameters and Activation Energies for Transition Structures for the Addition of Methylcarbene to Cyanoethylene..... | 147 |
| 4.8 | Selected Geometry Parameters and Activation Energies for Transition Structures for the Addition of Methyl Fluorocarbene to Cyanoethylene | 148 |
| 4.9 | Heats of Formation and Activation Energies of Transition States of Methylcarbene Addition to Various Push-Pull Olefins | 151 |
| 4.10 | Heats of Formation and Activation Energies of Transition States of Chlorocarbene Addition to Various Push-Pull Olefins | 152 |
| 4.11 | Heats of Formation and Activation Energies of Transition States of Bromocarbene Addition to Various Push-Pull Olefins | 153 |
| 4.12 | Heats of Formation and Activation Energies of Transition States of Methyl Fluorocarbene Addition to Various Push-Pull Olefins | 154 |
| 4.13 | Heats of Formation and Activation Energies of Transition States of Dichlorocarbene Addition to Various Push-Pull Olefins | 155 |
| 4.14 | Selected Geometry Parameters for Transition States for the Addition of Methylcarbene to the Various Push-Pull Olefins | 157 |
| 4.15 | Selected Geometry Parameters for Transition States for the Addition of Chlorocarbene to the Various Push-Pull Olefins | 159 |
| 4.16 | Selected Geometry Parameters for Transition States for the Addition of Bromocarbene to the Various Push-Pull Olefins | 161 |

| | | |
|------|--|-----|
| 4.17 | Selected Geometry Parameters for Transition States for the Addition of Methyl Fluorocarbene to the Various Push-Pull Olefins | 163 |
| 4.18 | Selected Geometry Parameters for Transition States for the Addition of Dichlorocarbene to the Various Push-Pull Olefins | 165 |
| 4.19 | Frontier Orbital Energies (eV) for Olefins | 170 |

LIST OF FIGURES

| | | |
|-----|---|----|
| 1.1 | Structures of 1.1A-3.1A calculated at the UHF/6-31G* and (MP2/6-31G*) levels of theory | 6 |
| 1.2 | The potential energy surface for C-O bond cleavage | 13 |
| 1.3 | Structures of 1.1B-3.1B calculated at the UHF/6-31G* level of theory | 21 |
| 1.4 | Structures of 1.1C-1.5C calculated at the UHF/6-31G* level of theory | 22 |
| 1.5 | Structures of 1.1D-1.5D calculated at the UHF/6-31G* level of theory | 23 |
| 1.6 | Structures of 1.1C'-1.5C' calculated at the UHF/6-31G* level of theory | 24 |
| 1.7 | Structures of 1.1D'-1.5D' calculated at the UHF/6-31G* level of theory | 25 |
| 2.1 | ESR Spectra for Irradiation of 9-Diazo fluorene with Phenylacetylene and 5-Phenyl-3-spirofluorenyl-3H-pyrazole at 77 K..... | 69 |
| 2.2 | ESR Spectrum for Irradiation of 9-Diazo fluorene with 1-Hexyne at 77 K | 70 |
| 2.3 | ESR Spectrum for Irradiation of 5- <i>t</i> -Butyl-3-spirofluorenyl-3H-pyrazole at 77 K..... | 71 |
| 2.4 | Calculated Geometries for Pyrazoles by MNDO | 80 |

| | | |
|-----|--|-----|
| 4.1 | Two possible transition states for carbene addition to a substituted olefin..... | 131 |
| 4.2 | The proposed preference of a singlet carbene reacting with a push-pull olefin..... | 132 |
| 4.3 | The interaction between a singlet carbene and an olefin at a long distance..... | 168 |
| 4.4 | A revised Figure 4.2 based on the computational results..... | 173 |

CHAPTER 1

α -Epoxyalkyl Radical Fragmentation: A Computational Study

PART I. The Parent System

PART II. Substituent Effects

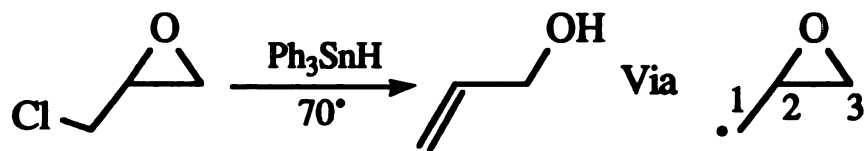
Abstract: The unusual regioselectivity of α -epoxymethyl radical ring-opening is studied by ab initio methods. Computational results at the PMP4/6-311G**//UMP2/6-31G* level indicate that the barrier for C-O bond cleavage is lower than that of C-C bond cleavage by about 7 kcal/mol. Interestingly, the heat of reaction for the C-C bond cleavage is ca. 3 kcal/mol more exothermic than for C-O bond cleavage. This suggests that the regioselectivity of the ring-opening is kinetically controlled. Several substituted α -epoxymethyl radical ring-openings are examined at the MP4/6-31G*//UHF/6-31G* level. In general, a π electron-withdrawing substituent favors C-C cleavage whereas a π electron-donating substituent favors C-O cleavage. Substituents on the epoxide ring show stronger substituent effects than on the α -methyl. A further study extended to substituents with charge, CH_2^+ , CNH^+ , NH_3^+ , CH_2^- , and BH_3^- is also discussed.

Part I. The Parent System

1.1 Introduction:

Ring-opening of α -epoxyalkyl radicals has recently emerged as a useful tool in organic synthesis.¹ In alkyl substituted cases, the epoxide ring opens at the C-O bond, leading to an oxygen-centered radical rather than the α -oxygen-stabilized carbon-centered radical obtained by C-C cleavage. This regioselectivity is opposite to that predicted from simple bond dissociation energies.² C-C opening can of course be favored by π -delocalizing groups on the 3-carbon (see numbering in Scheme 1.1).³ However, we wish to understand the fundamental origin of the unsubstituted system's seemingly anomalous regioselectivity. In light of the reaction's synthetic value, a predictive understanding of the factors that control the choice of cleavage path could aid in the design and control of new synthetic schemes.

Scheme 1.1



Thermochemical estimates for product radicals **1.3A** and **1.5A**, assuming no special role for the vinyl groups, yield a ΔH_f difference of ~ 5 kcal/mol in favor of vinyloxymethyl radical **1.3A**.⁴ However, K. W. Krosley et al. have recently observed that the α -chloromethyl epoxides react with Ph_3SnH to give only allyl alcohols.⁵ No oxiranylmethyl radicals were trapped at any Ph_3SnH concentration, suggesting that the initial radical's lifetime is vanishingly short. For comparison, the lifetime for rearrangement

of cyclopropylmethyl radical is 1.0×10^{-8} s at room temperature ($\Delta E_a = 5.9$ kcal/mol), and it can be trapped at high tin hydride concentrations.⁶ More recent work in which an intramolecular competition was set up between epoxide and cyclopropane ring cleavage showed only epoxide opening.⁷

A second issue of concern is the heat of reaction for the ring opening. From the above thermochemical estimates, a reaction exothermicity of only 4 kcal/mol is calculated for C-O ring opening; C-C cleavage would then be 9 kcal/mol exothermic. Combined with the rapid ring opening rate indicated by the above intramolecular selectivity, these numbers suggest that radicals 1.1A and 1.5A should equilibrate as in the cyclopropylmethyl system. Thus, even after opening, radical 1.5A could recyclize and access the more exothermic cleavage to 1.3A. The fact that this process is not seen hints at a substantial barrier to C-C cleavage.

We now report an ab initio molecular orbital study of this unique reaction, carried out to examine energies and conformations in the parent C_3H_5O system. In this work, we have sought to address the following questions: 1) What controls the epoxide ring-opening regioselectivity—relative energetics of the products or activation barriers? 2) What is the overall reaction exothermicity, and are these radicals in a mobile equilibrium as in the cyclopropylmethyl/prop-3-en-1-yl radical system? 3) What level of ab initio model is needed to describe this open-shell system adequately? 4) Can our calculations suggest new modes of control for these reactions?

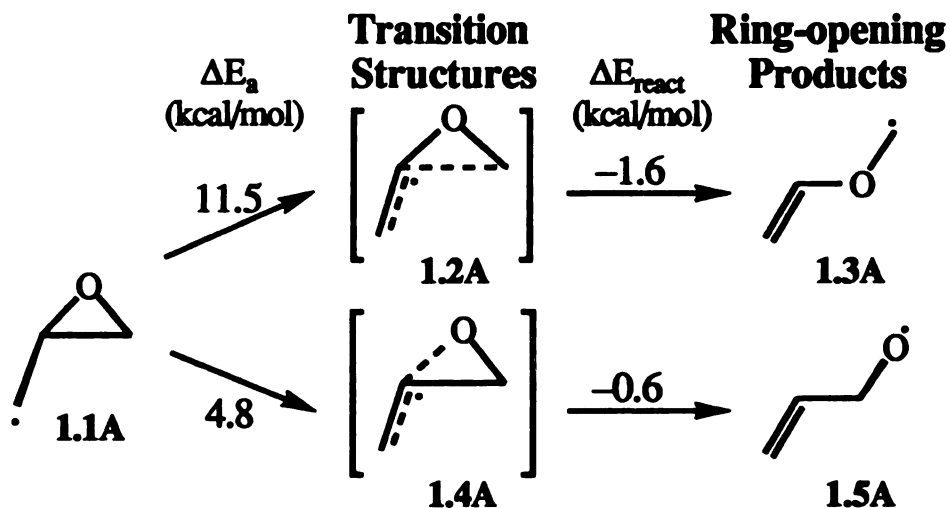
1.2 Methods:

Ab initio calculations were performed on the $\text{C}_3\text{H}_5\text{O}$ system with the GAUSSIAN 86⁸ and 90⁹ series of programs. Structures were fully optimized at the UHF/3-21G, UHF/6-31G*, MP2/3-21G, and MP2/6-31G* levels. Optimizations and vibrational frequency calculations used the analytical first and second derivative methods in the GAUSSIAN packages. The effects of electron correlation were included by way of Møller-Plesset perturbation theory up to fourth order, including single, double, triple and quadruple excitations (MP4(SDTQ), frozen core) with projection corrections for spin contamination (denoted PMP4) in the unrestricted open-shell wavefunctions; these corrections were especially significant in transition structures.¹⁰ Following conventional notation, the PMP4/6-311G**//MP2/6-31G* level represents PMP4 energies computed with the 6-311G** basis set, using geometries optimized with an MP2/6-31G* wavefunction. Energies for 1.1A-1.5A were computed at the PMP4/6-311G**//MP2/6-31G*, PMP4/6-31G*//MP2/6-31G*, PMP4/6-31G**//UHF/6-31G*, and PMP4/6-31G*//UHF/6-31G* levels. The latter method was also used for all reference species. Unscaled UHF/6-31G* vibrational frequencies for all species were used to characterize stationary points and to calculate zero point energies and thermal energies to 298 K for all structures. Each of the optimized transition structures (1.2A or 1.4A) has just one negative eigenvalue of the Hessian Matrix. Activation energies were computed from the calculated total energy differences between the starting radical (1.1A) and the transition structures (1.2A or 1.4A). Similarly, heats of reactions reflect total energy differences between the product radicals (1.3A or 1.5A) and the initial radical (1.1A) calculated at the vibrationally

corrected PMP4/6-311G**//MP2/6-31G* level. A second approach to calculation of the energies of 1.1A, 1.3A, and 1.5A was to estimate their heats of formation by combining the isodesmic reactions of Scheme 1.3 with the experimentally known heats of formation of the reference compounds propene oxide, methyl vinyl ether, allyl alcohol, ethyl radical, ethane, methoxymethyl radical, dimethyl ether, ethoxy radical, and ethanol.

Most computations were run on the MSU Chemistry Department's VAX cluster, while the Convex or Titan computers were used for some larger jobs, and the Cray YMP at San Diego Supercomputing Center ran the MP2/6-31G* optimizations. Some preliminary optimizations were run on the SPARTAN program (Wavefunction, Inc.; Irvine, CA) on Silicon Graphics Indigos at MSU. A generous grant of Cray YMP time from Cray Research, Inc. enabled higher level single-point calculations, detailed explorations of potential energy surfaces, and preliminary substituent effect studies.

Scheme 1.2



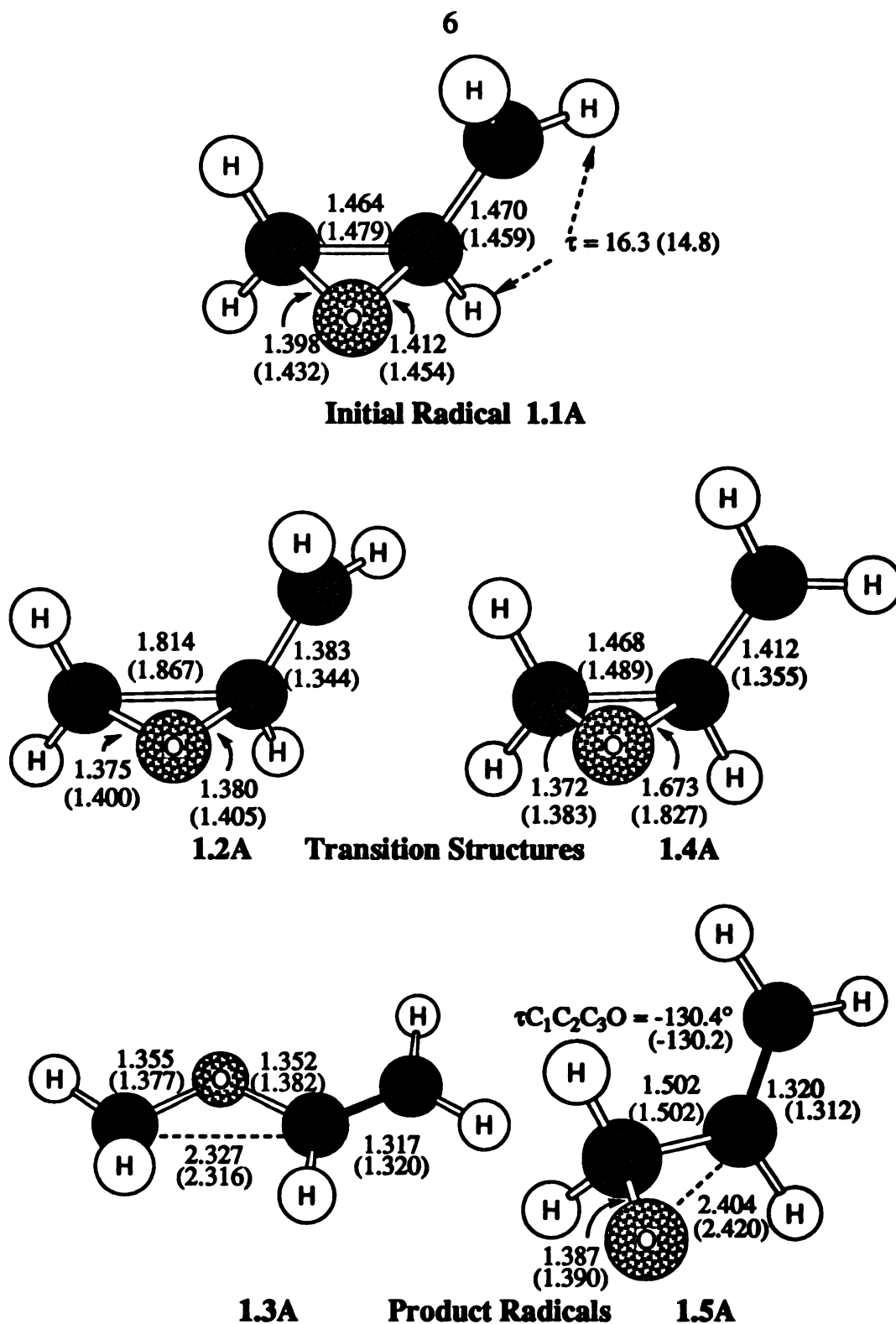


Figure 1.1. Structures of 1.1A-1.5A calculated at the UHF/6-31G* and (MP2/6-31G*) levels of theory, showing selected distances and torsion angles. For complete geometries, see appendix 1.1.

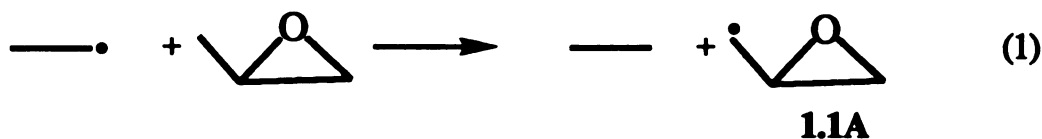
1.3 Results and Discussion:

Figure 1.1 shows the structures calculated for the species in Scheme 1.2, while Chart 1.1 and Table 1.1 summarize our energetic findings. Unless otherwise indicated, relative energies for 1.1A-1.5A cited in the following text denote 298 K vibrationally corrected PMP4/6-311G**//UMP2/6-31G* energies. Heats of formation in Chart 1.1 for 1.1A, 1.3A, 1.5A and their conformers were derived from known heats of formation for reference compounds and the heats of the isodesmic reactions of Scheme 1.3 calculated at the vibrationally corrected PMP4/6-31G**//UHF/6-31G* level. Explorations of the potential energy surface surrounding 1.4A are graphically presented in Figure 1.2.

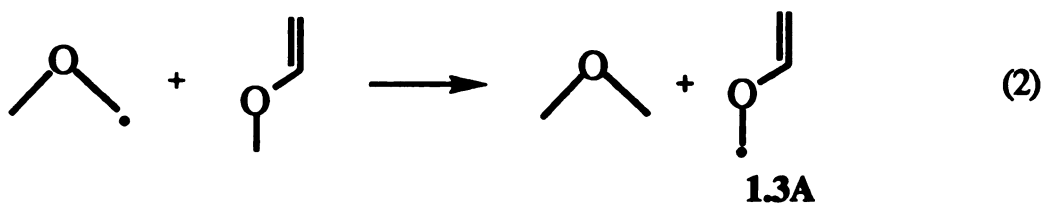
Product Structures and Energies: Product radicals 1.3A and 1.5A were optimized by slightly stretching the C-C and C-O distances in transition structures 1.2A and 1.4A and allowing them to relax to energy minima. Neither 1.3A nor 1.5A are the global minimum energy structures for vinyloxymethyl (1.3A) or allyloxy (1.5A) radicals; they are, nonetheless, no more than 2 kcal/mol above the lowest energy conformers (see Chart 1.1) as calculated at the PMP4/6-31G**//UHF/6-31G* level. The corresponding hydrogen-added C₃H₆O isomers methyl vinyl ether and allyl alcohol also have several close-lying conformational minima. For 1.3A and methyl vinyl ether, the lowest energy form is nearly planar in an *s-cis*-like conformation, while the structure first accessed by C-C bond cleavage is *s-trans*-like. Similarly, *s-cis*-like conformations ($\tau_{\text{CCCO}} \sim 0^\circ$) of 1.5A and allyl alcohol are lowest, but the initially accessed forms are staggered with $\tau_{\text{CCCO}} \sim 120^\circ$. In all cases these species are separated by barriers of less than 3 kcal/mol.

Ring opening by C-C bond cleavage to give 1.3A is calculated to be only 1.6 kcal/mol exothermic. Radical 1.3A is nearly planar, showing slight pyramidalization at the radical carbon, similar to that found in the methoxymethyl radical. Thus, there appears to be no special relationship in 1.3A between the vinyl group and the radical center, and 1.3A may be described as an ordinary α -alkoxymethyl radical. This view is supported by the theoretical finding of nearly thermoneutral hydrogen atom transfer from dimethyl ether to 1.3A (see Chart 1.1). We could not locate experimental data on methyl vinyl ether or anisole for comparison with the 93.1 kcal/mol C-H BDE for dimethyl ether.^{2a}

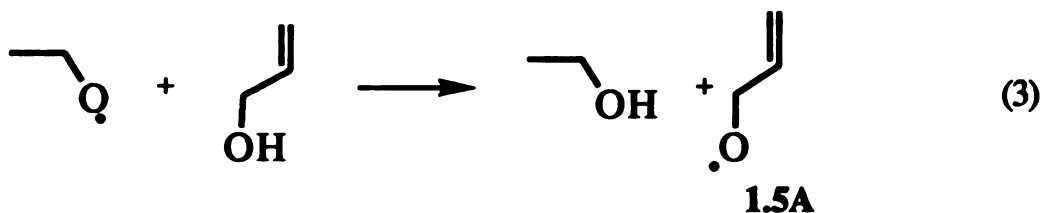
Ring opening by C-O bond cleavage to give the allyloxy radical 1.5A is calculated to be 0.6 kcal/mol exothermic, placing 1.5A only 1 kcal/mol above the quite ordinary radical 1.3A. At first, this result appears to suggest that allyl alcohol should have an anomalously low O-H BDE. However, the published BDE for benzyl alcohol is the same as that for ethanol (104 kcal/mol), suggesting no special stabilization in that case.^{2a} No compression of the \angle CCO angle is seen, nor are there significant differences in the double bond length. Resonance stabilization of 1.5A by a charge separated structure in which an electron has moved from the double bond to the oxygen center was considered, but the charges (Mulliken populations) computed for the oxygens in 1.5A and in ethoxy radical are essentially identical.¹¹ Furthermore, such an interaction would be expected to strongly affect the preferred conformation of the allyloxy radical, yet the staggered and *s-cis*-like forms are essentially isoenergetic, as shown in Chart 1.1. Finally, the isodesmic reactions of Scheme 1.3 (vide infra) show nearly thermoneutral hydrogen transfer from allyl alcohol to ethoxy radical.

Scheme 1.3 Isogyric Reactions

$\Delta H_{\text{rxn}}(\text{kcal/mol})^{\text{a}}$
 PMP4 -1.1(-1.0)



$\Delta H_{\text{rxn}}(\text{kcal/mol})^{\text{a}}$
 PMP4 0.1(-0.3)^b 1.8(1.5)^c



$\Delta H_{\text{rxn}}(\text{kcal/mol})^{\text{a}}$
 PMP4 -1.5(-1.3)^b -0.5(-0.5)^c



$\Delta H_{\text{rxn}}(\text{kcal/mol})^{\text{a}}$
 PMP4 -1.9(-1.6)
 EXP. -11.1

a Values listed in parentheses have been corrected for thermal energy contributions.

b These energies are estimated from the conformations obtained by allowing the corresponding transition states to relax to products, and the corresponding hydrogenated species.

c These energies are estimated from the most stable conformations found for all species.

Chart 1.1. Calculated Total Energies (in a.u.) and Estimated Heats of Formation

| | | | | |
|--------------------------------------|-------------|------------|------------|------------|
| | | | | |
| PMP4/6-31G* ^a | -79.53234 | -78.87326 | -154.54635 | -153.89497 |
| Thermal energy ^b | 0.08316 | 0.06719 | 0.09035 | 0.07529 |
| Corrected energy | -79.44918 | -78.80607 | -154.45600 | -153.81968 |
| ΔH_f (kcal/mol) ^c | -20.1±0.05 | 28.0±0.5 | -44.0±0.1 | -3.0±1.0 |
| | | | | |
| PMP4/6-31G* ^a | -154.55873 | -153.90435 | -192.52851 | -191.87114 |
| Thermal energy ^b | 0.09014 | 0.07474 | 0.09650 | 0.08060 |
| Corrected energy | -154.46859 | -153.82961 | -192.43201 | -191.79054 |
| ΔH_f (kcal/mol) ^c | -56.1±0.1 | -4.0±1.1 | -22.6±0.1 | [24.4±0.6] |
| | | | | |
| PMP4/6-31G* ^a | -192.52561 | -191.87415 | -192.52982 | -191.87558 |
| Thermal energy ^b | 0.09614 | 0.08056 | 0.09663 | 0.08113 |
| Corrected energy | -192.42947 | -191.79359 | -192.43319 | -191.79445 |
| ΔH_f (kcal/mol) ^c | [-22±2] | [19.1±3] | -24±2 | [18.5±3] |
| | | | | |
| PMP4/6-31G* ^a | -192.52859 | -191.87664 | -192.53030 | -191.87668 |
| Thermal energy ^b | 0.09652 | 0.08150 | 0.09666 | 0.08125 |
| Corrected energy | -192.43207 | -191.79514 | -192.43364 | -191.79543 |
| ΔH_f (kcal/mol) ^c | [-29.0±0.5] | [21.8±1.7] | -30.0±0.5 | [21.6±1.7] |

^a These values are calculated at the UHF/6-31G* geometries.

^b Thermal energies are sum of zero-point energy and thermal energy contributions at 298 K computed at the UHF/6-31G* level; frequency corrections were not applied as they make very little difference (< 0.2 kcal/mol) to the comparisons made here.

^c The values in square brackets are estimated from the isodemic reactions (1)-(3) in Scheme 1.3 and experimental heats of formation.

Since equations (1)-(3) are isodesmic, isogyric reactions, the errors therein should cancel. Thus, we can combine these isodesmic reaction energies with experimental heats of formation of reference compounds to estimate heats of formation for radicals 1.1A, 1.3A, 1.5A, and their conformers. The resulting energies, summarized in Chart 1.1, are close to those expected based on our original naive analogies.⁴ In other words, the vinyl groups in vinyloxymethyl radical and allyloxy radical do not significantly stabilize the radicals; in fact 1.3A appears to be slightly destabilized by the vinyl group. In equation (4), a nonisodesmic comparison of the BDEs for C-H of dimethyl ether and O-H of ethanol, there is a significant difference (> 9 kcal/mol) between computational and experimental estimations. This large discrepancy can be traced to two substantial errors: First, Hehre et al.¹² have shown that ab initio calculations underestimate heteroatom-hydrogen BDEs (i.e. O-H bond) by 5-10 kcal/mol even at a high level (MP4/6-31G**//UHF/6-31G*); this difficulty remains severe even when spin-projected wavefunctions are used. Second, the MP4/6-31G*//HF/6-31G* energy difference between the closed-shell C₂H₆O isomers dimethyl ether and ethanol is 7.9 kcal/mol (12.1 expt.) whereas the PMP4/6-31G*//UHF/6-31G* energy difference between C₂H₅O methoxymethyl and ethoxy radicals is 6.2 kcal/mol (1.0 expt.). These two errors add to give a 9.4 kcal/mol error for the reaction of equation (4).

Transition Structures and Activation Barriers: Transition structures 1.2A and 1.4A are shown in Figure 1.1. Our best calculated barrier for breaking the C-O bond of the epoxide (4.8 kcal/mol) is lower by 6.7 kcal/mol than for breaking the C-C bond (11.5 kcal/mol). In the UHF/6-31G* optimized structures, the shortening of the nascent double bond may

be used as a measure of reaction progress at the TS. At this level the vinyl groups in 1.3A and 1.5A are similar in length (1.317 and 1.320 Å, respectively), so the ending points are comparable. By this analysis the TSs for C-C (1.2A) and C-O (1.4A) bond cleavages are “late” and “early” (~57% and ~39%) respectively. In both cases, the erstwhile radical center has rotated to optimize π -overlap with the methine carbon, while the breaking bonds have stretched by 41 and 26% of their final extension. For TS 1.2A, the 3-carbon has not begun to rotate to allow π -stabilization by the neighboring oxygen; thus 1.2A does not yet “feel” the radical stabilizing effect of α -oxygen.

As a probe of the effects of electron correlation on geometry, structures 1.1A-1.5A were also optimized at the MP2/3-21G and MP2/6-31G* levels; MP4(SDTQ)/6-311G** and MP4(SDTQ)/6-31G* single point calculations were then run on the MP2/6-31G* geometries. For the radical minima 1.1A, 1.3A, and 1.5A, the geometry differences are minor between the UHF/3-21G, UHF/6-31G*, MP2/3-21G, and MP2/6-31G* levels (see Figure 1.1 and Appendix 1.1). However, both TSs 1.2A and 1.4A show significant geometrical changes on reoptimization at the MP2 levels (see Figure 1.1). Specifically, the breaking bonds are more extended than in the UHF/6-31G* TS structures, suggesting that the latter may not be adequate representations of the energy maxima for this reaction. Though the “late” vs. “early” timing of the TSs is retained, at the MP2/6-31G* level, both 1.2A and 1.4A are later (83% and 71%, respectively as defined previously), and their geometries are much more similar in reaction progress.

The higher barriers obtained at the MP2/6-31G* geometries suggest that these structures more accurately approximate the MP4 maxima

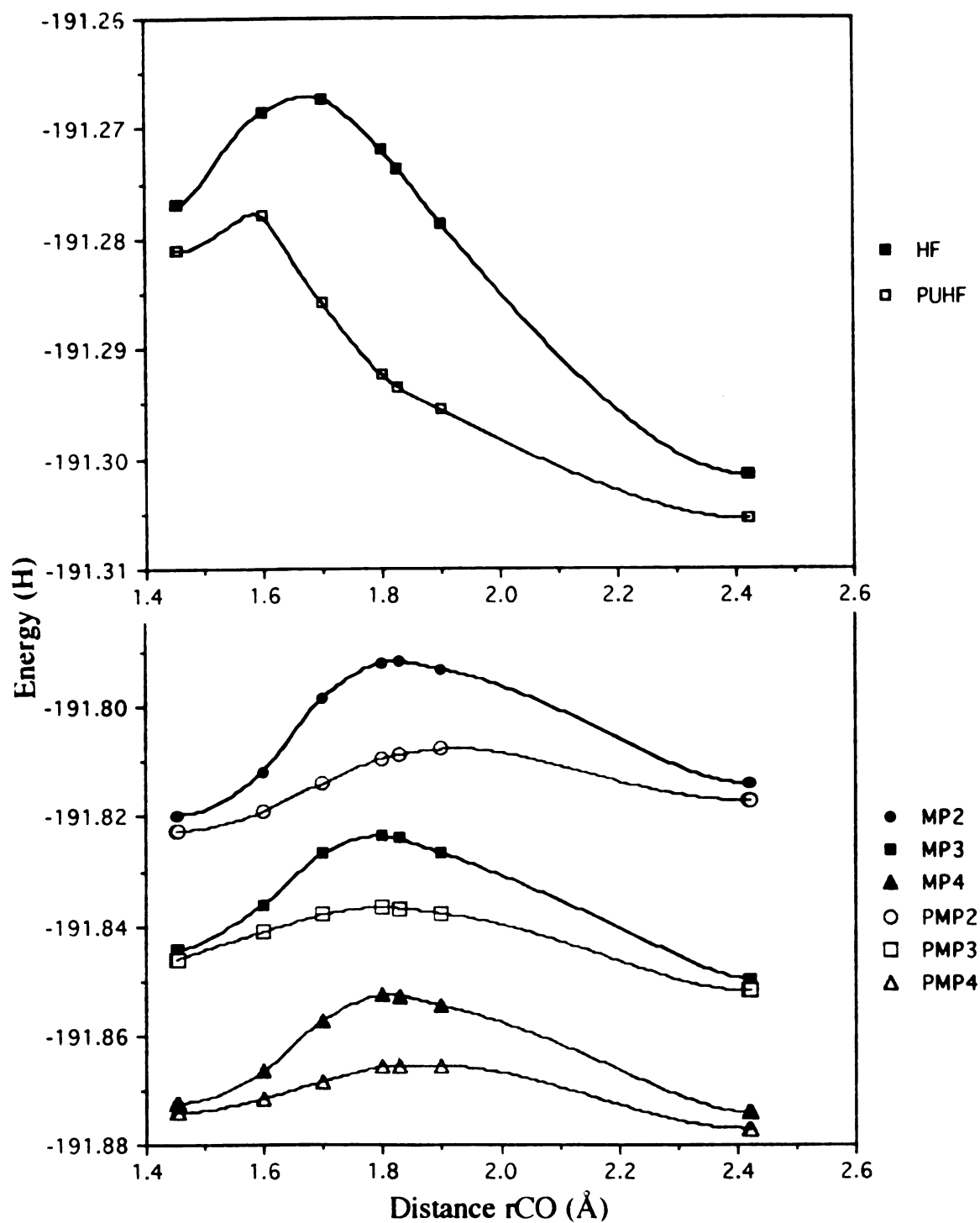


Figure 1.2. The potential energy surface for C-O bond cleavage generated by stepping the C-O length with reoptimization of all other geometry variables at the MP2/6-31G* level. Energies for the various levels are all in hartrees.

than do the UHF structures. To explore this interpretation, the potential energy surface for C-O bond cleavage was examined in the vicinity of the MP2/6-31G* transition structure by stepping the C-O length with reoptimization of all other geometry variables at the MP2/6-31G* level. Energy calculations at the MP4(STDQ) level were then run for each point. Results for UHF, MP2, MP3, MP4, and the corresponding spin polarization corrected PUHF, PMP2, PMP3, and PMP4/6-31G* calculations are shown in Figure 1.2. Three noteworthy items were uncovered: First, the PMP4 maximum is broad and flat and coincides with the optimized MP2/6-31G* maximum, so that the PMP4 energy barrier calculated at the MP2 geometry should be very close to the best value. Second, the HF energies calculated for MP2/6-31G* geometries peak close to the UHF/6-31G* optimized maximum; thus partially optimized "step" structures are not significantly distorted by the unbalanced treatment of geometrical variables (i.e. fixing one and optimizing all others). Third, spin projection hugely affects energies and calculated TS positions along the C-O distance; this last finding suggests that optimization with the spin-projected wavefunctions might be needed in some systems. We did not similarly analyze the potential energy along the C-C distance about 1.2Å. The geometry and the ΔE_a value for 1.2Å change much less than for 1.4Å between UHF/6-31G* to MP2/6-31G* structures (see Figure 1.1 and Table 1.1). Also, the MP2/6-31G* maximum had proven to be the proper choice for the higher level calculations on 1.4Å.

The calculated activation barriers, which clearly favor C-O over C-C cleavage, readily explain the experimental selectivities. The low barrier and near thermoneutrality of C-O bond opening suggest that fast equilibrium of closed and open forms (1.1Å and 1.5Å) would be expected, while access

to **1.3A** would be much slower. Thus, since all reports to date are based on product studies, the apparent selectivity for carbon vs. oxygen radical trapping may be affected by an imbalance in relative rates of hydrogen atom transfer to **1.1A** vs. **1.5A**. Nonetheless, C-C bond opening, when assisted by appropriate delocalizing 3-substitution, can lead to trappable carbon-centered radicals.

1.4 Conclusion:

Our calculations have established that (1) The apparent stability of the allyloxy radical **1.5A** compared with vinyloxymethyl radical **1.3A** results from over-estimation by the absolute energy calculations; (2) The vinyloxymethyl radical **1.3A**, also a homoallylic species, gains no special stability other than that afforded by α -oxy substitution; (3) The C-O ring-opening of α -epoxyalkyl radicals is a facile process whereas C-C cleavage is much more difficult; (4) The regioselectivity of α -epoxymethyl radical cleavage is controlled by relative rates for C-O vs. C-C bond breaking instead of the heats of reaction; (5) Spin contamination and electron correlation strongly affect the structures of TSs **1.2A** and **1.4A**, and the overall relative energetics in this system. We believe it may also be possible to control the C-C vs. C-O bond cleavage choice via substituents on the initial radical center, an unexpected locus of regiocontrol.

Table 1.1. Total and Relative Energies of Calculated Structures 1.1A-1.5A

| Basis set | Starting Radical | Transition Structures | | | Product Radicals |
|----------------------------|-------------------|-----------------------|-------------------|-------------------|-------------------|
| | 1.1A ^a | 1.2A ^b | 1.4A ^b | 1.3A ^b | 1.5A ^b |
| UHF/3-21G | -0.19959 | 10.2 | 0.2 | -15.7 | -26.1 |
| MP2/3-21G | -0.57739 | 16.9 | 9.8 | | |
| UHF/6-31G* | -1.27916 | 15.4 | 6.3 | -3.5 | -14.4 |
| UHF/6-31G**//UHF/6-31G* | -1.28777 | 15.2 | 6.3 | -3.9 | -14.2 |
| UHF/6-311G**//UMP2/6-31G* | -1.32562 | 13.6 | 1.5 | -5.9 | -16.6 |
| UMP2/6-31G**//UHF/6-31G* | -1.81752 | 22.5 | 11.2 | 0.5 | 2.7 |
| UMP2/6-31G**//UHF/6-31G* | 1.85757 | 22.6 | 11.2 | 0.1 | 3.0 |
| UMP2/6-31G**//UMP2/6-31G* | -1.81965 | 23.3 | 17.6 | 0.7 | 3.6 |
| UMP2/6-311G**//UMP2/6-31G* | -1.93386 | 21.3 | 17.3 | -0.9 | 2.7 |
| UMP3/6-31G**//UHF/6-31G* | -1.84277 | 20.8 | 9.5 | -0.6 | -3.9 |
| UMP3/6-31G**//UHF/6-31G* | -1.88548 | 20.9 | 9.5 | -1.0 | -3.6 |
| UMP3/6-31G**//UMP2/6-31G* | -1.84412 | 21.3 | 12.6 | -0.6 | -3.9 |
| UMP3/6-311G**//UMP2/6-31G* | -1.95940 | 19.1 | 12.1 | -2.3 | -4.6 |
| UMP4/6-31G**//UHF/6-31G* | -1.86950 | 19.7 | 7.7 | -1.5 | -2.8 |
| UMP4/6-31G**//UHF/6-31G* | -1.91210 | 19.8 | 7.7 | -1.8 | -2.4 |
| UMP4/6-31G**//UMP2/6-31G* | -1.87229 | 20.7 | 12.3 | -1.0 | -1.6 |
| UMP4/6-311G**//UMP2/6-31G* | -1.99323 | 19.0 | 12.6 | -2.1 | -1.1 |
| PUHF/6-31G**//UHF/6-31G* | -1.28306 | 6.2 | -1.9 | -3.6 | -14.8 |
| PUHF/6-31G**//UHF/6-31G* | -1.29116 | 5.8 | -2.2 | -4.4 | -15.0 |
| PUHF/6-31G**//UMP2/6-31G* | -1.28112 | 6.7 | -7.8 | -2.9 | -15.3 |
| PUHF/6-311G**//UMP2/6-31G* | -1.32989 | 5.6 | -8.2 | -4.9 | -16.3 |
| PMP2/6-31G**//UHF/6-31G* | -1.82017 | 14.3 | 4.0 | 0.1 | 2.1 |
| PMP2/6-31G**//UHF/6-31G* | -1.86017 | 14.4 | 4.0 | -0.3 | 2.2 |
| PMP2/6-31G**//UMP2/6-31G* | -1.82257 | 15.9 | 8.7 | 1.3 | 3.5 |
| PMP2/6-311G**//UMP2/6-31G* | -1.93679 | 14.1 | 8.5 | -0.2 | 2.7 |
| PMP3/6-31G**//UHF/6-31G* | -1.84441 | 14.4 | 4.3 | -1.0 | -4.5 |
| PMP3/6-31G**//UHF/6-31G* | -1.88709 | 14.5 | 4.3 | 2.3 | -4.4 |
| PMP3/6-31G**//UMP2/6-31G* | -1.84595 | 15.4 | 5.7 | -0.3 | -3.7 |
| PMP3/6-311G**//UMP2/6-31G* | -1.96122 | 13.5 | 5.3 | -1.9 | -4.8 |
| PMP4/6-31G**//UHF/6-31G* | -1.87114 | 13.3 | 2.5 | -1.9 | -3.4 |
| PMP4/6-31G**//UHF/6-31G* | -1.91370 | 13.7 | 2.5 | -2.2 | -3.2 |

| | | | | | |
|--|----------|------------|----------|------------|------------|
| PMP4/6-31G*//UMP2/6-31G* ^c | -1.87412 | 14.9(13.0) | 5.4(4.5) | -0.7(-0.7) | -1.8(-1.2) |
| PMP4/6-311G**//UMP2/6-31G* | -1.99506 | 13.4(11.5) | 5.7(4.8) | -1.6(-1.6) | -1.2(-0.6) |
| Zero-Point Energy ^d | 0.07603 | -1.6 | -0.6 | -0.3 | 0.7 |
| Σ Thermal Energies ^d | 0.08060 | -1.9 | -0.9 | -0.0 | 0.6 |
| Dipole (UHF/6-31G* geometries) | 2.28 D | 1.72 D | 2.35 D | 1.39 D | 1.96 D |
| Dipole (MP2/6-31G* geometries) | 2.47 D | 1.84 D | 2.10 D | 1.45 D | 1.97 D |

^a Total energies for radical **1.1A** are given in Hartrees (H) relative to -190.0 H (1 Hartree = 627.5 kcal/mol). Zero-point energies are directly reported in Hartrees, and dipole values are in debye.

^b Energies for **1.2A-1.5A** are given in kcal/mol, relative to the energy of **1.1A** at the corresponding level.

^c Values listed in parentheses have been corrected for thermal energy contributions and represent best estimates for the experimental activation energies/reaction exothermicities.

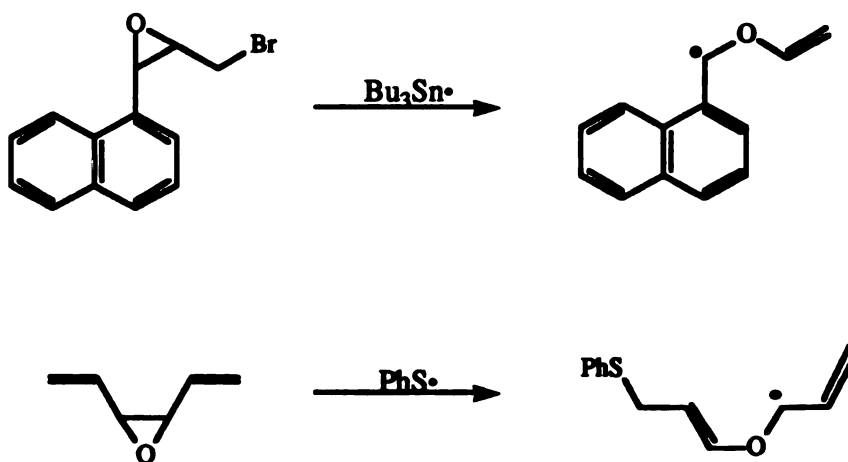
^d Zero-point and thermal energies were computed for 298 K at the UHF/6-31G*//UHF/6-31G* level and were used without scaling.

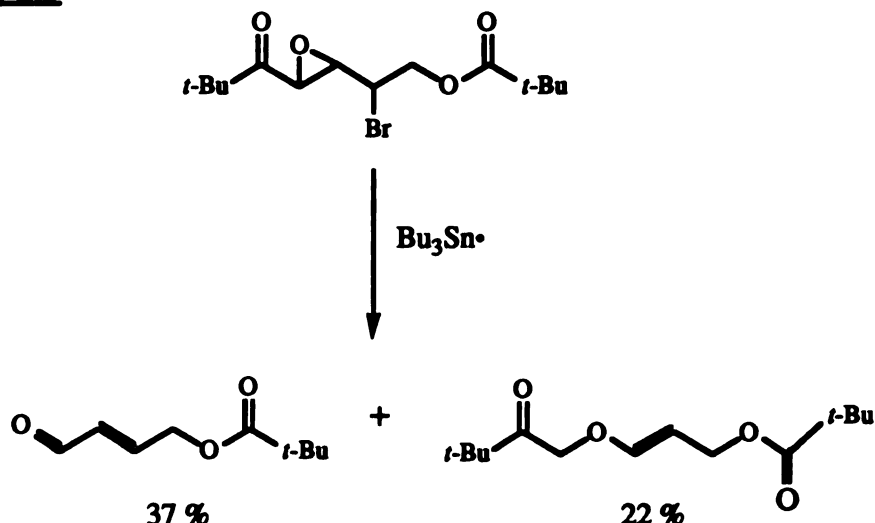
Part II: Substituent Effects

1.5 Introduction:

Ring-opening of α -epoxyalkyl radicals has been widely used in organic synthesis. The epoxide ring is easy to build, and this methodology can be used to generate cis-fused bicyclic systems through a highly regioselective C-O bond cleavage. Consistent with the experimental observations of Murphy et al., we have shown, by ab initio calculations, that the high regioselectivity of C-O bond cleavage of the epoxide is kinetically favored, even though C-C bond cleavage is more exothermic than C-O bond cleavage. However, Murphy et al.¹³ and Stogryn and Gianni¹⁴ have reported that substitution of an aryl group or simple vinyl group on the epoxide ring leads exclusively to products of C-C bond cleavage (Scheme 1.4). Additionally, Murphy and co-workers showed that C-C bond cleavage becomes competitive with C-O bond cleavage when a carbonyl group is placed on the epoxide ring, as shown in Scheme 1.5.

Scheme 1.4

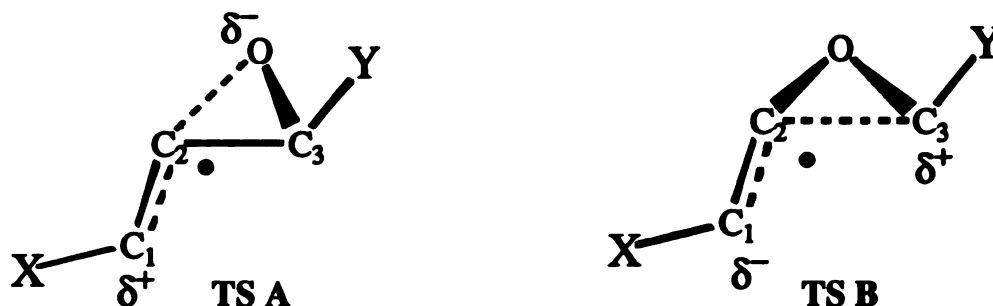


Scheme 1.5

If our prediction by ab initio calculation is correct, C-O bond cleavage of the parent epoxide is kinetically favored over C-C bond cleavage by ~ 6-7 kcal/mol. Thus, the activation energy difference between C-C and C-O bond cleavage can be decreased by a similar amount by putting proper substituents on the epoxide ring, as shown above.

Here, we attempt to answer the following questions using ab initio calculations: (1) How does such a simple electronic effect reverse the expected regioselectivity? (2) How do substituents on the α -methyl position influence the regioselectivities of the epoxide-ring opening? (3) Can we separate σ and π substituent effects?

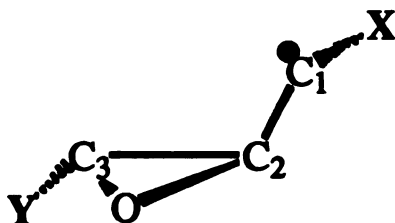
It is well-known that radicals are easily polarized.¹⁵ It seems reasonable, then, that the transition states for C-C and C-O cleavage of the epoxide should experience different degrees of polarization. Specifically, in the transition state for C-O bond cleavage (TS A), polarization may result in accumulation of negative charge on oxygen. In contrast, the transition state for C-C bond cleavage (TS B) would prefer positive charge build-up on C₃,



which could be stabilized by the neighboring oxygen. If these models are correct, then electron-withdrawing groups on C₁ and electron-donating groups on C₃ should prefer TS B; electron-donating substituents on C₁ should favor TS A, and those on C₃ should not significantly affect TS A.

1.6 Results:

Geometries: Three different substituents on either α -methyl or epoxide ring of α -epoxymethyl radical have been calculated, as shown in below. All structures were fully optimized at the UHF level using a 6-31G*



- | | |
|---------------------------------|--------------------------------|
| A: X = H; Y = H | |
| B: X = NH ₂ ; Y = H, | B': X = H; Y = NH ₂ |
| C: X = CN; Y = H, | C': X = H; Y = CN |
| D: X = BH ₂ ; Y = H, | D': X = H; Y = BH ₂ |

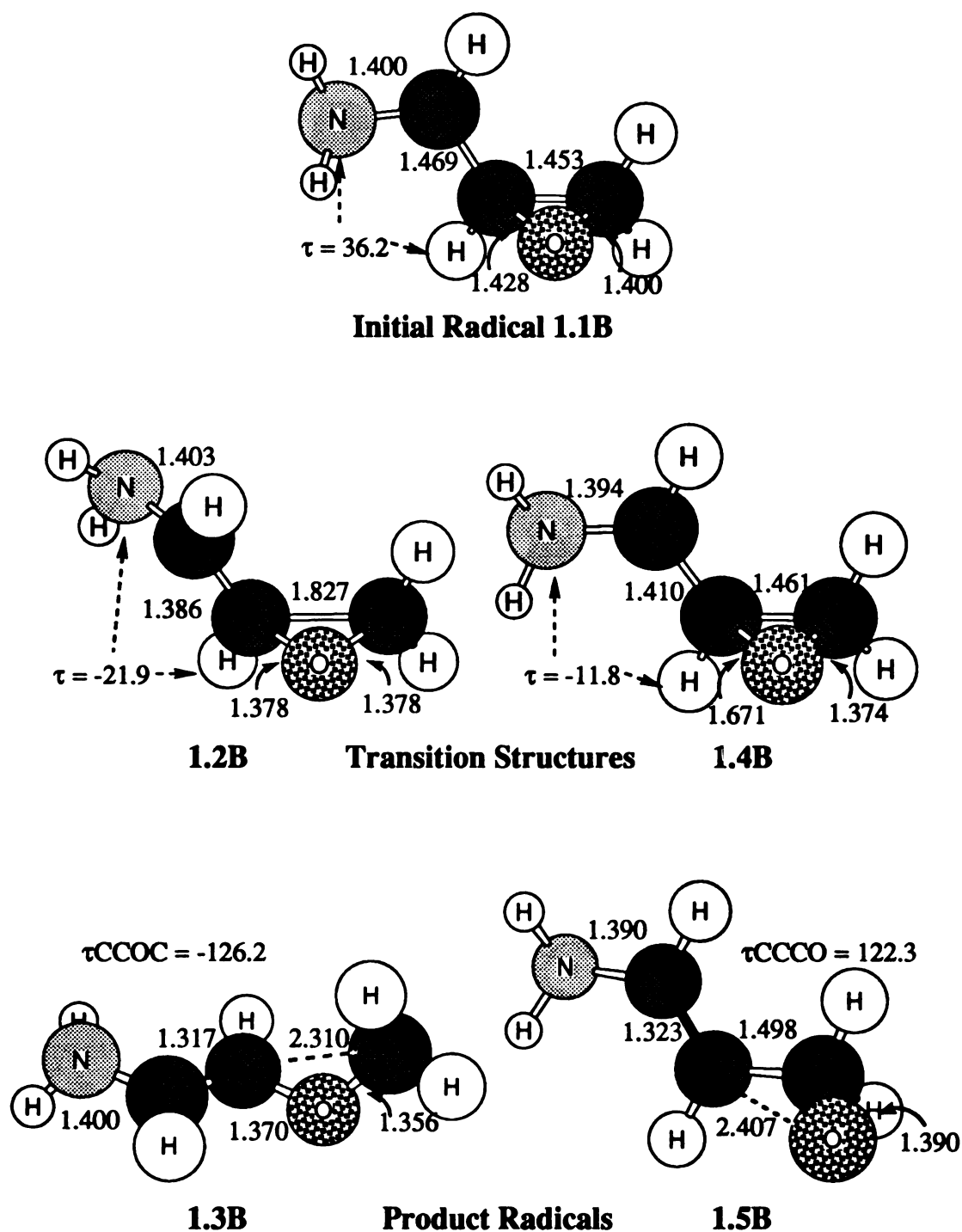


Figure 1.3. Structures of 1.1B-1.5B calculated at the UHF/6-31G* level of theory, showing selected distances and torsion angles.

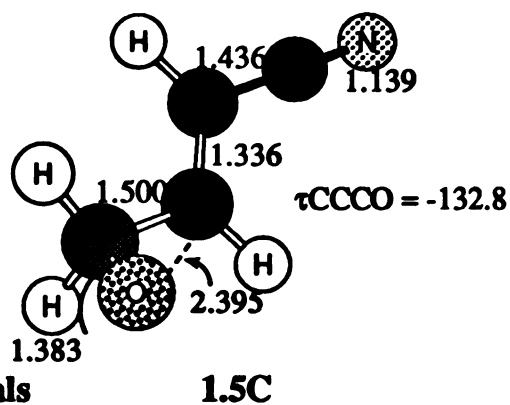
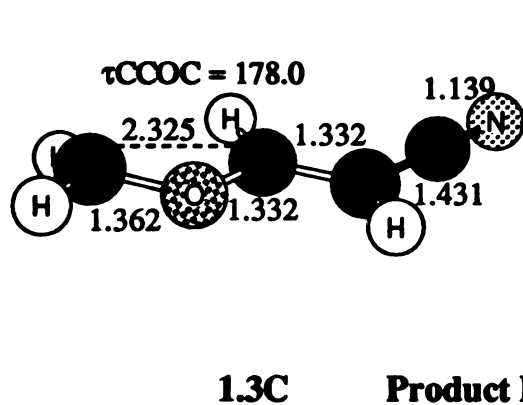
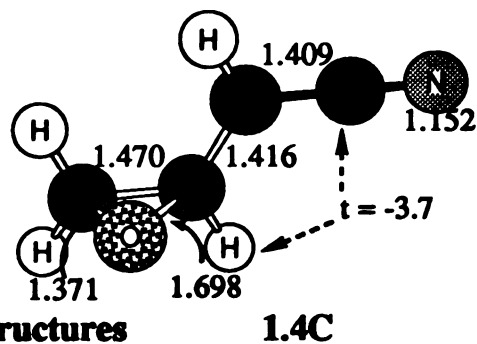
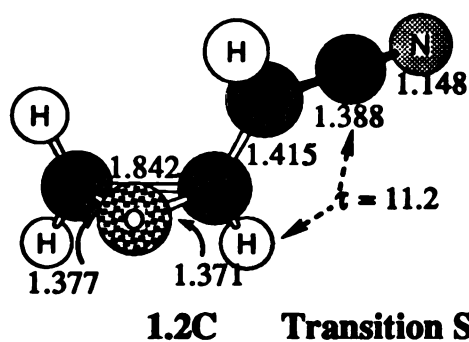
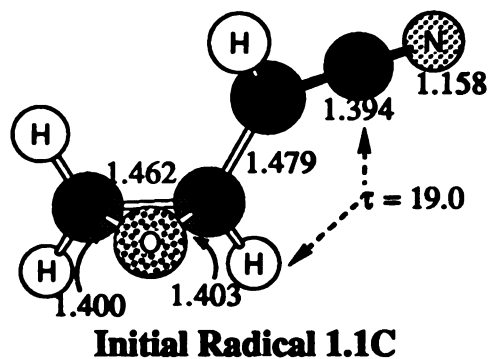


Figure 1.4. Structures of 1.1C-1.5C calculated at the UHF/6-31G* level of theory, showing selected distances and torsion angles.

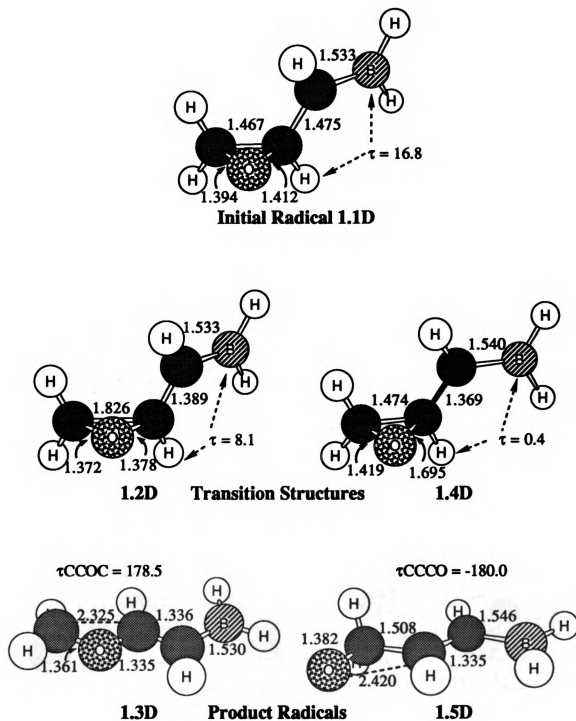


Figure 1.5. Structures of 1.1D-1.5D calculated at the UHF/6-31G* level of theory, showing selected distances and torsion angles.

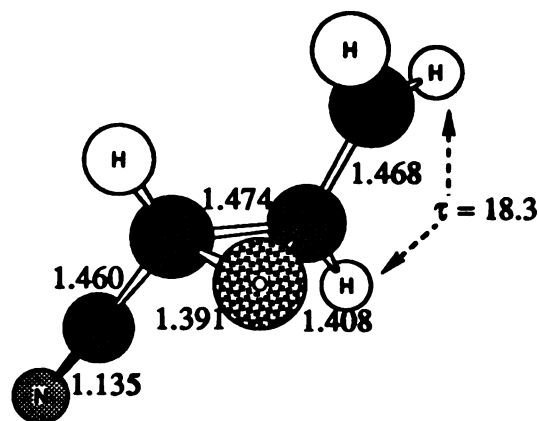
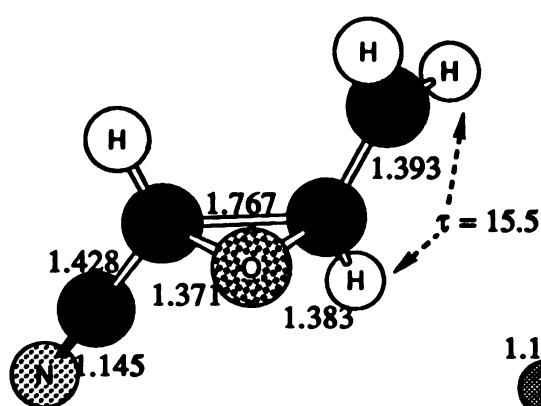
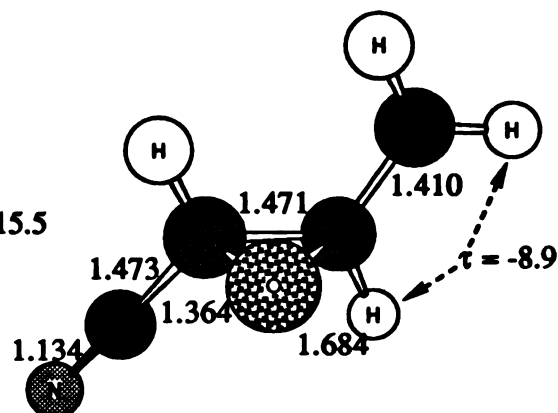
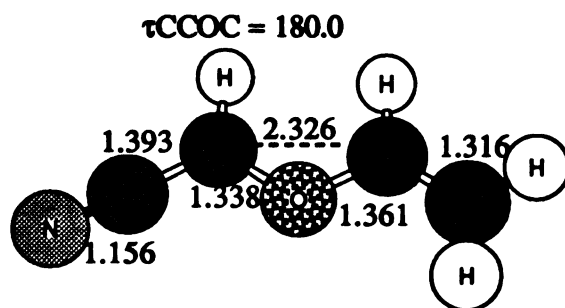
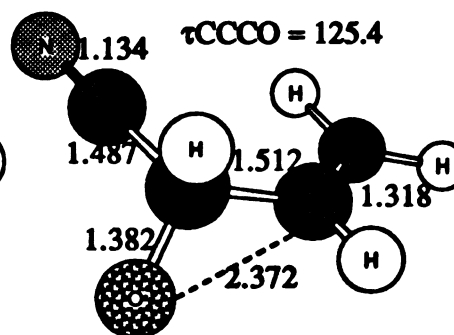
**Initial Radical 1.1C'****1.2C'****Transition Structures****1.4C'****1.3C'****Product Radicals****1.5C'**

Figure 1.6. Structures of 1.1C'-1.5C' calculated at the UHF/6-31G* level of theory, showing selected distances and torsion angles.

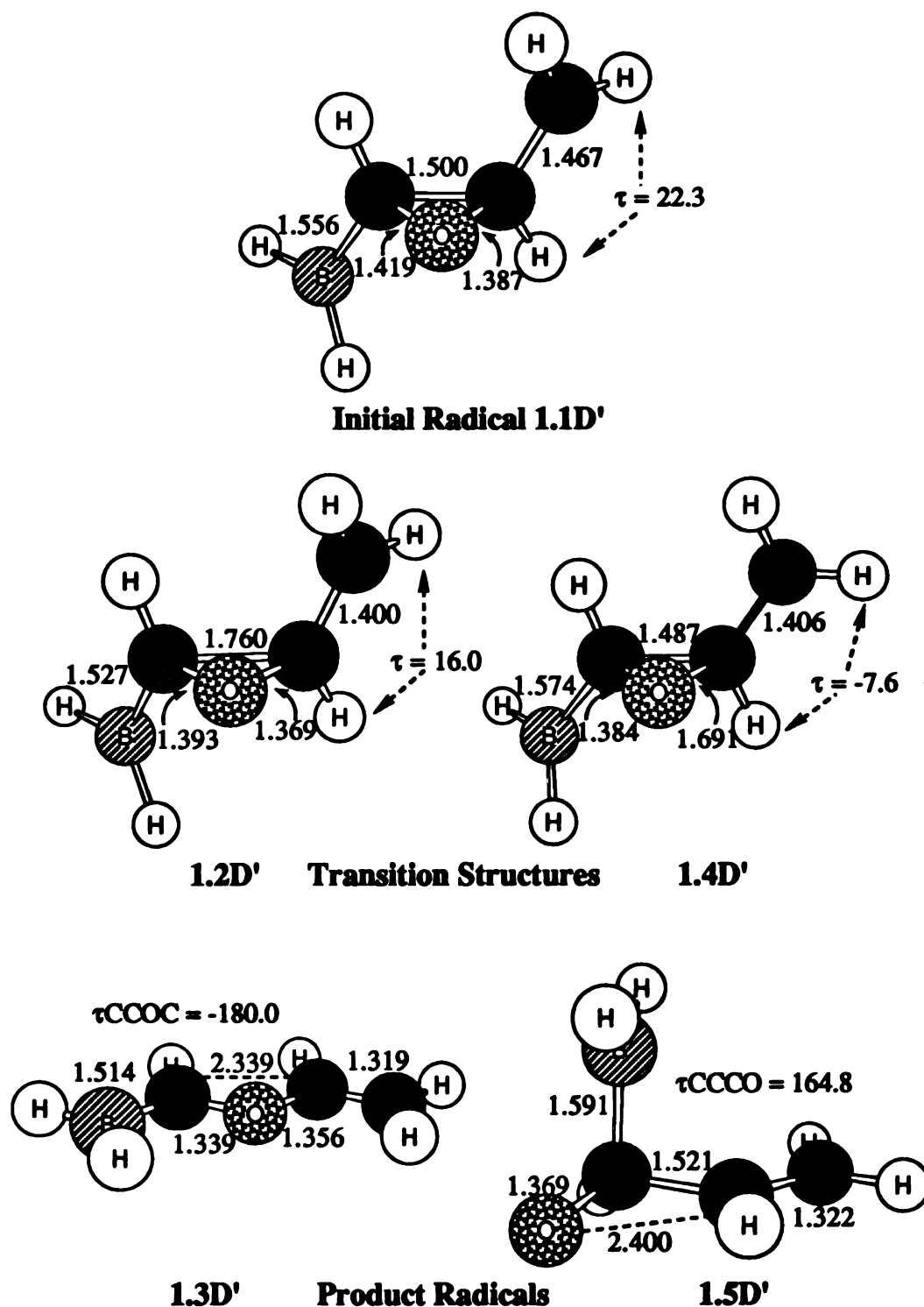


Figure 1.7. Structures of 1.1D'-1.5D' calculated at the UHF/6-31G* level of theory, showing selected distances and torsion angles.

basis set. Geometries of the initial radicals (1.1), transition states (1.2 for C-C and 1.3 for C-O bond breaking), and final radicals (1.4 for C-C and 1.5 for C-O bond cleavage) incorporating different substituents, are summarized in Tables 1.2-1.6 and Figures 1.3-1.7. The starting geometries (1.1) of the α -epoxymethyl radicals basically are very similar, as shown in Table 1.2. Bond distances of future breaking-bonds, C_2C_3 or C_2O , are ca. 1.5 Å and 1.4 Å, respectively. The transition states for the C-C bond cleavage of the substituted α -epoxymethyl radicals are also similar to the transition state of the parent radical, as shown in Table 1.3. For all substituents at the X position, the rC_2C_3 for the transition states of C-C bond cleavage are about 1.8 Å; they become just a little shorter (~ 1.76 Å) when $Y = CN$ or BH_2 , the electron-acceptors. There is not much geometry variation among the transition states for C-O bond cleavage either, as shown in Table 1.4. For the X or Y substituted radicals, the rC_2O values are ca. 1.68 Å, which is a little longer than that of the parent system ($X = Y = H$; 1.64 Å). Unfortunately, we were unable to locate the initial radical or transition states for C-C and C-O bond cleavages for α -epoxymethyl radical with an NH_2 substituent on the Y position; the initial radical fell monotonically down hill to generate the C-O bond cleavage product radical. Repeated attempts at locating a minimum for the amino substituted radical failed, suggesting that with such a strong electron donor, C-O cleavage occurs without a barrier.

The broken bond (rC_2C_3) distances for the product radicals obtained from C-C bond cleavage are all about 2.3 Å (Table 1.5). The broken bond (rC_2O) distances for the C-O bond cleavage product radical are around 2.4 Å (Table 1.6) except that the distance is a little shorter for the

NH₂-substituted epoxide ring (1.5B) (C-O cleavage product when Y = NH₂).

Generally speaking, comparing the corresponding radicals, the geometries of substituted α -epoxymethyl radical ring-opening transition structures are not changed much by changes in the nature— π electron-donors or acceptors—or the position—X or Y—of the substituents. Even though the distances of the breaking bond at the transition states are slightly sensitive to substituents, the changes are trivial (< 0.1 Å).

Energies: Total energies were calculated at the MP4(SDTQ)/6-31G*//UHF/6-31G* level including projection correction for spin contamination (PMP4) for all substituted systems. The results are summarized in Tables 1.7-1.11 and heats of reaction and activation energies calculated at the PMP4/6-31G*//UHF/6-31G* level are listed in Table 1.12.

Activation Energies: For substituents NH₂, CN, and BH₂ on the α -methyl position (X position) the activation energies of C-C bond cleavage increase by 2.2, 3.1, and 0.7 kcal/mol, respectively, with respect to the 13.3 kcal/mol activation barrier in the parent system (Table 1.12). However, these substituents have different effects on the energy barriers for C-O bond cleavage. With electron-donating groups like NH₂, the energy barrier for C-O bond breaking is just 0.8 kcal/mol, which is 1.7 kcal/mol less than for the parent system. However, electron-withdrawing groups CN and BH₂ increase the barrier by ~ 3 kcal/mol with respect to the parent system.

For substituents on the epoxide ring (Y position), electron-withdrawing groups dramatically decrease the activation energies for C-C bond cleavage. With a CN group at the Y position, the activation energy for

C-C bond cleavage is 6.6 kcal/mol, 6.7 kcal/mol lower than that for the parent system, and the barrier for C-O bond cleavage (3.1 kcal/mol) is essentially the same as the parent system. The activation energy difference between C-C and C-O bond cleavage is then narrowed from 10.8 kcal/mol for parent system, to just 3.5 kcal/mol for the α -cyanoepoxymethyl radical. In the case of BH₂, an even stronger π electron-withdrawing group (but sigmatropic donor), the activation energy for C-C bond cleavage is decreased to 2.3 kcal/mol, while the barrier to C-O bond cleavage is increased. At this level of calculation, a BH₂ group at the Y position of the α -epoxymethyl radical changes the selectivity of the ring opening to favor C-C bond cleavage over C-O bond cleavage by 4.1 kcal/mol.

Energies of Reaction: The energies of reactions shown in Table 1.12 clearly show that the stronger the electron-withdrawing substituent at Y, the more C-C bond cleavage is favored. For substituents on the α -methyl position (X), the energy differences between C-C bond cleavage (vinyloxymethyl radicals) and C-O bond cleavage (allyloxy radicals) are 6.6, 1.5, -0.3, and -4.3 kcal/mol for NH₂, H, CN, and BH₂, respectively.

Compared to substituents on C₁ (X position), the same substituents at the Y position have stronger effects favoring C-C bond cleavage over C-O bond cleavage. When Y is CN or BH₂, the C-C bond cleavages (1.3C' and 1.3D') are calculated to be about 10 and 15 kcal/mol, respectively, more exothermic than C-O bond cleavage (1.5C' and 1.5D').

Other Substituents: In order to broaden our understanding of the substituent effects, we pushed the edge of the electron-donor and

acceptor to charged groups with and without π -conjugation abilities at the UHF/3-21G**//UHF/3-21G* level, as shown in Table 1.13.

For substituents at the X position, generally, the stronger the electron-acceptor, the more favored is C-C bond cleavage, relative to the parent system. Different from other substituents which increase the exothermicity for the C-C bond cleavage and slightly decrease the exothermicity for the C-O bond cleavage, NH_3^+ dramatically increases the exothermicity for both cleavages, in which it turns out that C-O bond cleavage is favored over C-C bond cleavage by 11.3 kcal/mol. Interestingly, the CN group has exactly the opposite effects for both bond cleavages; however, the results are the same as for NH_3^+ ; C-O bond cleavage is favored over C-C bond cleavage by 11.3 kcal/mol. For electron-donors, compared to the parent system the heats of reaction for C-C bond cleavage are essentially the same, while the exothermicity for the C-O bond cleavage is slightly increased (~ 2 kcal/mol).

For the substituents at the Y position, the trend is similar to those described above. The electron-acceptors favor C-C bond cleavage over C-O bond cleavage; however, the effects are stronger than for substituents at the X position: Except for NH_3^+ , all electron-acceptors increase the exothermicities for the C-C bond cleavage by more than 10 kcal/mol relative to that for parent system; meanwhile, the exothermicities for the C-O bond cleavage are basically the same as for the parent system. For NH_3^+ , again, the epoxide ring-opening still favors C-O bond cleavage over C-C bond cleavage by 3.0 kcal/mol. For both NH_3^+ and CH_2^+ , we cannot locate a minimum for the initial substituted radicals, which directly

fell down to bond cleavage products; C-O cleavage for NH_3^+ and C-C cleavage for CH_2^+ .

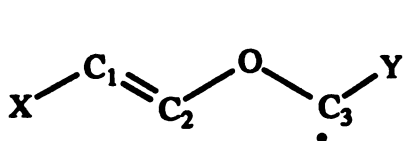
For electron-donors at the Y position, NH_3^+ , CH_3 , and BH_3^- are the same as for the parent system, favoring C-O bond cleavage. But it is a different story for CH_2^- , which shows the opposite trend compared with the other substituents. Again, unfortunately, we could not find a minimum for the initial CH_2^- substituted radical which directly fell down to the C-O bond cleavage product radical.

1.7 Discussion:

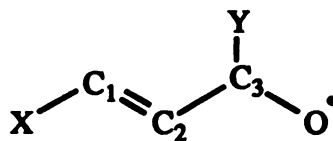
Basically, placing substituents either on the methyl (X position) or directly on the epoxide ring (Y position) does not change the geometries of the initial radicals, transition structures, or final radicals too much from the parent system ($\text{X} = \text{Y} = \text{H}$), regardless of the group's nature. This means that the substituents do not significantly change the relative location of the transition states along the reaction coordinates. Therefore, changes in barrier heights are hard to interpret in terms of early or late transition states using the Hammond postulate. Nevertheless, relative barriers and relative reaction exothermicities do tend vary together. This finding is not surprising since the more exothermic process already is seen to have the higher energy barrier (i.e. non-Hammond postulate behavior). Substituent effects for regioselectivity of the epoxide ring-opening just, then, result from the substituents having different effects on stability of the starting point (initial radical), mid-point (transition states), and final point (final radical) along the reaction coordinate, not the shapes of the molecule.

For substituents on the X position, the electron-withdrawing groups, CN and BH₂, increase energy barriers for both C-C and C-O bond cleavage; the electron-donating group, NH₂, decreases the activation energy for C-O bond cleavage but increases the energy for C-C bond cleavage. This is different from what we postulated in the introduction — that the stronger the electron-withdrawing group, the more favorable C-C bond cleavage would become, even though relative activation energies ($\Delta\Delta E_a$) still points in the predicted direction. Obviously, these substituents, especially the electron-withdrawing groups, can also stabilize the initial radicals. During bond breaking, either C-O or C-C bond, the unpaired electron's locus moves away from the initial radical center, thereby losing the X-substituent's stabilization and increasing the barrier.

For the same reason, the heats of reaction become more endothermic compared to the parent system, since the final radical center has completely lost the stabilization from the substituents. Nevertheless, the reactions still should favor C-C bond cleavage if only the exothermicities of the reactions are considered. Electron-acceptors at the X position in the vinyloxymethyl radical, as shown below, should stabilize the double bond between C₁ and C₂ via push-pull conjugation between the electron-acceptor and the electron-donor (alkoxy group).



vinyloxymethyl radical



allyloxy radical

Because of the compensation for losing the stabilization of the initial radical by the neighboring substituents, substituents on the X position

do not have much effect on the bond cleavage selectivity of α -epoxymethyl radical ring-opening.

For substituents on the Y position, the same radical stabilization concept applies as well for the epoxide ring-opening. For C-C bond cleavage, the further bond-breaking proceeds, the more radical electron density shifts to C₃, and the more stabilization the radical "feels". As shown in Table 1.12, for C-C bond cleavage, the activation energies are substantially decreased and the heats of reaction are also about 10 kcal/mole more exothermic than those of C-O bond cleavage.

As shown in Table 1.13, the π electron donors or acceptors are the major players here. The ionic species NH_3^+ and BH_3^- , which do not have unshared p-orbitals, do not affect much about the preference and both substituents either X or Y substituents are still in favor of C-O over C-C bond cleavage of the α -epoxymethyl radical ring-opening. Even though the UHF/3-21G//UHF/3-21G level of description may not be good enough, we still can observe the trend shown in $\Delta\Delta E_{\text{rel}}$ in Table 1.13: For either at X or Y positions, the π electron-acceptor substituted epoxide rings favors the C-C bond cleavage and π electron-donor substituted epoxide rings favors the C-O bond cleavage. As we discussed previously, though the regioselectivity of α -epoxymethyl radical ring-opening is determined by the preference between the transition states of C-O and C-C bond cleavage, the heats of reaction are do respond to substituent effects.

1.8 Conclusion:

We have clearly demonstrated that putting a substituent on the α -epoxyalkyl radical can change the ring-opening pathway of the epoxide. Electron-withdrawing substituents at C₁ (X position) stabilize the initial radical (1.1); however, the net effect is not as strong as for substituents at C₃ (Y position) which can form captodatively stabilized radicals after the epoxide ring-opening. Stabilization of the radical is mainly a result of π -conjugation between the π -electron-acceptor and the oxygen of the epoxide or its opened form. Polarization through the σ -bond has little or no effect on the α -epoxyalkyl radical ring-opening.

1.9 References and Notes:

- 1 (a) Carlson, R. G.; Huber, J. H. A.; Henton, D. E. *J. Chem. Soc. Chem. Commun.* **1973**, 223. (b) Barton, D. H. R.; Motherwell, R. S. H.; Motherwell, W. B. *J. Chem. Soc., Perkin Trans. I* **1981**, 2363. (c) Johns, A.; Murphy, J. A. *Tetrahedron Lett.* **1988**, 29, 837. (d) Johns, A.; Murphy, J. A.; Patterson, C. W.; Wooster, N. F. *J. Chem. Soc. Chem. Commun* **1988**, 294. (e) Rawal, V. H.; Newton, R. C.; Krishnamurthy, V. *J. Org. Chem.* **1990**, 55, 5181.
- 2 (a) Lias, S. G.; Bartmess, J. E.; Liebman, J. F.; Holmes, J. L.; Levin, R. D.; Mallard, W. G.; "Gas Phase Ion and Neutral Thermochemistry" *J. Phys. Chem. Ref. Data* **1988**, 17, Suppl. 1. (b) Heusler, K.; Kalvoda, J. *Angew., Chem. Int. Ed. Engl.* **1964**, 3, 525. (c) Brun, P.; Waegell, B. In

- Reactive Intermediates*; Abramovich, R. A., Ed.; Plenum Press: New York, 1983; vol. 3, p 367.
- 3 (a) Strogryn, E. L.; Gianni, M. H.; *Tetrahedron Lett.* 1970, 34, 3025. (b) Cook, M.; Hares, O.; Johns, A.; Murphy, J. A.; Patterson, C. W. *J. Chem. Soc., Chem. Commun.* 1986, 1419.
- 4 We naively estimate heats of formation of 17 and 22 kcal/mol for vinyloxymethyl radical 3.3A and allyloxy radical 3.5A by combining the ΔH_f values^{2a} for vinyl methyl ether (-24 kcal/mol) and allyl alcohol (-30 kcal/mol) with the appropriate BDEs (93.1 and 104.2 kcal/mol, respectively) of dimethyl ether (C-H) and ethanol (O-H) and subtracting the ΔH_f of a hydrogen atom (52.1 kcal/mol).
- 5 Krosley, K. W.; Gleicher, G. J.; Clapp, G. E. *J. Org. Chem.* 1992, 57, 840. These authors note the possibility of epoxide opening concerted with stannyl radical attack on the β -chlorine on the grounds of the enhanced reactivity of chloromethyl oxirane relative to chlorocyclohexane. However, various α -oxiranylalkyl radical systems have been generated via routes in which tin does not directly participate in the radical-forming step; see Sabatini, E. C.; Gritter, R. J. *J. Org. Chem.* 1963, 28, 3437. (See also refs. 1, 3, especially 1a, 3a).
- 6 Newcomb, M.; Glenn, A. G. *J. Am. Chem. Soc.* 1989, 111, 275.
- 7 Krosley, K. W.; Gleicher, G. J. *J. phys Org. Chem.* 1993, 6, 228-232.
- 8 Frisch, M. J.; Binkley, J. S.; Schlegel, H. B.; Ragavachari, K.; Melius, C. F.; Martin, R. L.; Stewart, J. J. P.; Bobrowicz, F. W.; Rohlfing, C. M.;

- Kahn, L. R.; Defrees, D. J.; Seeger, R.; Whiteside, R. A.; Fox, D. J.; Fleuder, E. M.; Pople, J. A. *Gaussian 86*; Carnegie-Mellon Quantum Chemistry Publishing Unit: Pittsburgh, PA, 1984; Revision C.
- 9 Frisch, M. J.; Head-Gordon, M; Trucks, G. W; Foresman, J. B.; Schlegel, H. B.; Ragavachari, K.; Robb, M. A.; Binkley, J. S.; Gonzalez, C.; Defrees, D. J.; Fox, D. J.; Whiteside, R. A.; Seeger, R.; Melius, C. F.; Baker, J.; Martin, R. L.; Kahn, L. R.; Stewart, J. J. P.; Topiol, S.; Pople, J. A. *Gaussian Inc.*; Pittsburgh, PA, 1990.
- 10 Schlegel, H. B., *J. Chem. Phys.* **1986**, 84(8), 4530.
- 11 Oxygen charges were -0.338 for 1.5A and -0.348 for ethoxy radical at the UHF/6-31G* level.
- 12 Hehre, W. J.; Radom, L.; Schleyer, P. v. R.; Pople, J. A. *Ab Initio Molecular Orbital Theory*; John Wiley & Sons: New York, 1986, pp 272-279.
- 13 Cook, M.; Hares, O.; Johns, A.; Murphy, J. A.; Patterson, C. W. *J. Chem. Soc., Chem. Commun.*, **1986**, 1419-1420.
- 14 Stogryn, E. L.; Gianni, M. H. *Tetrahedron Lett.* **1970**, 34, 3025-3028.
- 15 Fleming, I. *Frontier Orbitals and Organic Chemical Reactions*; Wiley: London, 1976, Chap. 5

Table 1.2. Calculated Geometries (UHF/6-31G*) of Initial Substituted Radicals (1.1)

| X | Y | rC ₁ C ₂ | rC ₂ C ₃ | rC ₂ O | rC ₃ O | τCCCO | τCCOC |
|-----------------|-----------------|--------------------------------|--------------------------------|-------------------|-------------------|--------|-------|
| H | H | 1.470 | 1.464 | 1.412 | 1.398 | -130.5 | 113.3 |
| NH ₂ | H | 1.469 | 1.453 | 1.428 | 1.400 | -105.2 | 122.8 |
| CN | H | 1.479 | 1.462 | 1.403 | 1.400 | -102.5 | 112.3 |
| BH ₂ | H | 1.457 | 1.467 | 1.412 | 1.394 | -104.0 | 111.8 |
| H | H | 1.470 | 1.464 | 1.412 | 1.398 | -130.5 | 113.3 |
| H | NH ₂ | — | — | — | — | — | — |
| H | CN | 1.468 | 1.474 | 1.408 | 1.391 | -104.2 | 112.1 |
| H | BH ₂ | 1.467 | 1.500 | 1.387 | 1.419 | -105.5 | 111.5 |

Table 1.3. Calculated Geometries (UHF/6-31G*) of Transition Structures for CC Bond Cleavage (1.2)

| X | Y | rC ₁ C ₂ | rC ₂ C ₃ | rC ₂ O | rC ₃ O | τCCCO | τCCOC |
|-----------------|-----------------|--------------------------------|--------------------------------|-------------------|-------------------|--------|-------|
| H | H | 1.383 | 1.814 | 1.380 | 1.375 | -106.6 | 104.9 |
| NH ₂ | H | 1.386 | 1.827 | 1.378 | 1.378 | -103.8 | 107.7 |
| CN | H | 1.388 | 1.842 | 1.371 | 1.377 | -105.9 | 103.6 |
| BH ₂ | H | 1.389 | 1.826 | 1.378 | 1.372 | -109.0 | 101.6 |
| H | H | 1.383 | 1.814 | 1.380 | 1.375 | -106.6 | 104.9 |
| H | NH ₂ | — | — | — | — | — | — |
| H | CN | 1.393 | 1.767 | 1.383 | 1.371 | -106.8 | 104.5 |
| H | BH ₂ | 1.400 | 1.760 | 1.369 | 1.393 | -109.0 | 102.2 |

Table 1.4. Calculated Geometries (UHF/6-31G*) of Transition Structures for CO Bond Cleavage (1.4)

| X | Y | rC ₁ C ₂ | rC ₂ C ₃ | rC ₂ O | rC ₃ O | τCCCO | τCCOC |
|-----------------|-----------------|--------------------------------|--------------------------------|-------------------|-------------------|-------|-------|
| H | H | 1.412 | 1.468 | 1.637 | 1.372 | -95.5 | 114.6 |
| NH ₂ | H | 1.410 | 1.461 | 1.671 | 1.374 | -98.1 | 113.5 |
| CN | H | 1.416 | 1.470 | 1.698 | 1.371 | -92.9 | 114.6 |
| BH ₂ | H | 1.419 | 1.474 | 1.695 | 1.369 | -92.4 | 116.0 |
| H | H | 1.412 | 1.468 | 1.637 | 1.372 | -95.5 | 114.6 |
| H | NH ₂ | — | — | — | — | — | — |
| H | CN | 1.410 | 1.471 | 1.684 | 1.364 | -96.3 | 113.3 |
| H | BH ₂ | 1.406 | 1.487 | 1.691 | 1.384 | -96.3 | 113.9 |

Table 1.5. Calculated Geometries (UHF/6-31G*) of Substituted Product Radicals 1.3 from CC Bond Cleavage

| X | Y | rC ₁ C ₂ | rC ₂ C ₃ | rC ₂ O | rC ₃ O | τCCCO | τCCOC |
|-----------------|-----------------|--------------------------------|--------------------------------|-------------------|-------------------|-------|-------|
| H | H | 1.317 | 2.327 | 1.352 | 1.355 | -2.0 | 178.9 |
| NH ₂ | H | 1.317 | 2.310 | 1.370 | 1.356 | -77.0 | 126.2 |
| CN | H | 1.332 | 2.325 | 1.332 | 1.362 | -3.6 | 178.0 |
| BH ₂ | H | 1.336 | 2.325 | 1.335 | 1.361 | -3.0 | 178.5 |
| H | H | 1.317 | 2.327 | 1.352 | 1.355 | -2.0 | 178.9 |
| H | NH ₂ | 1.320 | 2.372 | 1.351 | 1.368 | -40.8 | 155.1 |
| H | CN | 1.316 | 2.326 | 1.361 | 1.338 | 0.0 | 180.0 |
| H | BH ₂ | 1.319 | 2.339 | 1.356 | 1.339 | 0.0 | 180.0 |

Table 1.6. Calculated Geometries (UHF/6-31G*) of Substituted Product Radicals 1.5 from CO Bond Cleavage

| X | Y | rC ₁ C ₂ | rC ₂ C ₃ | rC ₂ O | rC ₃ O | τCCCO | τCCOC |
|-----------------|-----------------|--------------------------------|--------------------------------|-------------------|-------------------|--------|-------|
| H | H | 1.320 | 1.502 | 2.404 | 1.387 | -129.7 | 76.7 |
| NH ₂ | H | 1.323 | 1.498 | 2.407 | 1.390 | 122.3 | -82.6 |
| CN | H | 1.336 | 1.500 | 2.395 | 1.383 | -132.8 | 73.0 |
| BH ₂ | H | 1.335 | 1.508 | 2.420 | 1.382 | -180.0 | 0.0 |
| H | H | 1.320 | 1.502 | 2.404 | 1.387 | -129.7 | 76.7 |
| H | NH ₂ | 1.324 | 1.507 | 2.292 | 1.397 | -105.9 | 100.5 |
| H | CN | 1.318 | 1.512 | 2.372 | 1.382 | 125.4 | -83.7 |
| H | BH ₂ | 1.322 | 1.521 | 2.400 | 1.369 | 164.8 | -30.0 |

Table 1.7. Total Energies for 1.1B-1.5B (Amino Group on α -Methyl)*

| Basis Set (//UHF/6-31G*) | Initial radical 1.1B | Transition states | | Final radicals | |
|-----------------------------|-------------------------|-------------------|------------|----------------|------------|
| | | 1.2B | 1.4B | 1.3B | 1.5B |
| UHF/6-31G* | -246.30598 | -246.27885 | -246.29731 | -246.30714 | -246.33213 |
| MP2/6-31G* | -247.01018 | -246.96990 | -246.99718 | -247.00291 | -247.00782 |
| MP3/6-31G* | -247.03922 | -247.00217 | -247.02787 | -247.03420 | -247.04665 |
| MP4/6-31G* | -247.07277 | -247.03723 | -247.06439 | -247.06798 | -247.07791 |
| PUHF/6-31G* | -246.30970 | -246.29724 | -246.31222 | -246.30988 | -246.33556 |
| PMP2/6-31G* | -247.01258 | -246.98566 | -247.00942 | -247.00468 | -247.01027 |
| PMP3/6-31G* | -247.04065 | -247.01413 | -247.03632 | -247.03530 | -247.04831 |
| PMP4/6-31G* | -247.07420 | -247.04920 | -247.07285 | -247.06908 | -247.07956 |
| Zero-point energies | 0.09595 | 0.09260 | 0.09454 | 0.09500 | 0.09654 |
| Thermal energies | 0.10171 | 0.09810 | 0.09996 | 0.10109 | 0.10212 |

* All values are in hartrees

Table 1.8. Total Energies for 1.1C-1.5C (Cyano Group on α -Methyl)*

| Basis Set (//UHF/6-31G*) | Initial radical | | Transition states | | Final radicals | |
|-----------------------------|-----------------|------------|-------------------|------------|----------------|--|
| | 1.1C | 1.2C | 1.4C | 1.3C | 1.5C | |
| UHF/6-31G* | -283.02536 | -282.99617 | -283.01027 | -283.02350 | -283.03683 | |
| MP2/6-31G* | -283.82154 | -283.78431 | -283.79749 | -283.82242 | -283.81468 | |
| MP3/6-31G* | -283.84682 | -283.81003 | -283.82511 | -283.84389 | -283.84548 | |
| MP4/6-31G* | -283.89517 | -283.86008 | -283.87662 | -283.89371 | -283.89245 | |
| PUHF/6-31G* | -283.04295 | -283.02432 | -283.04191 | -283.03163 | -283.04586 | |
| PMP2/6-31G* | -283.83622 | -283.80905 | -283.82495 | -283.82951 | -283.82268 | |
| PMP3/6-31G* | -283.85709 | -283.82931 | -283.84582 | -283.84917 | -283.85151 | |
| PMP4/6-31G* | -283.90545 | -283.87936 | -283.89733 | -283.89899 | -283.89848 | |
| Zero-point energies | 0.07596 | 0.07246 | 0.07418 | 0.07457 | 0.06946 | |
| Thermal energies | 0.08166 | 0.07813 | 0.07917 | 0.08098 | 0.07428 | |

*All values are in hartrees

Table 1.2. Total Energies for 1.1D-1.5D (Boron Group on α -Methyl)*

| Basis Set (//UHF/6-31G*) | Initial radical | | Transition states | | Final radicals | |
|-----------------------------|-----------------|------------|-------------------|------------|----------------|--|
| | 1.1D | 1.2D | 1.4D | 1.3D | 1.5D | |
| UHF/6-31G* | -216.54558 | -216.52021 | -216.53184 | -216.55158 | -216.56075 | |
| MP2/6-31G* | -217.15529 | -217.11975 | -217.13092 | -217.15494 | -217.13999 | |
| MP3/6-31G* | -217.18909 | -217.15541 | -217.16784 | -217.18824 | -217.18370 | |
| MP4/6-31G* | -217.22034 | -217.18895 | -217.20232 | -217.22184 | -217.21350 | |
| PUHF/6-31G* | -216.54862 | -216.53626 | -216.54912 | -216.55510 | -216.56691 | |
| PMP2/6-31G* | -217.15706 | -217.13346 | -217.14548 | -217.15772 | -217.14456 | |
| PMP3/6-31G* | -217.19016 | -217.16567 | -217.17830 | -217.19020 | -217.18710 | |
| PMP4/6-31G* | -217.22141 | -217.19915 | -217.21278 | -217.22380 | -217.21689 | |
| Zero-point energies | 0.09010 | 0.08637 | 0.08802 | 0.08801 | 0.08853 | |
| Thermal energies | 0.09550 | 0.09180 | 0.09337 | 0.09419 | 0.09442 | |

* All values are in hartrees

Table 1.10. Total Energies for 1.1C'-1.5C' (Cyano Group on Epoxide Ring)*

| Basis Set (//UHF/6-31G*) | Initial radical | | Transition states | | Final radicals | |
|-----------------------------|-----------------|------------|-------------------|------------|----------------|--|
| | 1.1C' | 1.2C' | 1.4C' | 1.3C' | 1.5C' | |
| UHF/6-31G* | -283.00866 | -282.99202 | -283.99737 | -283.02699 | -283.02694 | |
| MP2/6-31G* | -283.81949 | -283.78740 | -283.80039 | -283.81753 | -283.81122 | |
| MP3/6-31G* | -283.83818 | -283.81092 | -283.82181 | -283.84479 | -283.84078 | |
| MP4/6-31G* | -283.88696 | -283.86190 | -283.87359 | -283.89464 | -283.88760 | |
| PUHF/6-31G* | -283.01266 | -283.01674 | -283.01454 | -283.04594 | -283.03127 | |
| PMP2/6-31G* | -283.88226 | -283.80879 | -283.81467 | -283.83365 | -283.81474 | |
| PMP3/6-31G* | -283.83992 | -283.82713 | -283.83193 | -283.85641 | -283.84331 | |
| PMP4/6-31G* | -283.88870 | -283.87811 | -283.88371 | -283.90627 | -283.89013 | |
| Zero-point energies | 0.07508 | 0.07250 | 0.07403 | 0.07352 | 0.07508 | |
| Thermal energies | 0.08104 | 0.07807 | 0.07953 | 0.08018 | 0.08104 | |

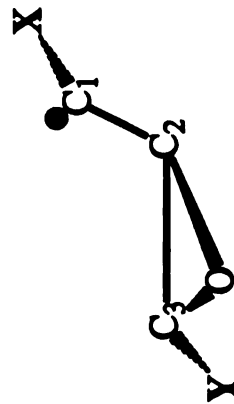
*All values are in hartrees

Table 1.11. Total Energies for 1.1D'-1.5D' (Boron Group on Epoxide Ring)*

| Basis Set (//UHF/6-31G*) | Initial radical 1.1D | Transition states | | Final radicals | |
|-----------------------------|-------------------------|-------------------|-------------|----------------|-------------|
| | | 1.2D' | 1.4D' | 1.3D' | 1.5D' |
| UHF/6-31G* | -216.530342 | -216.520968 | -216.514899 | -216.559535 | -216.855187 |
| MP2/6-31G* | -217.140546 | -217.126000 | -217.114339 | -217.165321 | -217.139837 |
| MP3/6-31G* | -217.173157 | -217.160355 | -217.150715 | -217.200607 | -217.181694 |
| MP4/6-31G* | -217.205304 | -217.194466 | -217.185618 | -217.234439 | -217.212494 |
| PUHF/6-31G* | -216.534413 | -216.536167 | -216.533351 | -216.564508 | -216.554414 |
| PMP2/6-31G* | -217.143390 | -217.138782 | -217.129762 | -217.169505 | -217.142042 |
| PMP3/6-31G* | -217.174986 | -217.169755 | -217.161742 | -217.203634 | -217.183050 |
| PMP4/6-31G* | -217.207134 | -217.203866 | -217.196645 | -217.237467 | -217.213850 |
| Zero-point energies | 0.08710 | 0.08620 | 0.08576 | 0.08863 | 0.08875 |
| Thermal energies | 0.09298 | 0.09150 | 0.09133 | 0.09459 | 0.09453 |

* All values are in hartrees

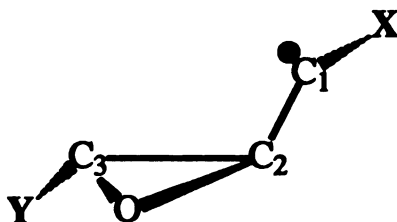
Table 1.12. Reaction Barriers and Heats of Reactions for Ring-Openings of Substituted α -Epoxyethyl Radicals



| Substituents | | Transition States (ΔE_a)* | | | Final Radicals (ΔE_{rxn})* | | |
|-----------------|-----------------|-------------------------------------|-----|---------------------|--------------------------------------|------|-------------------------|
| X | Y | BCC | BCO | $\Delta \Delta E_a$ | BCC | BCO | $\Delta \Delta E_{rxn}$ |
| H | H | 13.3 | 2.5 | 10.8 | -1.9 | -3.4 | 1.5 |
| NH ₂ | H | 15.7 | 0.8 | 14.9 | 3.2 | -3.4 | 6.6 |
| CN | H | 16.4 | 5.1 | 10.3 | 4.1 | 4.4 | -0.3 |
| BH ₂ | H | 14.0 | 5.4 | 8.6 | -1.5 | 2.8 | -4.3 |
| H | NH ₂ | — | — | — | — | — | — |
| H | CN | 6.6 | 3.1 | 3.5 | -11.0 | -0.9 | -10.1 |
| H | BH ₂ | 2.3 | 6.6 | -4.3 | -19.0 | -4.2 | -14.8 |

* PMP4/6-31G**/UHF/6-31G*

* All values are in kcal/mol

Table 1.13. Heats of Reaction for Ring-Opening of Various Substituted α -Epoxyethyl Radicals

| Substituents | | Final Radicals (ΔE_{rxn})* | | | |
|------------------------------|------------------------------|---|-------|--------------------------------|----------------------------------|
| X | Y | BCC | BCO | $\Delta \Delta E_{\text{rxn}}$ | $\Delta \Delta E_{\text{rel}}$ † |
| H | H | -15.7 | -26.1 | 10.4 | (0.0) |
| CN | H | -9.5 | -20.8 | 11.3 | 0.9 |
| BH ₂ | H | -16.4 | -24.1 | 7.7 | -2.7 |
| CNH [⊕] | H | -22.3 | -25.5 | 3.2 | -7.2 |
| CH ₂ [⊕] | H | — | — | -17.6‡ | -27.6 |
| NH ₃ [⊕] | H | -21.9 | -33.2 | 11.3 | 0.9 |
| NH ₂ | H | — | — | — | — |
| CH ₃ | H | -15.2 | -29.0 | 13.8 | 3.4 |
| BH ₃ [⊖] | H | -15.0 | -28.3 | 13.3 | 2.9 |
| H | CN | -24.4 | -26.2 | -1.8 | -12.2 |
| H | BH ₂ | -29.2 | -27.2 | -2.0 | -12.4 |
| H | CNH [⊕] | -35.4 | -26.2 | -9.2 | -19.6 |
| H | CH ₂ [⊕] | — | — | -13.4‡ | -23.8 |
| H | NH ₃ [⊕] | — | — | 13.4‡ | 3.0 |
| H | NH ₂ | — | — | 13.4‡ | 3.0 |
| H | CH ₃ | -9.6 | -27.2 | 17.6 | 7.2 |
| H | CH ₂ [⊖] | — | — | 5.0‡ | -5.4 |
| H | BH ₃ [⊖] | -19.9 | -32.1 | 12.2 | 1.8 |

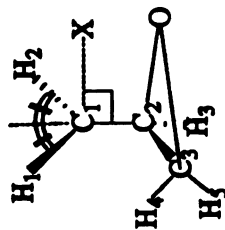
* UHF/3-21G//UHF/3-21G

* All values are in kcal/mol

† Energy difference between $\Delta \Delta E_{\text{rxn}}$ for the substituted case and $\Delta \Delta E_{\text{rxn}}$ (X = Y = H)

‡ Note that in these cases, no minimum could be located for the starting radical 1.1.

Appendix 1.1. Geometrical Parameters for Parent Radicals (Figure 1.1)



| Structure | 1.1A | | | | 1.2A | | | | 1.4A | | | |
|--|--------|--------|--------|--------|--------|--------|--------|--------|-------|-------|--------|--------|
| | 3-21G | | 6-31G* | | 3-21G | | 6-31G* | | 3-21G | | 6-31G* | |
| Variable | UHF | UMP2 | UHF | UMP2 | UHF | UMP2 | UHF | UMP2 | UHF | UMP2 | UHF | UMP2 |
| rC ₁ C ₂ | 1.452 | 1.467 | 1.470 | 1.459 | 1.390 | 1.362 | 1.383 | 1.344 | 1.434 | 1.379 | 1.412 | 1.355 |
| rC ₂ C ₃ | 1.482 | 1.507 | 1.464 | 1.479 | 1.795 | 1.866 | 1.814 | 1.867 | 1.480 | 1.503 | 1.468 | 1.489 |
| rC ₂ O | 1.517 | 1.525 | 1.412 | 1.454 | 1.442 | 1.476 | 1.380 | 1.405 | 1.586 | 1.774 | 1.673 | 1.827 |
| rC ₃ O | 1.462 | 1.518 | 1.398 | 1.432 | 1.437 | 1.469 | 1.375 | 1.400 | 1.456 | 1.474 | 1.372 | 1.383 |
| rC ₁ H ₁ | 1.072 | 1.083 | 1.074 | 1.082 | 1.071 | 1.083 | 1.074 | 1.083 | 1.072 | 1.084 | 1.074 | 1.084 |
| rC ₁ H ₂ | 1.071 | 1.081 | 1.073 | 1.081 | 1.071 | 1.082 | 1.073 | 1.082 | 1.071 | 1.083 | 1.074 | 1.083 |
| rC ₂ H ₃ | 1.071 | 1.086 | 1.078 | 1.090 | 1.070 | 1.084 | 1.075 | 1.088 | 1.070 | 1.082 | 1.072 | 1.083 |
| rC ₃ H ₄ | 1.072 | 1.085 | 1.077 | 1.089 | 1.069 | 1.081 | 1.074 | 1.083 | 1.073 | 1.090 | 1.082 | 1.096 |
| rC ₃ H ₅ | 1.072 | 1.085 | 1.078 | 1.089 | 1.070 | 1.083 | 1.075 | 1.086 | 1.073 | 1.089 | 1.081 | 1.095 |
| ∠C ₁ C ₂ H ₃ | 117.7 | 117.5 | 115.7 | 116.8 | 122.6 | 123.0 | 121.6 | 122.6 | 118.6 | 120.6 | 119.0 | 121.0 |
| ∠H ₁ C ₁ H ₂ | 119.0 | 119.5 | 119.3 | 119.2 | 119.3 | 118.6 | 118.9 | 118.7 | 118.6 | 117.4 | 118.0 | 117.5 |
| ∠C ₁ C ₂ O | 115.0 | 115.0 | 116.8 | 116.0 | 119.7 | 121.0 | 121.3 | 122.0 | 114.3 | 111.9 | 114.0 | 110.8 |
| ∠C ₁ C ₂ C ₃ | 120.9 | 120.3 | 122.5 | 121.9 | 118.6 | 118.9 | 120.6 | 120.9 | 121.6 | 122.5 | 123.5 | 122.5 |
| ∠C ₂ C ₃ O | 62.0 | 60.6 | 62.8 | 58.4 | 51.6 | 50.9 | 48.9 | 48.4 | 65.4 | 73.0 | 72.0 | 78.9 |
| ∠C ₃ OC ₂ | 59.6 | 59.4 | 58.0 | 61.6 | 77.0 | 78.6 | 82.4 | 83.5 | 58.0 | 54.2 | 56.6 | 53.0 |
| ∠OC ₂ C ₃ | 58.3 | 60.6 | 59.0 | 59.9 | 51.3 | 50.5 | 48.7 | 48.0 | 56.6 | 52.7 | 51.3 | 48.0 |
| ∠H ₄ C ₃ H ₅ | 115.9 | 116.3 | 115.2 | 115.6 | 119.3 | 121.4 | 120.2 | 121.2 | 115.2 | 113.6 | 112.8 | 112.0 |
| ∠C ₁ C ₂ C ₃ O | -102.2 | -103.0 | -103.5 | -103.0 | -106.7 | -108.0 | -106.6 | -107.0 | -99.9 | -94.0 | -95.5 | -89.6 |
| ∠C ₁ C ₂ OC ₃ | 112.2 | 102.0 | 113.3 | 112.9 | 104.4 | 103.5 | 104.9 | 104.6 | 113.0 | 115.0 | 114.6 | 115.6 |
| ∠XC ₁ C ₂ O | 43.7 | 63.2 | 62.2 | 61.0 | 83.9 | 85.2 | 84.4 | 86.1 | 35.2 | 30.9 | 33.0 | 33.8 |
| ∠H ₁ C ₁ C ₂ H ₂ | 172.6 | -178.2 | 176.4 | 176.9 | -176.7 | -177.8 | 175.4 | 178.2 | 171.9 | 176.0 | 173.4 | -178.4 |
| ∠H ₃ C ₂ C ₃ O | 100.5 | 103.2 | 102.2 | 102.0 | 107.5 | 109.7 | 108.7 | 111.5 | 97.3 | 90.2 | 90.9 | 86.8 |
| ∠H ₁ C ₁ C ₂ H ₃ | -178.7 | -165.4 | -167.3 | -168.3 | -167.6 | -172.0 | -171.0 | -174.0 | 176.3 | 177.4 | 178.0 | -179.0 |

| Structure Variable | 1.3A | | | | 1.5A | | | |
|--|--------|------|--------|--------|--------|------|--------|--------|
| | 3-21G | | 6-31G* | | 3-21G | | 6-31G* | |
| | UHF | UMP2 | UHF | UMP2 | UHF | UMP2 | UHF | UMP2 |
| rC ₁ C ₂ | 1.314 | | 1.317 | 1.320 | 1.316 | | 1.320 | 1.312 |
| rC ₂ C ₃ | 2.404 | | 2.327 | 2.316 | 1.510 | | 1.502 | 1.502 |
| rC ₂ O | 1.380 | | 1.352 | 1.382 | 2.411 | | 2.404 | 2.420 |
| rC ₃ O | 1.386 | | 1.355 | 1.377 | 1.456 | | 1.387 | 1.390 |
| rC ₁ H ₁ | 1.070 | | 1.074 | 1.083 | 1.074 | | 1.077 | 1.087 |
| rC ₁ H ₂ | 1.070 | | 1.073 | 1.082 | 1.073 | | 1.075 | 1.084 |
| rC ₂ H ₃ | 1.074 | | 1.076 | 1.089 | 1.074 | | 1.078 | 1.088 |
| rC ₃ H ₄ | 1.069 | | 1.077 | 1.087 | 1.082 | | 1.087 | 1.100 |
| rC ₃ H ₅ | 1.074 | | 1.072 | 1.081 | 1.082 | | 1.091 | 1.104 |
| ∠C ₁ C ₂ H ₃ | 123.0 | | 122.7 | 123.6 | 120.6 | | 120.5 | 121.1 |
| ∠H ₁ C ₁ H ₂ | 118.6 | | 118.6 | 118.8 | 116.4 | | 116.5 | 116.4 |
| ∠C ₁ C ₂ O | 121.5 | | 122.0 | 121.4 | 137.0 | | 139.0 | 138.6 |
| ∠C ₁ C ₂ C ₃ | 151.0 | | 152.9 | 150.6 | 123.9 | | 124.0 | 123.3 |
| ∠C ₂ C ₃ O | 29.6 | | 30.7 | 33.0 | 108.7 | | 112.6 | 113.5 |
| ∠C ₃ OC ₂ | 120.7 | | 118.5 | 114.2 | 36.4 | | 35.2 | 34.7 |
| ∠OC ₂ C ₃ | 29.7 | | 30.8 | 32.9 | 34.9 | | 32.2 | 31.8 |
| ∠H ₄ C ₃ H ₅ | 121.2 | | 119.6 | 120.2 | 109.6 | | 107.2 | 106.3 |
| ∠C ₁ C ₂ C ₃ O | 7.9 | | -2.0 | 37.7 | -125.4 | | -129.7 | -130.2 |
| ∠C ₁ C ₂ OC ₃ | -175.5 | | 178.9 | -159.4 | 83.7 | | 76.7 | 75.1 |
| ∠XC ₁ C ₂ O | -89.5 | | -90.0 | -87.5 | 48.2 | | 52.4 | 53.7 |
| ∠H ₁ C ₁ C ₂ H ₂ | 180.0 | | 180.0 | -180.0 | 180.0 | | 180.0 | 179.7 |
| ∠H ₃ C ₂ C ₃ O | -175.6 | | 179.0 | -159.6 | 55.6 | | 50.5 | 49.7 |
| ∠H ₁ C ₁ C ₂ H ₃ | -180.0 | | 180.0 | 180.0 | -180.0 | | -179.5 | -179.2 |

Appendix 1.2. Cartesian Coordinates for Figure 1.3.**1.1B**

| | | | |
|---|-----------|-----------|-----------|
| O | 1.071732 | -1.285583 | 0.834793 |
| C | 0.278564 | -0.671371 | -0.181870 |
| C | 1.730026 | -0.684174 | -0.243546 |
| C | -0.487915 | 0.531235 | 0.169479 |
| H | 0.018555 | 1.416916 | 0.508240 |
| N | -1.854080 | 0.393555 | 0.435257 |
| H | -0.256653 | -1.390808 | -0.780548 |
| H | 2.280991 | 0.211060 | -0.004990 |
| H | 2.234268 | -1.359300 | -0.914780 |
| H | -2.254929 | 1.170853 | 0.914764 |
| H | -2.105850 | -0.458694 | 0.895355 |

1.2B

| | | | |
|---|-----------|-----------|-----------|
| O | 1.213654 | -1.171478 | 1.059860 |
| C | 0.118149 | -0.715424 | 0.358795 |
| C | 1.903214 | -0.677353 | -0.026321 |
| C | -0.563080 | 0.411789 | 0.789810 |
| H | -0.142303 | 1.022964 | 1.565811 |
| N | -1.656281 | 0.955093 | 0.099289 |
| H | -0.337250 | -1.427994 | -0.307236 |
| H | 2.405136 | 0.261246 | 0.118179 |
| H | 2.310700 | -1.406616 | -0.704117 |
| H | -2.310700 | 1.406631 | 0.704117 |
| H | -2.138107 | 0.291977 | -0.473114 |

1.4B

| | | | |
|---|-----------|-----------|-----------|
| O | 1.182678 | -1.144012 | 1.116104 |
| C | 0.317902 | -0.522400 | -0.171143 |
| C | 1.765976 | -0.546112 | 0.024796 |
| C | -0.487808 | 0.598465 | 0.114288 |
| H | -0.052795 | 1.507141 | 0.484009 |
| N | -1.876068 | 0.578064 | -0.011002 |
| H | -0.123810 | -1.360229 | -0.676254 |
| H | 2.261307 | 0.397095 | 0.217560 |
| H | 2.350662 | -1.196854 | -0.611633 |
| H | -2.350677 | 1.196854 | 0.611633 |
| H | -2.281600 | -0.333679 | 0.033234 |

1.3B

| | | | |
|---|-----------|-----------|-----------|
| O | 1.172653 | -0.508438 | -0.372345 |
| C | -0.042100 | 0.076965 | -0.614990 |
| C | 2.184570 | 0.338486 | -0.058380 |
| C | -1.119431 | -0.310944 | 0.036057 |
| H | -1.032745 | -1.080887 | 0.781250 |
| N | -2.403015 | 0.232742 | -0.103729 |
| H | -0.044205 | 0.841934 | -1.372650 |
| H | 1.938660 | 1.191879 | 0.551010 |
| H | 3.118271 | -0.169098 | 0.090439 |
| H | -3.118256 | -0.464676 | -0.127533 |
| H | -2.497650 | 0.834229 | -0.896300 |

1.5B

| | | | |
|---|-----------|-----------|-----------|
| O | -2.574753 | -0.506943 | 0.835007 |
| C | -0.337845 | 0.191376 | 0.286377 |
| C | -1.713837 | -0.150436 | -0.196762 |
| C | 0.746552 | -0.437408 | -0.138229 |
| H | 0.657928 | -1.243744 | -0.847290 |
| N | 2.063629 | -0.125854 | 0.180008 |
| H | -0.262512 | 0.992630 | 1.004150 |
| H | -1.686188 | -0.932220 | -0.952316 |
| H | -2.202728 | 0.712784 | -0.651154 |
| H | 2.668121 | -0.916840 | 0.244751 |
| H | 2.166840 | 0.467743 | 0.976227 |

Appendix 1.3. Cartesian Coordinates for Figure 1.4.**1.1C**

| | | | |
|---|-----------|-----------|-----------|
| O | -0.702530 | -1.042618 | 1.151108 |
| C | 0.004349 | -0.554703 | 0.042068 |
| C | -1.456696 | -0.617004 | 0.052322 |
| C | 0.715759 | 0.724000 | 0.256058 |
| H | 0.368759 | 1.395432 | 1.018677 |
| C | 1.803650 | 1.102646 | -0.529022 |
| N | 2.707367 | 1.408752 | -1.185730 |
| H | 0.543533 | -1.301666 | -0.514954 |
| H | -2.028763 | 0.281830 | 0.206238 |
| H | -1.955643 | -1.396729 | -0.496811 |

1.2C

| | | | |
|---|-----------|-----------|-----------|
| O | -1.319611 | -1.008636 | 1.752502 |
| C | -0.256882 | -0.602783 | 0.987808 |
| C | -2.073502 | -0.573212 | 0.686264 |
| C | 0.399902 | 0.585236 | 1.278275 |
| H | 0.026657 | 1.237640 | 2.044662 |
| C | 1.542007 | 0.994476 | 0.549683 |
| N | 2.471558 | 1.328918 | -0.035065 |
| H | 0.165848 | -1.338364 | 0.329346 |
| H | -2.566040 | 0.372925 | 0.802124 |
| H | -2.471558 | -1.328918 | 0.035065 |

1.4C

| | | | |
|---|-----------|-----------|-----------|
| O | -1.435760 | -0.925354 | 1.590897 |
| C | -0.626617 | -0.277863 | 0.245789 |
| C | -2.070358 | -0.412918 | 0.488480 |
| C | 0.090652 | 0.897064 | 0.577667 |
| H | -0.402176 | 1.715897 | 1.067017 |
| C | 1.473312 | 1.018890 | 0.336868 |
| N | 2.599136 | 1.132309 | 0.120132 |
| H | -0.120453 | -1.078018 | -0.254990 |
| H | -2.635620 | 0.493591 | 0.656342 |
| H | -2.599136 | -1.132309 | -0.120148 |

1.3C

| | | | |
|---|-----------|-----------|-----------|
| C | 2.134613 | 0.188950 | -0.826172 |
| C | 1.216324 | -0.253815 | 0.177704 |
| C | -0.083969 | 0.016357 | 0.071518 |
| H | 1.604935 | -0.805389 | 1.011780 |
| H | -0.490417 | 0.572205 | -0.754578 |
| O | -0.948181 | -0.399353 | 0.995880 |
| C | -2.263809 | -0.069687 | 0.875229 |
| H | -2.871017 | -0.537628 | 1.622162 |
| H | -2.641739 | 0.080353 | -0.120377 |
| N | 2.871017 | 0.537628 | -1.622162 |

1.5C

| | | | |
|---|-----------|-----------|-----------|
| C | -0.649185 | -0.442596 | 0.022690 |
| O | -1.369125 | -1.497421 | 2.048996 |
| H | -2.477432 | -0.074081 | 1.105530 |
| C | -1.796097 | -0.890060 | 0.882263 |
| H | -2.372787 | -1.659622 | 0.366882 |
| C | -0.580048 | 0.770752 | -0.531189 |
| H | 0.135071 | -1.161148 | -0.139191 |
| H | -1.343155 | 1.511063 | -0.371552 |
| C | 0.511261 | 1.169159 | -1.374756 |
| N | 1.369125 | 1.497421 | -2.048981 |

Appendix 1.4. Cartesian Coordinates for Figure 1.5.**1.1D**

| | | | |
|---|-----------|-----------|-----------|
| H | 0.303909 | -1.415176 | -0.503189 |
| C | -1.670654 | -0.702835 | 0.084915 |
| H | 0.123703 | 1.188019 | 1.121323 |
| C | -0.204544 | -0.667267 | 0.082123 |
| H | -2.225952 | 0.200226 | 0.275300 |
| O | -0.940277 | -1.196060 | 1.165024 |
| C | 0.534653 | 0.585754 | 0.325958 |
| B | 1.765366 | 1.033905 | -0.471573 |
| H | -2.182419 | -1.442383 | -0.507858 |
| H | 2.211700 | 0.335693 | -1.329224 |
| H | 2.284485 | 2.079926 | -0.242706 |

1.2D

| | | | |
|---|-----------|-----------|-----------|
| O | -1.093369 | -1.377258 | 1.124466 |
| C | -0.161102 | -0.963867 | 0.197067 |
| C | -1.985748 | -1.005219 | 0.150421 |
| C | 0.478775 | 0.265366 | 0.285416 |
| H | 0.133621 | 0.920639 | 1.069489 |
| B | 1.597641 | 0.660675 | -0.685669 |
| H | 0.183640 | -1.734970 | -0.468048 |
| H | -2.497559 | -0.073151 | 0.295578 |
| H | -2.435303 | -1.793594 | -0.425156 |
| H | 2.152298 | 1.709854 | -0.589584 |
| H | 1.928787 | -0.091415 | -1.550705 |

1.4D

| | | | |
|---|-----------|-----------|-----------|
| O | -1.474579 | -1.362778 | 0.937042 |
| C | -0.471359 | -0.638916 | -0.222061 |
| C | -1.938019 | -0.785172 | -0.214325 |
| C | 0.206894 | 0.497100 | 0.290558 |
| H | -0.416200 | 1.236282 | 0.769073 |
| B | 1.733871 | 0.677048 | 0.197266 |
| H | 0.091949 | -1.420074 | -0.693802 |
| H | -2.527374 | 0.111800 | -0.081085 |
| H | -2.364594 | -1.467056 | -0.937042 |
| H | 2.253983 | 1.670380 | 0.595428 |
| H | 2.405106 | -0.178300 | -0.290771 |

1.3D

| | | | |
|---|-----------|-----------|-----------|
| B | 2.073074 | 0.862732 | -0.773804 |
| C | 1.022522 | 0.066132 | 0.002945 |
| C | -0.272156 | 0.290009 | -0.238159 |
| H | 1.266342 | -0.675888 | 0.745544 |
| H | -0.600510 | 1.017578 | -0.961044 |
| O | -1.251190 | -0.365570 | 0.388565 |
| C | -2.545303 | -0.053391 | 0.106857 |
| H | -2.756546 | 0.322876 | -0.878433 |
| H | 3.240600 | 0.703064 | -0.597931 |
| H | -3.240585 | -0.703064 | 0.597931 |
| H | 1.723190 | 1.670029 | -1.582581 |

1.5D

| | | | |
|---|-----------|-----------|-----------|
| B | 1.961029 | 0.061234 | 0.030914 |
| C | 0.508621 | 0.250229 | -0.464264 |
| C | -0.527695 | -0.155838 | 0.272568 |
| H | 0.302872 | 0.715820 | -1.418945 |
| H | -0.362686 | -0.623962 | 1.229065 |
| C | -1.976776 | -0.017456 | -0.120377 |
| O | -2.856461 | -0.518814 | 0.820908 |
| H | -2.178970 | -0.532547 | -1.058029 |
| H | -2.239838 | 1.026184 | -0.284668 |
| H | 2.157410 | -0.455322 | 1.087494 |
| H | 2.894424 | 0.419327 | -0.617400 |

Appendix 1.5. Cartesian Coordinates for Figure 1.6.**1.1C'**

| | | | |
|---|-----------|-----------|-----------|
| O | 0.069794 | -0.786026 | 1.104553 |
| C | 0.567963 | -0.137375 | -0.041885 |
| C | -0.875504 | -0.283432 | 0.216263 |
| C | 1.264908 | 1.138763 | 0.157532 |
| H | 1.955338 | 1.498413 | -0.579926 |
| H | 1.035278 | 1.746140 | 1.012100 |
| H | 0.993744 | -0.809006 | -0.767227 |
| H | -1.445007 | 0.558731 | 0.565475 |
| C | -1.661606 | -1.266769 | -0.523102 |
| N | -2.279648 | -2.008774 | -1.118652 |

1.2C'

| | | | |
|---|-----------|-----------|-----------|
| O | -0.089310 | -0.721283 | 1.053665 |
| C | 0.715942 | -0.176163 | 0.070236 |
| C | -1.045685 | -0.245193 | 0.194763 |
| C | 1.374832 | 1.033508 | 0.278854 |
| H | 2.045090 | 1.413437 | -0.467500 |
| H | 1.162888 | 1.632080 | 1.144394 |
| H | 1.029694 | -0.865738 | -0.690933 |
| H | -1.530350 | 0.672897 | 0.460022 |
| C | -1.752000 | -1.179688 | -0.621979 |
| N | -2.300446 | -1.898926 | -1.323532 |

1.4C'

| | | | |
|---|-----------|-----------|-----------|
| O | -0.097656 | -0.665421 | 1.294861 |
| C | 0.586000 | -0.111053 | -0.140808 |
| C | -0.826981 | -0.145966 | 0.265869 |
| C | 1.392960 | 1.036179 | 0.001434 |
| H | 2.428146 | 1.010040 | -0.278992 |
| H | 1.015396 | 1.920715 | 0.478760 |
| H | 0.959686 | -0.970856 | -0.658707 |
| H | -1.318100 | 0.795273 | 0.463211 |
| C | -1.721802 | -1.082153 | -0.436417 |
| N | -2.417648 | -1.786621 | -0.989258 |

1.3C'

| | | | |
|---|-----------|-----------|-----------|
| H | 1.262085 | 1.282120 | -0.422516 |
| C | 1.275070 | 0.272705 | -0.053009 |
| C | 2.378738 | -0.367096 | 0.270782 |
| O | 0.055115 | -0.320419 | 0.063538 |
| H | 3.326920 | 0.123535 | 0.169266 |
| H | 2.356491 | -1.375946 | 0.637161 |
| C | -1.037781 | 0.371078 | -0.278107 |
| C | -2.278015 | -0.250610 | -0.152679 |
| N | -3.326920 | -0.729400 | -0.063766 |
| H | -0.946136 | 1.375931 | -0.637161 |

1.5C'

| | | | |
|---|-----------|-----------|-----------|
| C | -1.543304 | 0.690598 | -0.033630 |
| C | -0.652039 | -0.205400 | 0.750336 |
| C | 0.725647 | -0.361496 | 0.147736 |
| O | -1.226410 | -1.446381 | 0.947937 |
| H | -0.558334 | 0.223100 | 1.747177 |
| C | 1.149078 | 0.206848 | -0.963196 |
| H | 1.364670 | -1.008621 | 0.722153 |
| H | 0.528259 | 0.850540 | -1.559097 |
| H | 2.151978 | 0.040787 | -1.311096 |
| N | -2.219604 | 1.383820 | -0.623566 |

Appendix 1.6. Cartesian Coordinates for Figure 1.7.**1.1D'**

| | | | |
|---|-----------|-----------|-----------|
| H | 1.226883 | -0.817261 | -0.374985 |
| C | -0.768738 | -0.050598 | 0.195114 |
| B | -1.481110 | -1.064438 | -0.745728 |
| C | 0.731339 | -0.054900 | 0.204575 |
| H | -1.213608 | 0.909409 | 0.404007 |
| O | 0.002609 | -0.544327 | 1.278534 |
| C | 1.494125 | 1.182419 | 0.405029 |
| H | 2.286285 | 1.447479 | -0.268677 |
| H | -2.260742 | -0.674622 | -1.555817 |
| H | 1.182343 | 1.884537 | 1.154953 |
| H | -1.199265 | -2.217682 | -0.697006 |

1.2D'

| | | | |
|---|-----------|-----------|-----------|
| O | -0.137573 | -0.622314 | 1.654419 |
| C | 0.780304 | -0.186432 | 0.736923 |
| C | -0.975342 | -0.222794 | 0.614990 |
| C | 1.397888 | 1.063187 | 0.869812 |
| H | 2.172958 | 1.355850 | 0.188019 |
| H | 1.045929 | 1.772507 | 1.594650 |
| H | 1.230011 | -0.956300 | 0.137451 |
| H | -1.381866 | 0.762787 | 0.763077 |
| B | -1.445480 | -1.197723 | -0.462341 |
| H | -2.202057 | -0.819260 | -1.299210 |
| H | -1.026169 | -2.310623 | -0.487381 |

1.4D'

| | | | |
|---|-----------|-----------|-----------|
| O | -0.110809 | -0.545883 | 1.762985 |
| C | 0.724747 | -0.090408 | 0.365570 |
| C | -0.741669 | -0.100098 | 0.614273 |
| C | 1.523468 | 1.057419 | 0.509964 |
| H | 2.584396 | 1.009689 | 0.351257 |
| H | 1.106110 | 1.976517 | 0.876236 |
| H | 1.169022 | -0.985748 | -0.023666 |
| H | -1.166275 | 0.893097 | 0.715378 |
| B | -1.556213 | -1.121521 | -0.263824 |
| H | -2.179626 | -0.720596 | -1.194733 |
| H | -1.505737 | -2.285950 | -0.036438 |

1.3D'

| | | | |
|---|-----------|-----------|-----------|
| H | 3.307983 | 0.433456 | -1.061600 |
| C | 2.519730 | 0.111298 | -0.409256 |
| C | 1.262833 | 0.356979 | -0.724548 |
| H | 2.779083 | -0.408400 | 0.493637 |
| H | 0.969620 | 0.874710 | -1.620590 |
| O | 0.241592 | -0.035217 | 0.076538 |
| C | -1.026932 | 0.224396 | -0.263779 |
| B | -2.172485 | -0.210876 | 0.625946 |
| H | -1.139175 | 0.753265 | -1.197891 |
| H | -3.284439 | 0.041626 | 0.283585 |
| H | -1.962997 | -0.790710 | 1.641830 |

1.5D'

| | | | |
|---|-----------|-----------|-----------|
| H | 1.970490 | -0.476547 | -0.270920 |
| C | 0.957550 | -0.323959 | -0.596176 |
| C | -0.067841 | -0.601227 | 0.191620 |
| H | 0.824081 | 0.045563 | -1.598495 |
| H | 0.090744 | -0.964462 | 1.192535 |
| C | -1.524857 | -0.353989 | -0.168304 |
| O | -2.384933 | -1.022858 | 0.660858 |
| H | -1.727798 | -0.572205 | -1.212067 |
| B | -1.492645 | 1.204605 | 0.151230 |
| H | -1.222412 | 1.956512 | -0.725250 |
| H | -1.656357 | 1.586900 | 1.261642 |

CHAPTER 2

Low Temperature Carbene-to-Carbene Homologations

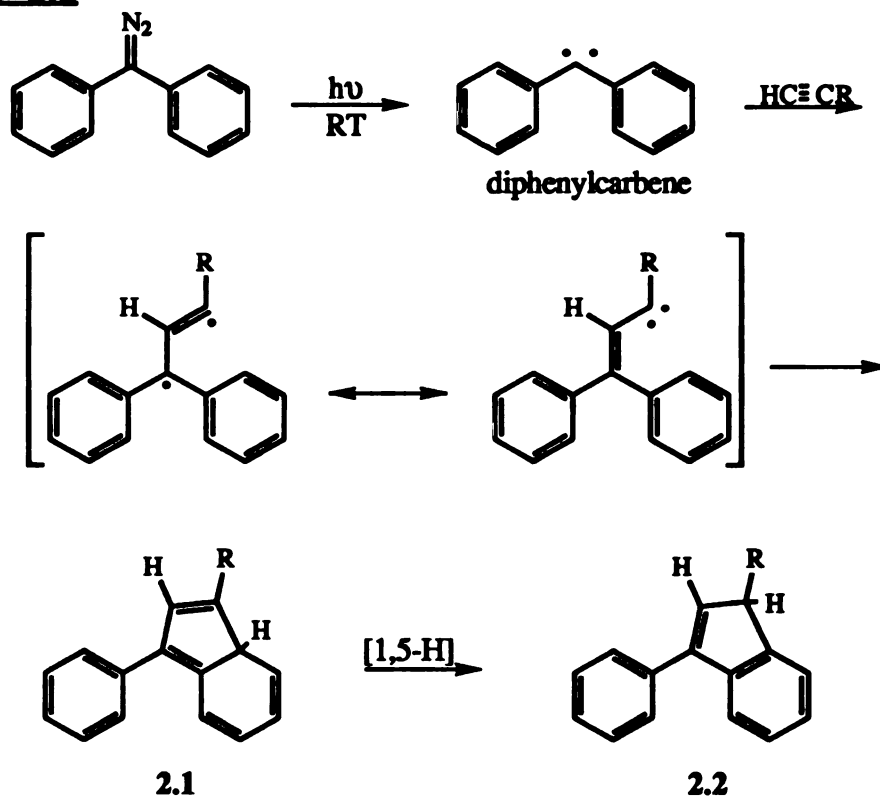
Abstract: Since alkynes have higher symmetry than olefins, it is not easy to infer the mechanism of a triplet carbene's addition to an alkyne by traditional product analysis studies. Specifically, no stereochemical information which might offer insight into the carbene's spin state can be extracted from the cyclopropene products. In 1971, Hendrick, Baron, and Jones showed that diphenylcarbene reacts with terminal alkynes in solution to produce indenenes via a "self-trapping" vinylcarbene. They also examined the diphenylcarbene reaction with disubstituted alkynes and found at most trace amounts of the "self-trapping" indene product.

In this work, we report the direct observation by organic matrix EPR of the vinylcarbenes generated from triplet fluorenylidene and terminal alkynes, our attempts at their structural confirmation by independent synthesis, and trapping the intermediate by another "self-trapping" method — halogen-migration.

2.1 Introduction:

Reactions of triplet diphenylcarbene with monosubstituted acetylenes (Scheme 2.1) were reported 20 years ago by Baron, Hendrick and Jones. They found that the addition of triplet diphenylcarbene to acetylenes went through a self-trapping 2,2-diphenylvinylcarbene, described as its 1,3-diradical resonance form, to generate the corresponding substituted phenyl indene. Furthermore, by studying deuterium isotope effects, they showed that the formation of indene proceeded via addition to the phenyl ring to give 2.1 followed by a 1,5-hydrogen shift.¹

Scheme 2.1

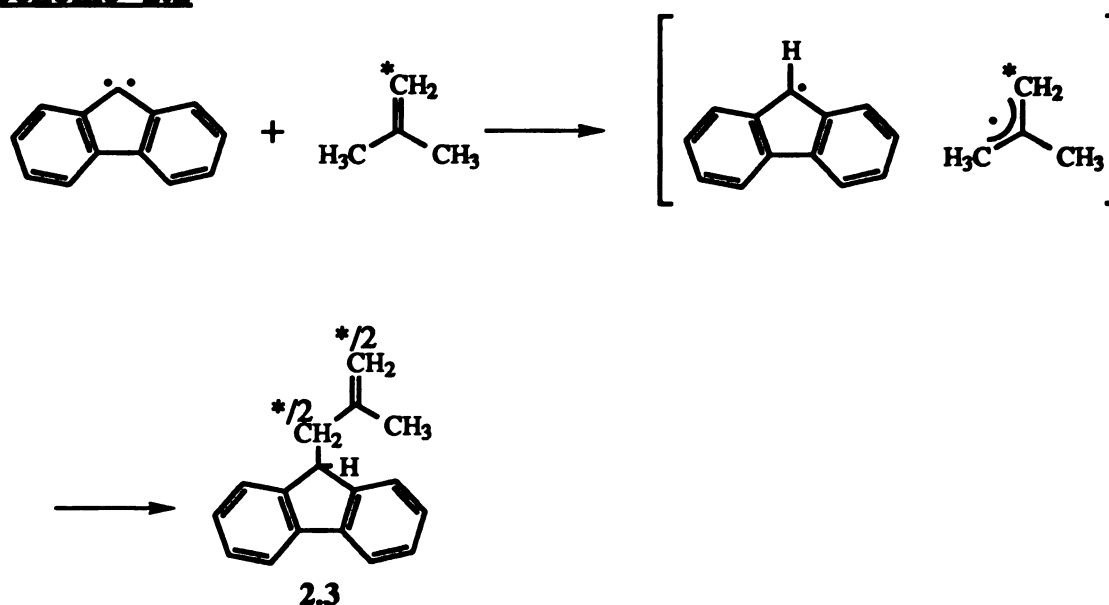


R = Ph, CH₃, *t*-Bu

Similarities in the reactivities of diphenylcarbene and fluorenylidene has drawn a lot of attention.²⁻⁶ The reactions of triplet fluorenylidene and monosubstituted acetylenes, however, have not been addressed. Diphenylcarbene and fluorenylidene are both known to have ground-state triplet multiplicities⁷, but their chemistries are quite different. The reactions of fluorenylidene in solution show more "singlet" character than the reactions of diphenylcarbene. Two arguments have been advanced to explain the differing behaviors. One is steric; fluorenylidene is planar and "tied back" but diphenylcarbene, being bent less than fluorenylidene and also twisted, may experience more steric interactions in the transition states of addition reactions.¹ The other argument centers on the equilibrium population of singlet and triplet states of fluorenylidene and diphenylcarbene. The singlet-triplet gaps of diphenylcarbene and fluorenylidene are approximately 5 kcal/mol⁷ and 1 kcal/mol,⁸ respectively. It is generally believed that the singlet and triplet states of diphenylcarbene are in rapid equilibrium before being trapped by other species. However, because of its small singlet-triplet energy gap and the greater reactivity of singlet compared to triplet carbene, the chemistry of fluorenylidene shows primarily singlet behavior. From laser flash photolysis studies of 9-diazafluorene with methanol, Schuster et al. calculated that ~ 5% or more singlet fluorenylidene is present at equilibrium at room temperature.⁸ Moss and Joyce also estimated that the ratio of singlet to triplet fluorenylidene was ~1.2 by product analysis of the reaction of fluorenylidene and cis-butene at room temperature. However, this earlier estimate was based on same flawed assumptions concerning the relative reactivities of singlet and triplet fluorenylidene.

As Grasse, Brauer, Zupancic, Kaufmann, and Schuster have pointed out, it is difficult to assign a particular chemical behavior to a specific electronic state of a carbene such as fluorenylidene, which has such a small energy difference between the lowest states. Then, if one wants to investigate the chemistry of triplet fluorenylidene, how can one be sure the species examined is the pure triplet state? At least, how can one be confident that the triplet dominates the observed chemistry?

Scheme 2.2



In 1978, Moss and Joyce convincingly demonstrated that fluorenylidene reacts with ¹³C labeled isobutene at 77 K through a triplet carbene mechanism hydrogen atom abstraction/radical recombination⁹ (Scheme 2.2). The reaction of fluorenylidene with ¹³CH₂=C(CH₃)₂ at 77 K gave fluorenylalkene (2.3) in which the label was equally distributed between C(1) and C(3). Furthermore, those workers examined the reaction of fluorenylidene with various butene isomers over a wide temperature range, from solution experiments at 0 °C down to solid

mixtures at 77 K. The yield of cyclopropane decreased dramatically in the solid phase, from ~ 85% at 273 K to ~ 20% at 77 K, but the cyclopropane stereoisomer ratio from *cis*-2-butene changed very little. They believed that the cold temperature enhanced the triplet abstraction-recombination by decreasing the reaction rate of the singlet addition and also moving the singlet - triplet equilibrium over to the triplet state. Tomioka found similar changes in the reactions of arylcarbenes with alcohols and alkanes at low temperature and showed that this phenomenon applies only to those carbenes which have triplet ground states. Later, Platz and co-workers suggested that the changing chemistry of fluorenylidene at low temperature in frozen organic matrices would be better interpreted in terms of matrix effects; he pointed out that even if singlet fluorenylidene reacts with the organic glass at a diffusion-controlled rate ($k_{\text{diff}} \approx 10^5 \text{ M}^{-1}\text{s}^{-1}$, 120 K relatively warm, soft glass), this is much too slow to compete with intersystem crossing ($k_{\text{ST}} \approx 10^{10} \text{ s}^{-1}$).^{4,10}

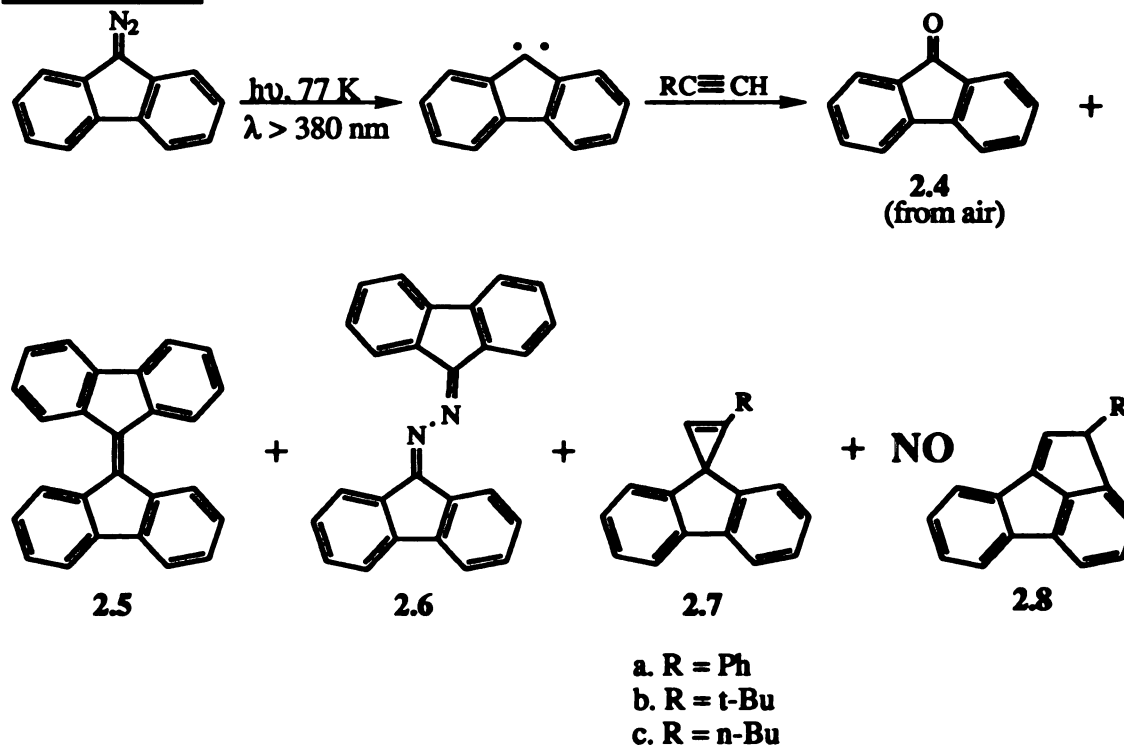
In this work we have tried to examine the reaction of triplet fluorenylidene with terminal alkynes by direct observation of organic matrix EPR and analysis of the various trapping products in low temperature glasses.

2.2 Results:

Reaction of Fluorenylidene with Phenylacetylene, 1-Hexyne and 3,3-Dimethyl-1-butyne. Degassed solutions (0.1 M) of diazofluorene in the monosubstituted acetylenes were irradiated at 77 K with light from a 500W high pressure mercury arc lamp, filtered with

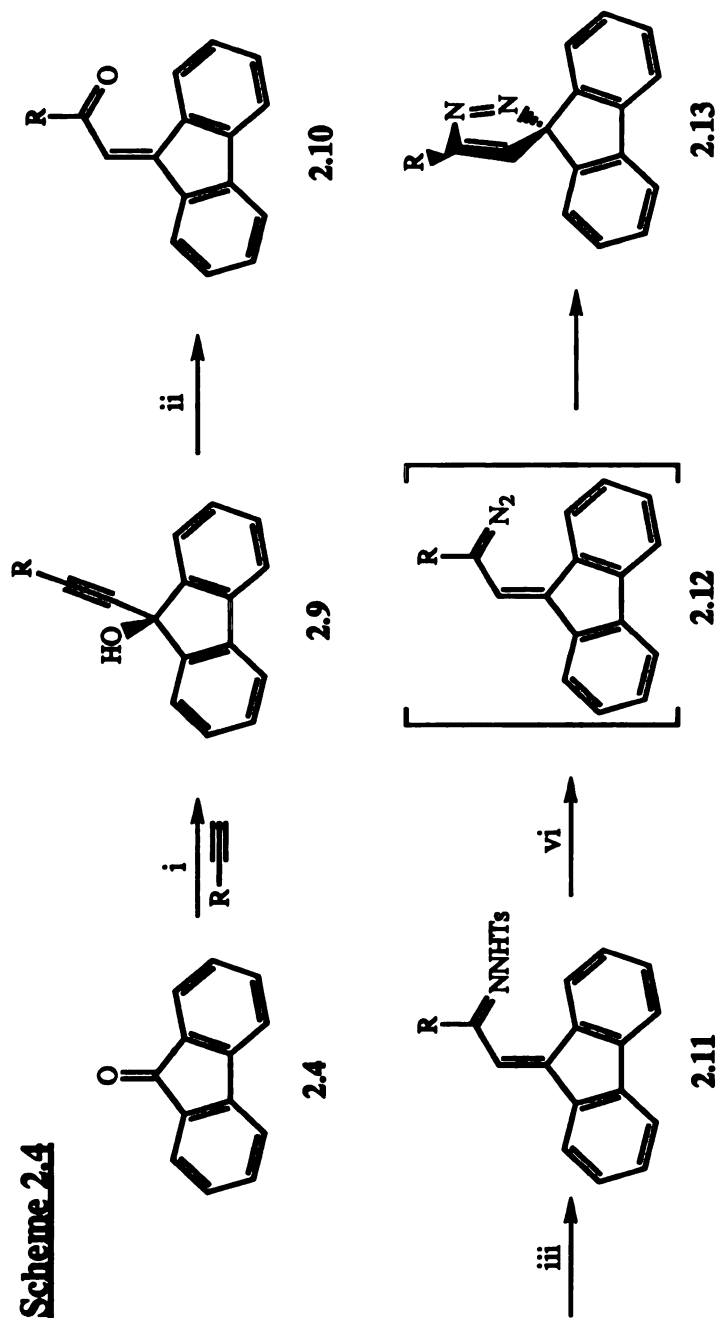
uranium and pyrex glasses as described in the Experimental Section. The product mixtures were separated by flash column chromatography over silica gel using hexane as eluent. Besides the major product cyclopropene (2.7), three other products were indentified: 9-fluorenone (2.4), bifluorenylidene (2.5) and fluorenone ketazine (2.6); no compound 2.8, which corresponds to 2.2 obtained from diphenylcarbene, was found. All cyclopropenes were identified by ^1H NMR, ^{13}C NMR and mass

Scheme 2.3



spectrometry. For comparison, the above photolyses were repeated at room temperature; the product distributions were essentially the same as in the low temperature matrix photolyses.

Scheme 2.4

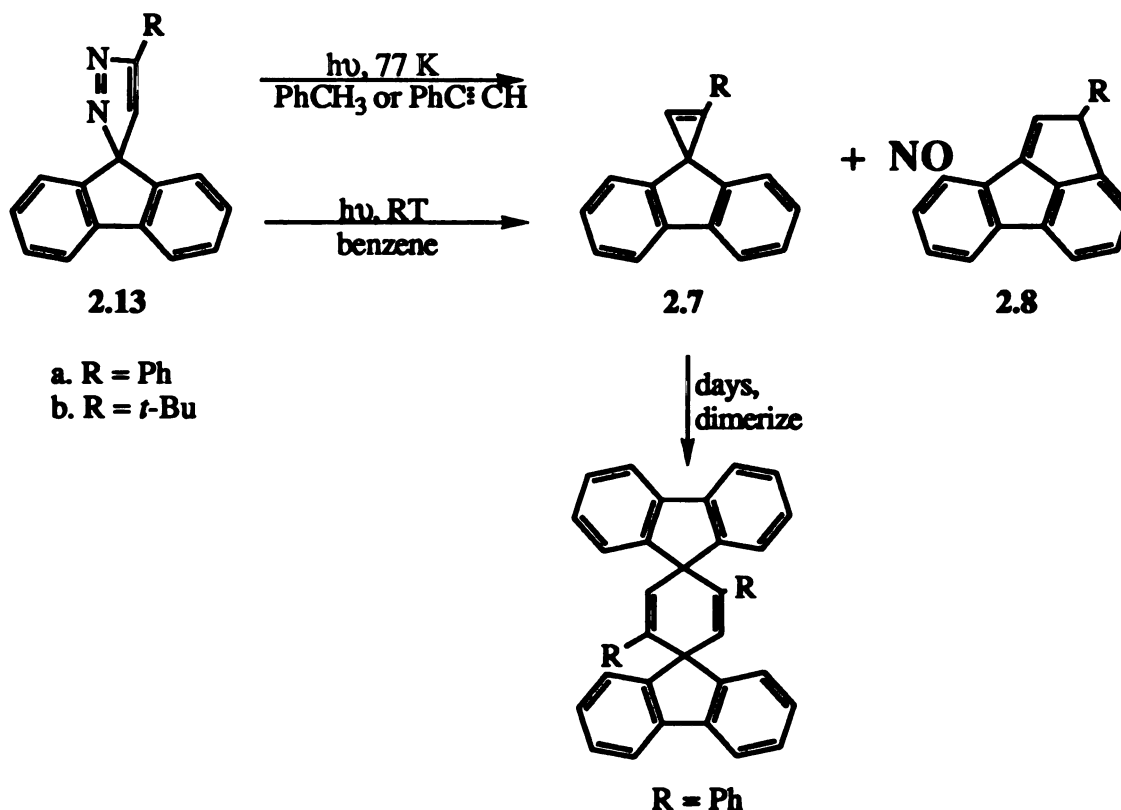


a R = Ph
b R = *t*-Bu
c R = *n*-Bu

i. Mg, $\text{C}_2\text{H}_5\text{Br}$, $(\text{C}_2\text{H}_5)_2\text{O}$. ii. H^+ , THF. iii. H_2NNHTs , $\text{C}_2\text{H}_5\text{OH}$. vi. NaH, pyridine.

Synthesis of Pyrazoles. Pyrazoles were prepared from 9-fluorenone (2.4) according to the reaction sequence shown in Scheme 2.4. Treatment of 9-fluorenone with phenyl ethynlmagnesium bromide in diethyl ether gave the ynol 2.9. Exposure of 2.9 to dilute sulfuric acid in THF resulted in yneol isomerization to enone 2.10. Then, the ketone reacted with toluenesulfonylhydrazide in ethanol, followed by base-induced detosylation to afford pyrazole 2.13. We failed to generate the n-butyl pyrazole 2.13c, presumably due to the α -hydrogens next to the hydrazone 2.11c.

Scheme 2.5



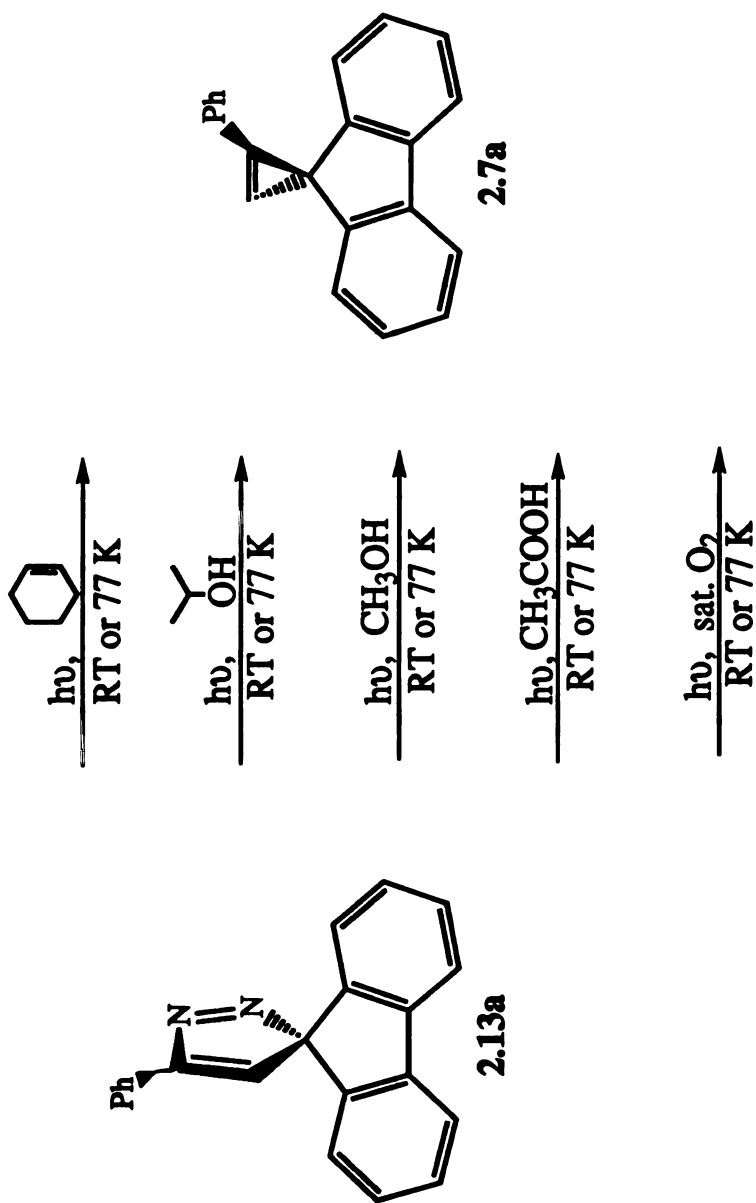
Photolyses of Pyrazole (2.13). Photolysis of pyrazole in low temperature toluene or phenylacetylene (0.1 M) matrices using light from a 500W mercury arc lamp, filtered with uranium and pyrex glasses,

was a very clean reaction and only cyclopropene (2.7) was identified (Scheme 2.5). Photolyses of pyrazoles in benzene were carried out at room temperature and the results were the same as in the low temperature matrix. No indene (2.8) was found.

Photolyses of 5-Phenyl-3-spirofluorenyl-3H-pyrazole (2.13a) with Various Trapping Reagents. A degassed solution of the pyrazole (0.05 M) in cyclohexene containing 30% (by volume) of toluene was photolyzed at 77 K and gave only 1-phenylspiro[cyclopropene-3,9'-fluorene] (2.7a). The same photolyses were carried out in methanol, isopropanol, and acetic acid with the same results as in the cyclohexene matrix. (Scheme 2.6) In order to use oxygen as a trapping reagent, a solution of the pyrazole in methylene chloride (0.08 M) was oxygenated by bubbling with oxygen gas for 10 minutes before being frozen at liquid nitrogen temperature and photolyzed. Photolyses of the pyrazole in the oxygen-saturated methylene chloride gave only the cyclopropene (2.7a).

The above reactions were also carried out in solution at room temperature and still the cyclopropene (2.7a) was the only product.

Thermolyses of 5-Phenyl-3-spirofluorenyl-3H-pyrazole. A solution of the pyrazole (14.7 mg) in 4 ml of acetic acid was refluxed for one and a half hours until no starting material remained, as assessed by TLC. The solution was diluted with 100 ml of benzene, washed with saturated aqueous sodium bicarbonate solution and dried over magnesium sulfate. After removal of solvent, the residue was separated by flash chromatography over silica gel eluting with hexane. Only the cyclopropene (2.7a) could be identified.

Scheme 2.6

Electron Spin Resonance Studies. Irradiation of a dilute degassed solution ($\sim 5 \times 10^{-3}$ M) of 9-diazofluorene in phenylacetylene cooled to 77 K in the microwave cavity of an ESR spectrometer gave rise not to the well-known ESR spectrum of triplet fluorenylidene formed in other matrices but to the triplet spectrum shown in Figure 2.1. The lifetime of the triplet species was at least several hours in the low temperature matrix. A similar triplet ESR spectrum was obtained from irradiation of a dilute degassed solution ($\sim 5 \times 10^{-3}$ M) of 5-Phenyl-3-spirofluorenyl-3H-pyrazole in toluene/pentane (1:1) or phenylacetylene matrices at 77 K, as shown in Figure 2.1.

Irradiations of 9-diazofluorene in 1-hexyne were carried out as described above in the neat alkyne or in dry toluene/pentane (1:1), yielding the ESR spectra shown in Figure 2.2.

Irradiations of 9-diazofluorene in 3,3-dimethylbutyne were carried out as described above in the neat alkyne or in dry toluene/pentane (1:1). A triplet ESR spectrum was obtained which also showed significant radical contamination; however, this spectrum, judging from non-free-radical region, is significantly different from the ESR spectrum of triplet fluorenylidene.

A procedure analogous to that given above was used for irradiation of 5-*t*-butyl-3-spirofluorenyl-3H-pyrazole in toluene/pentane (1:1) or 3,3-dimethyl-1-butyne matrices at 77 K; the resulting spectrum are shown in Figure 2.3.

Figure 2.1. ESR Spectra for Irradiation of 9-Diazo fluorene with Phenylacetylene and 5-Phenyl-3-spirofluorenyl-3H-pyrazole at 77 K

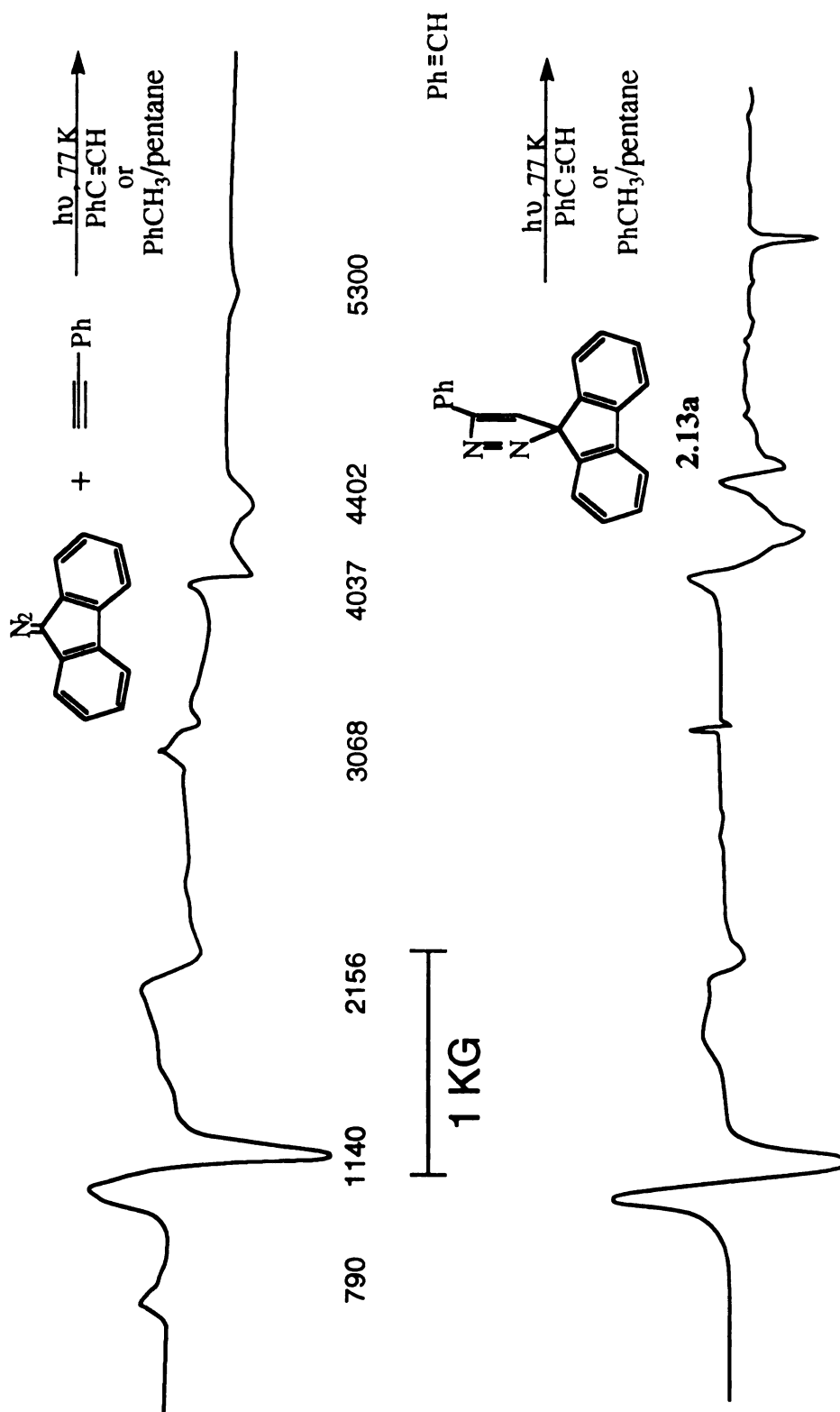


Figure 2.2. ESR Spectrum for Irradiation of 9-Diazafluorene with 1-Hexyne at 77 K

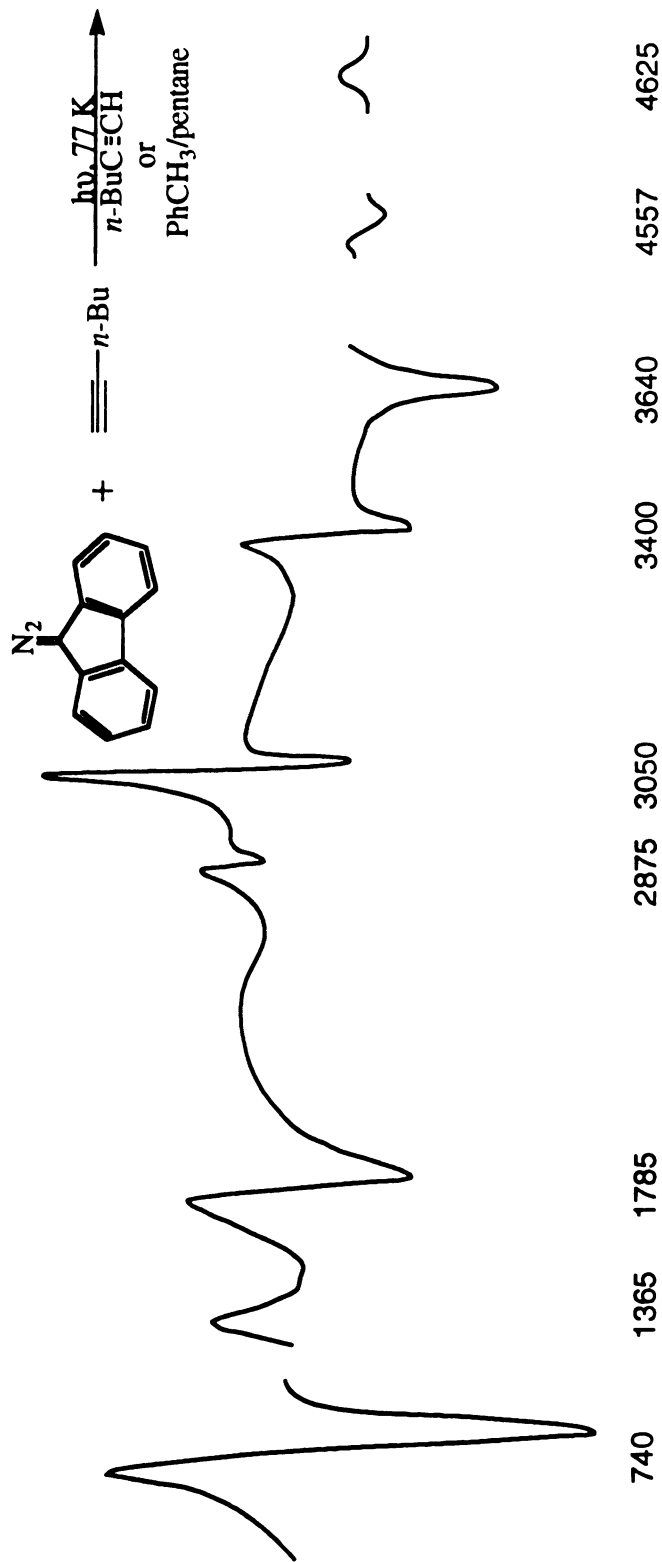
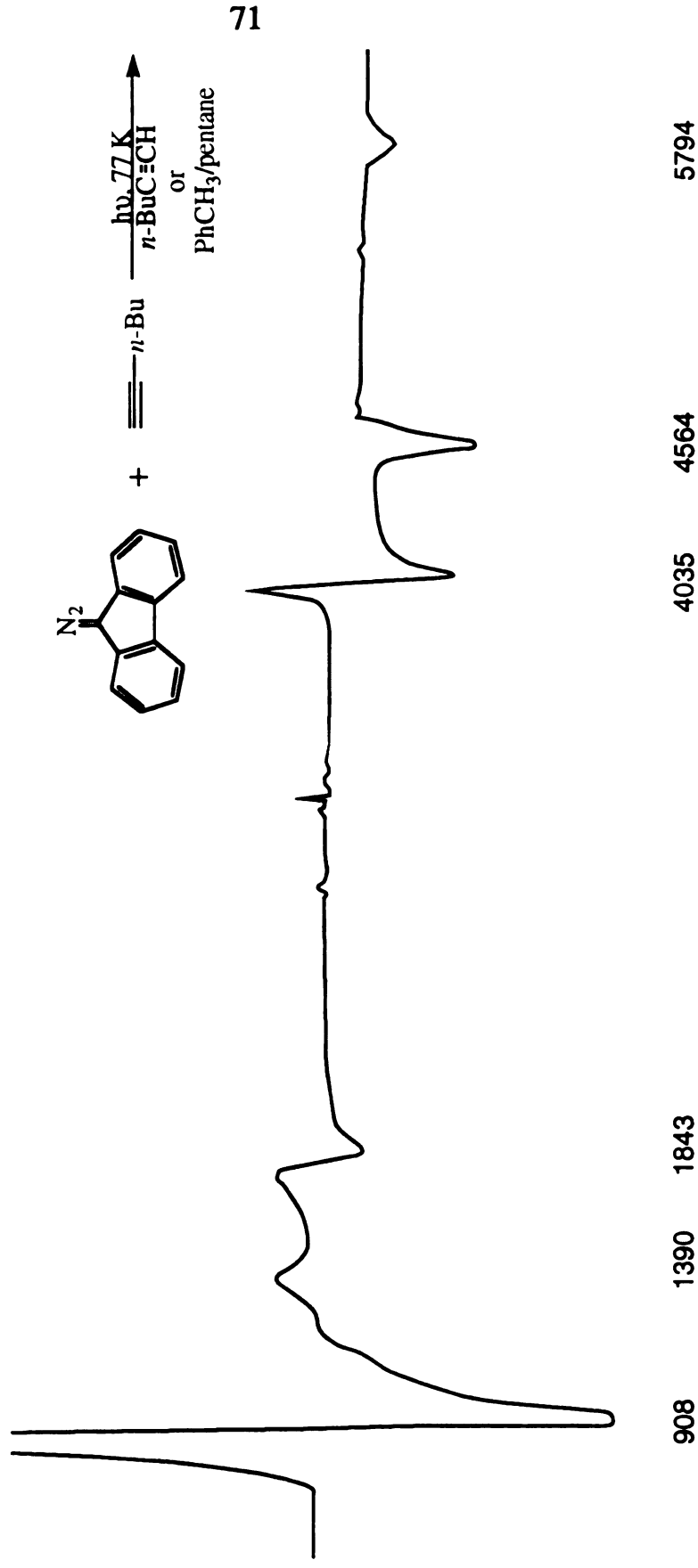
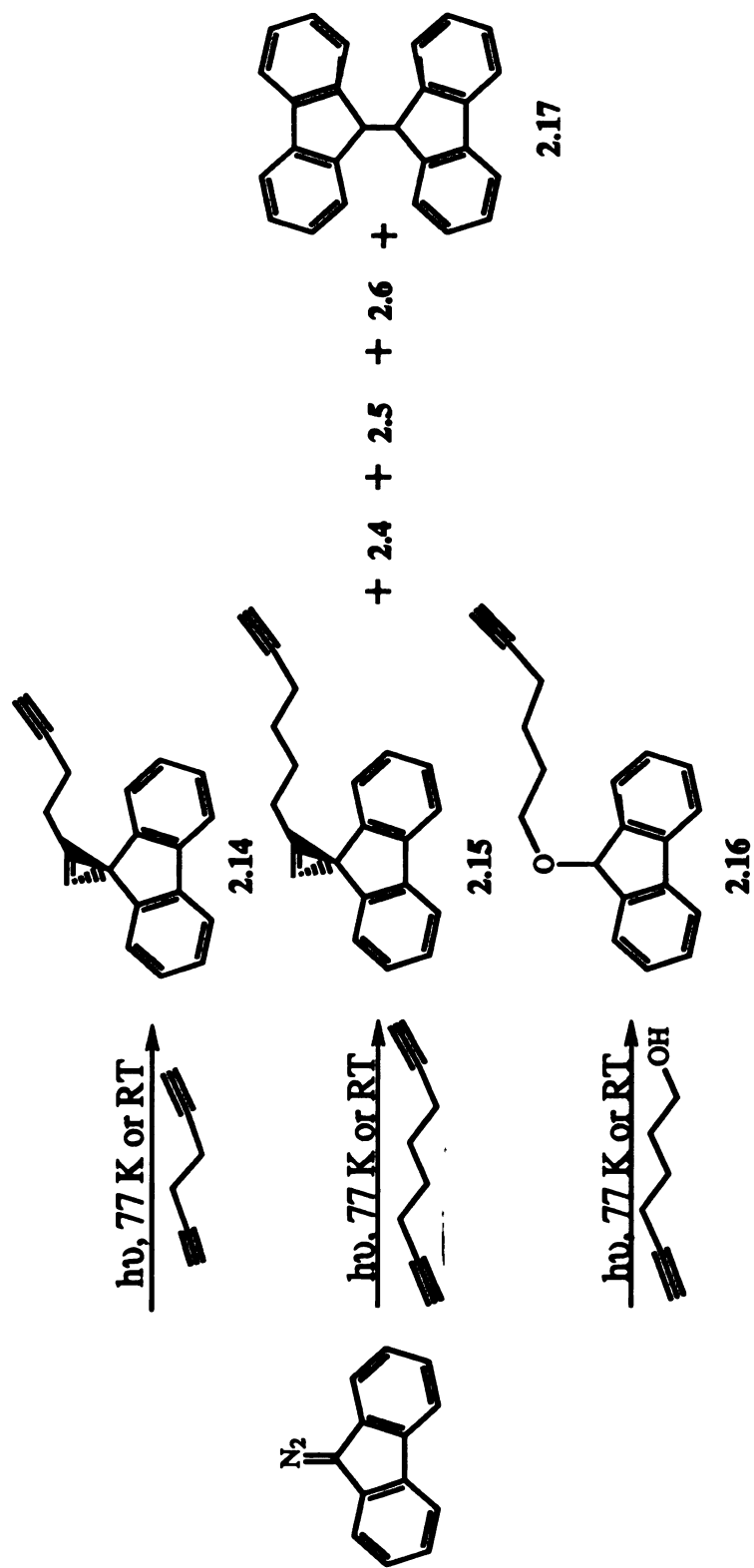


Figure 2.3. ESR Spectrum for Irradiation of 9-Diazo fluorene with 5-*t*-Butyl-3-spirofluorenyl-3H-pyrazole at 77K



Scheme 2.7.

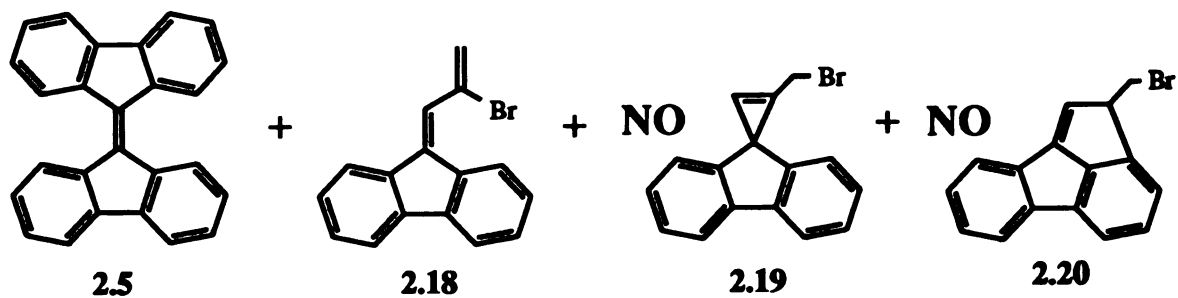
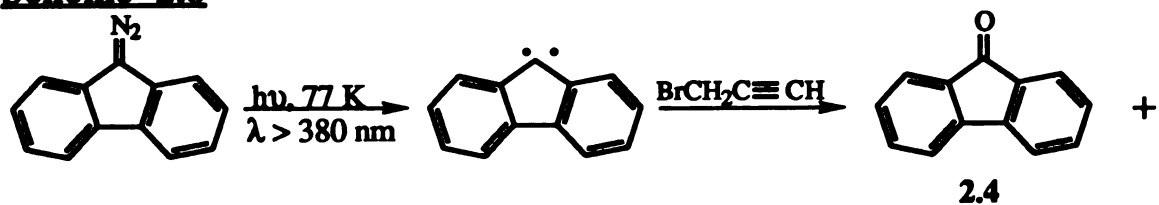
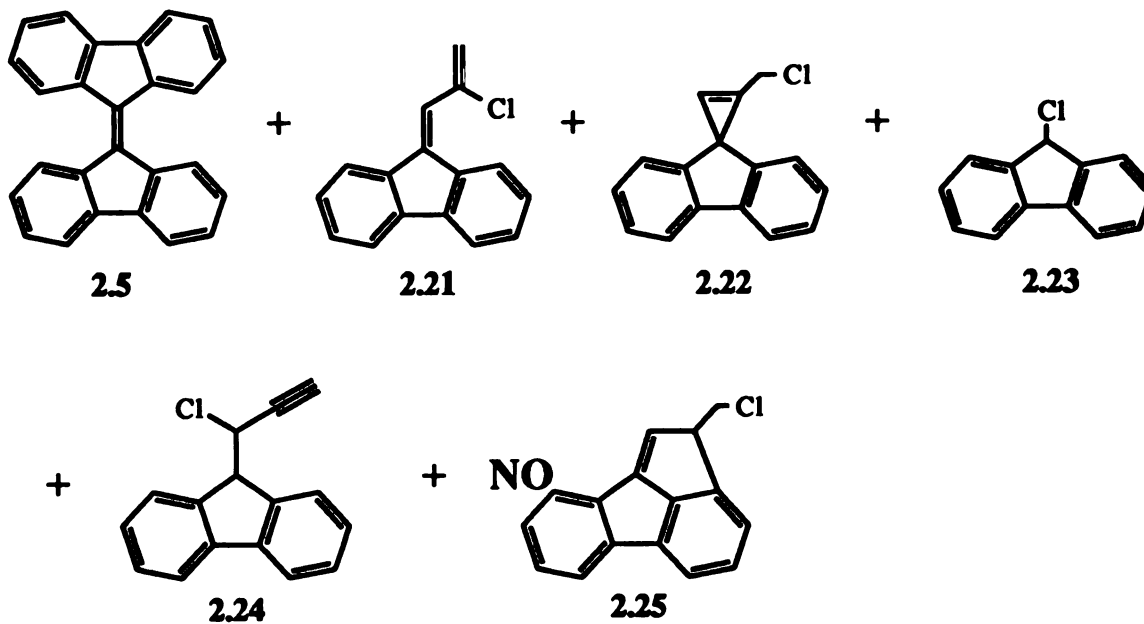
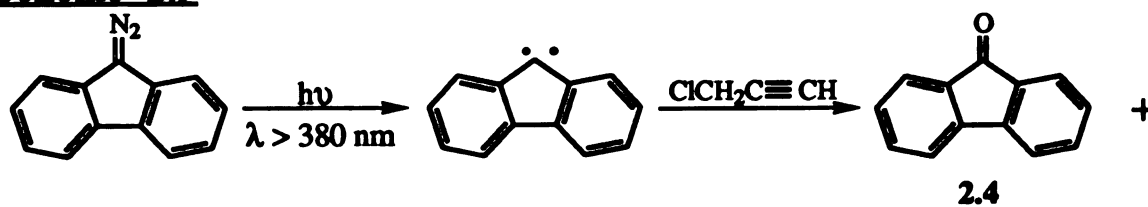
Irradiation of 1-phenylspiro[cyclopropene-3,9'-fluorene] (2.7a) in phenylacetylene or dry toluene/pentane (1:1) matrices at 77 K gave only a featureless free-radical signal.

Only the triplet fluorenylidene ESR spectra were obtained from the irradiation of 9-diazo fluorene in neat propargyl chloride or propargyl bromide (80% w/w in toluene) at 77 K following similar procedures described above.

Photolyses of 9-Diazo fluorene in 1,5-Hexadiyne and 1,7-Octadiyne. Photolyses of 9-diazo fluorene in 1,5-hexadiyne and 1,7-octadiyne were carried out as above, and giving only cyclopropene addition products 2.14 and 2.15, respectively (Scheme 2.7). Both the cyclopropenes were identified by ^1H NMR, ^{13}C NMR and mass spectrometry.

Photolyses of 9-Diazo fluorene in 6-Hexyn-1-ol. Photolysis of 9-diazo fluorene in 6-hexyn-1-ol were carried out similar to previous procedure, and gave only one product ether 2.16, which was identified by ^1H NMR, ^{13}C NMR and mass spectra (Scheme 2.7).

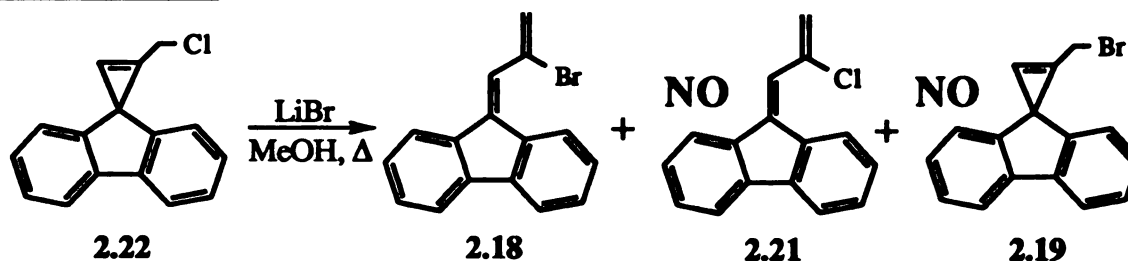
Photolyses of 9-Diazo fluorene in Propargyl Bromide. Photolyses of 9-diazo fluorene in propargyl bromide containing 20% (by weight) of toluene were carried out similarly to the previous procedure and gave 9-fluorenone, bifluorenylidene and 2-bromo-3,9'-fluorenylidenylpropene (2.18) (Scheme 2.8).

Scheme 2.8**Scheme 2.9**

Photolyses of 9-Diazafluorene in Propargyl Chloride.

These experiments were carried out as in the case of propargyl bromide; the reaction mixture was separated by flash column chromatography over silica gel to give 9-fluorenone, bifluorenylidene, 9-chlorofluorene (2.23), 2-chloro-3,9'-fluorenylidene-propene (2.21), 1-(chloromethyl)-spiro[cyclopropene-3,9'-fluorene] (2.22) and 3-chloro-3,9'-fluorenyl-propyne (2.24) (Scheme 2.9).

Scheme 2.10

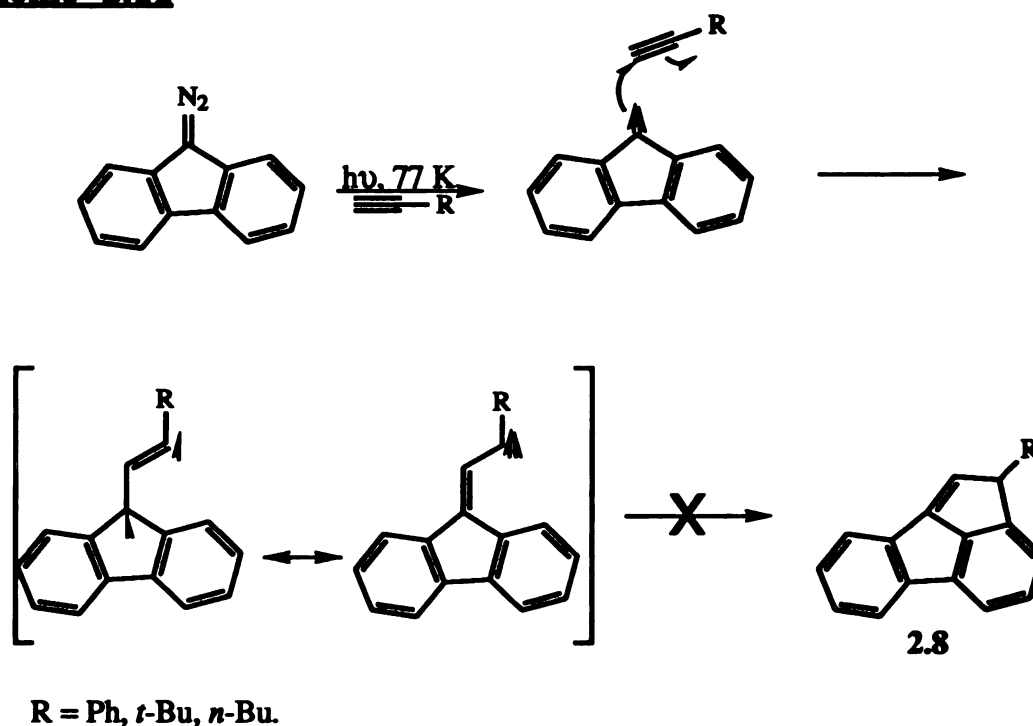


Bromide Exchange of 1-(Chloromethyl)-spiro[cyclopropene-3,9'-fluorene] (2.22). A solution of 2.22 and lithium bromide in 10 ml of methanol was refluxed for 10 hours and the solvent was removed. The residue was directly subjected to ^1H NMR. Only 1-(chloromethyl)-spiro[cyclopropene-3,9'-fluorene] (2.22) and 2-bromo-3,9'-fluorenylidene-propene (2.18) were identified and in product mixture, as shown in Scheme 2.10.

Product Ratio Studies. Product distributions of irradiation of 9-diazafluorene in propargyl chloride and 1,2-dichloroethane are summarized in Table 2.1. All product yields were absolute yields and were determined by ^1H NMR using toluene as the internal standard which was added just prior to analysis.

Table 2.1. Irradiation of 9-Diazo fluorene in Mixtures of Propargyl Chloride and 1,2-Dichloroethane

| Temp. K | % v/v of C ₂ H ₄ Cl ₂ | product yield, % (absolute) | | | | | |
|---------|---|-----------------------------|------|------|------|------|-----------|
| | | 2.5 | 2.21 | 2.22 | 2.23 | 2.23 | 2.22/2.21 |
| 77 | 50 | 18 | 14 | 9 | 5 | 7 | 0.6 |
| 298 | 0 | 1 | 4 | 28 | 5 | 3 | 7.0 |
| 298 | 50 | 3 | 12 | 52 | 14 | 8 | 4.3 |
| 298 | 90 | 11 | 24 | 39 | 16 | 10 | 1.6 |
| 298 | 95 | 10 | 21 | 31 | 7 | 8 | 1.5 |

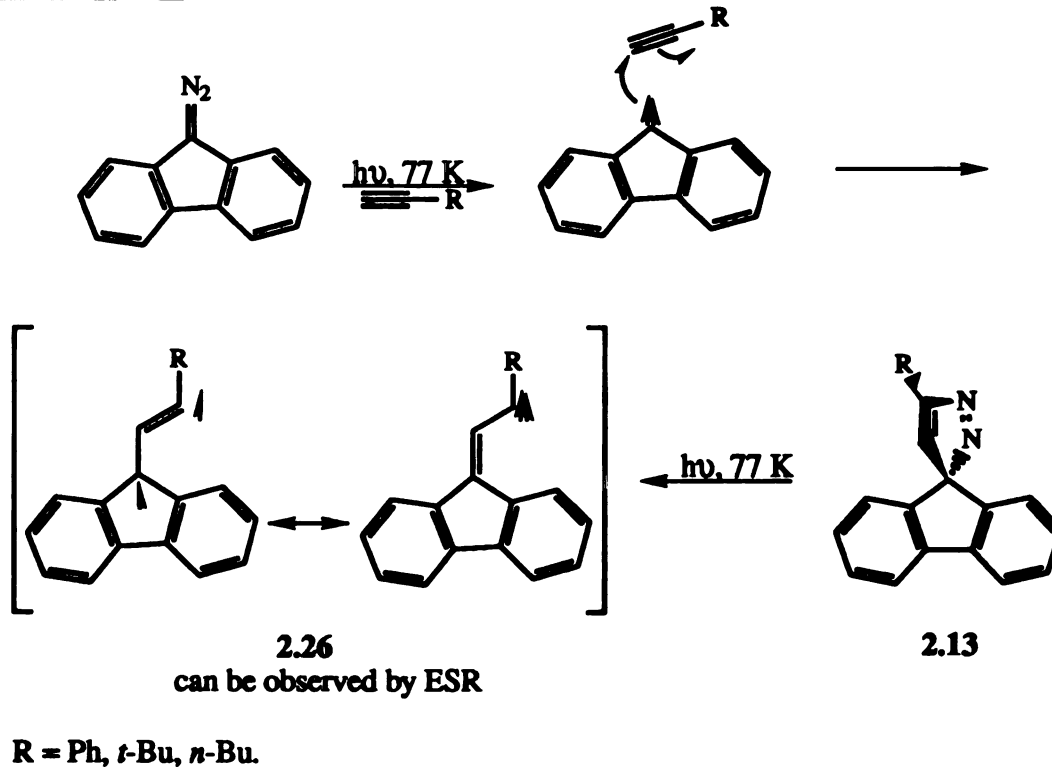
Scheme 2.11**2.3 Discussion**

Just as a triplet carbene reacts with an alkene via a stepwise mechanism, it should similarly react with an alkyne in a stepwise manner via an intermediate biradical. Jones et al. demonstrated the stepwise mechanism of the reaction of triplet diphenylcarbene and monosubstituted alkynes by intramolecularly trapping the vinylcarbene intermediate with one of the phenyl rings of the original diphenylcarbene.¹ However, our attempt to follow the same strategy failed, as shown in Scheme 2.11. The only adduct of triplet fluorenylidene and acetylene was cyclopropene (2.7) both in solution and in the low temperature matrices. As mentioned in the introduction, the reported literature rules out the explanation that the indene (2.8) was not observed because the only reactive species in the

reaction is singlet fluorenylidene. Additionally, the ESR spectrum of an irradiated sample of 9-diazafluorene in a phenylacetylene matrix at 77 K shows a triplet species that is not triplet fluorenylidene. Since similar ESR spectra were obtained from photolyses of 5-phenyl-3-spirofluorenyl-3H-pyrazole (2.13a) in toluene/pentane or phenylacetylene matrices (Figure 2.1), it seems reasonable that a similar or even the same type of intermediate was generated during these photolyses.

As shown in Figures 2.2 and 2.3, it is clear that there is a triplet carbene other than simple triplet fluorenylidene generated in the reactions, although we were unsuccessful in making direct comparisons of the corresponding ESR spectra for irradiation of 9-diazafluorene with 3,3-dimethyl-butyne or 5-*n*-butyl-3-spirofluorenyl-3H-pyrazole at 77 K.

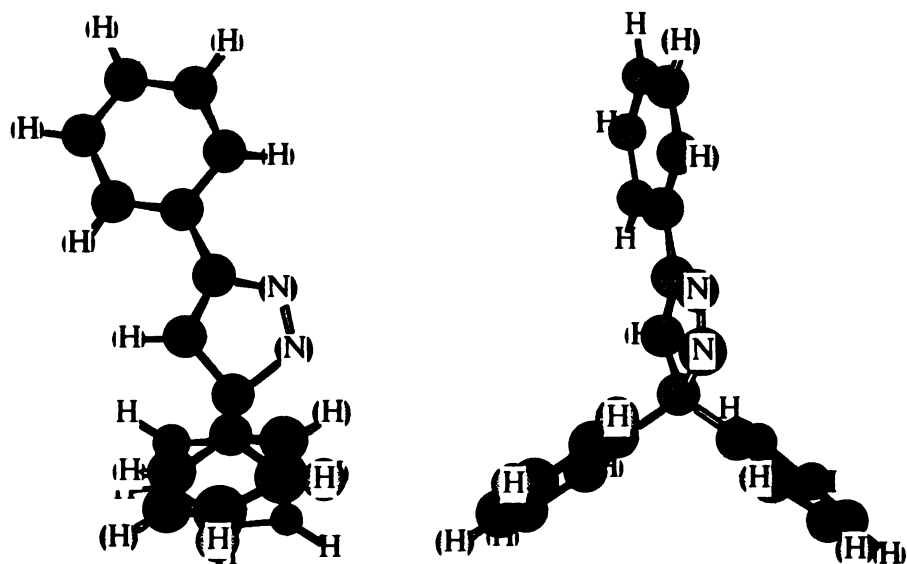
Scheme 2.12



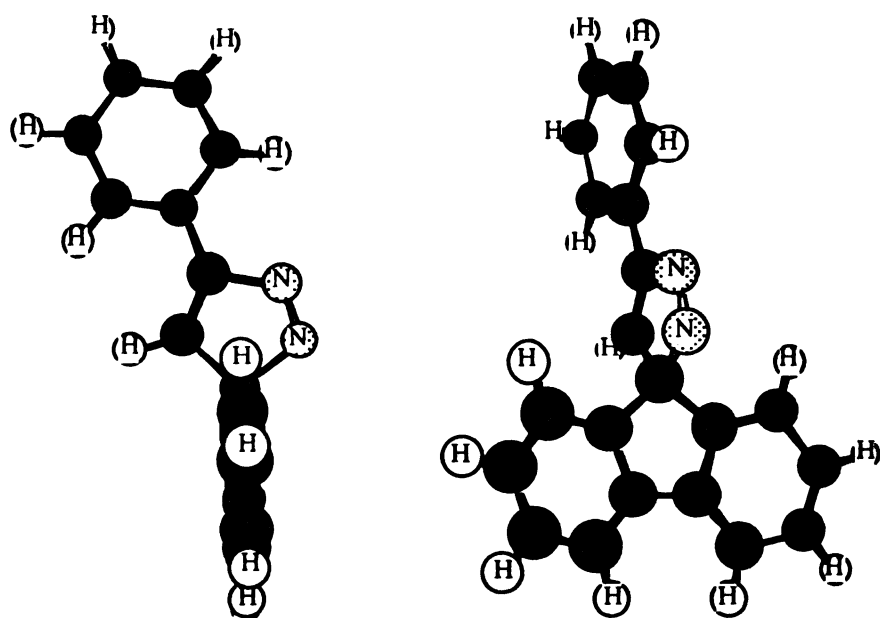
The ESR studies obviously show that a secondary triplet species was generated in organic alkyne matrices. Then the question becomes what is the triplet carbene? Is it the analogue to the vinylcarbene intermediate proposed by Jones et al? Actually, we can not think of any intermediate other than the vinylcarbene (2.26) or its diradical resonance form, as shown in Scheme 2.12.

Unfortunately, as shown in Scheme 2.6, attempts to trap 2.26 were not very successful. Even thermolyses of 5-phenyl-3-spirofluorenyl-3H-pyrazole (2.13a) in acetic acid did not trap the intermediate. Assuming the loss of N₂ must yield an intermediate before product, the rate of ring-closure of the intermediate (2.26) to form cyclopropene (2.17) must exceed the rate of intermolecular reaction even though most carbenes react with carboxylic acids at rates near the diffusion limit. Some insight may be gained by comparing the geometries of 3,3,5-triphenyl-3H-pyrazole and 5-phenyl-3-spirofluorenyl-3H-pyrazole (2.13a) calculated by the MNDO method (Figure 2.4).¹¹ The plane of the fluorenyl group is perpendicular to the plane of the pyrazole ring and the whole molecule is rigid. After extrusion of nitrogen, the orbitals on the carbene center can not overlap with the p-orbitals of the fluorenyl ring because of the rigidity of the ring. However, for triphenyl-pyrazole, the dihedral angle between the planes of the phenyl groups at C₃ and the plane of the pyrazole are around 120 degree. More important, after extrusion of the nitrogen in the pyrazole ring, those two phenyl rings can free rotately to develop overlap between the orbitals on the carbene center and on the phenyl ring. The overlap of those orbitals is even better during the addition of diphenylcarbene and acetylene. Because of the twisted and bent

Figure 2.4. Calculated Geometries for Pyrazoles by MNDO

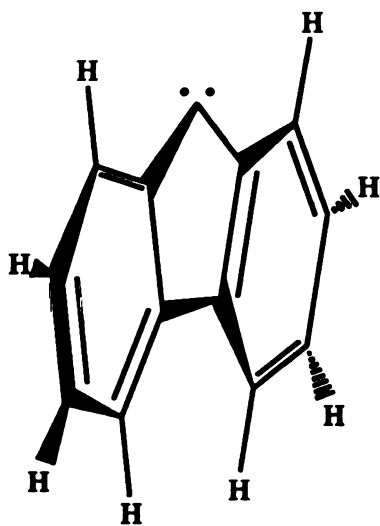


3,3,5-Triphenyl-3H-pyrazole

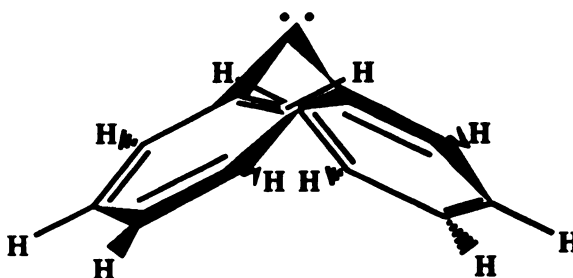


5-Phenyl-3-spirofluorenyl-3H-pyrazole

geometry of diphenyl carbene, the approaching acetylene can interact with the carbene in any orientation without suffering much steric hindrance from the ortho hydrogens on the phenyl rings of the carbene. However, in the case of the planar fluorenylidene, because of blocking by the hydrogens on the 2 and 8 positions, the acetylene can only approach the carbene in a perpendicular orientation. Jackson and O'Brien found that,



Fluorenylidene



Diphenylcarbene

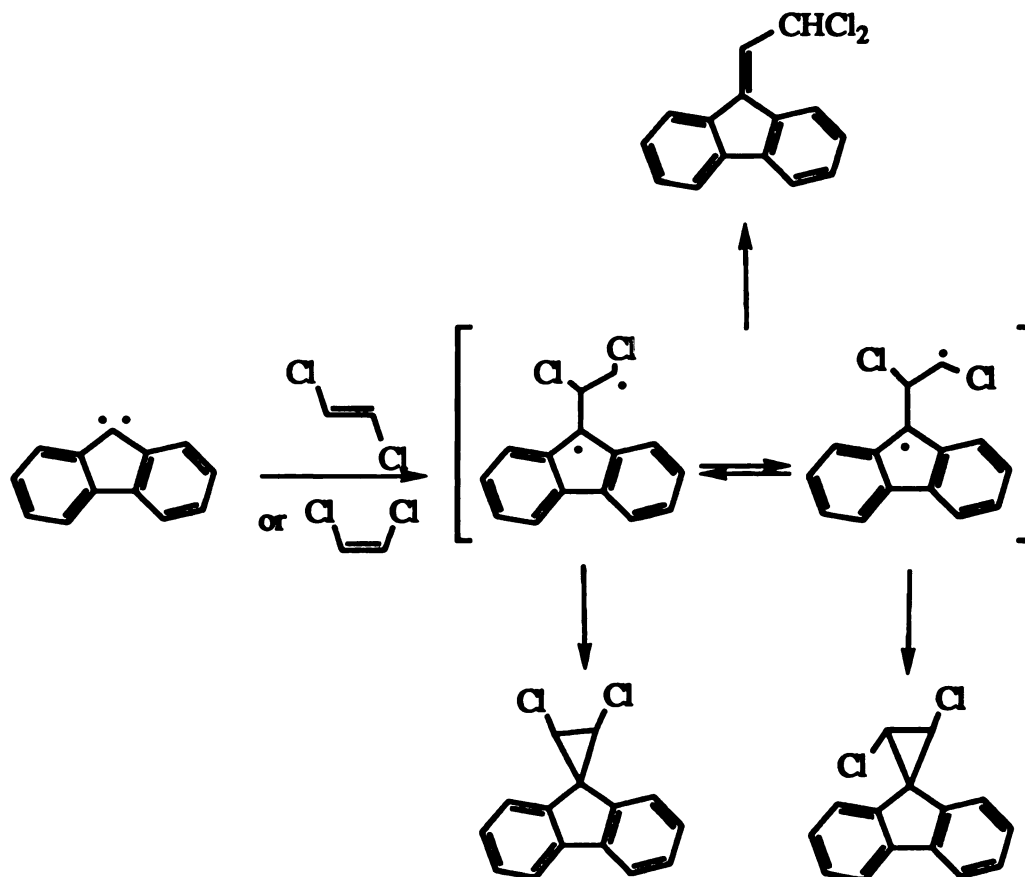
by MNDO and ab initio calculations, there is no rotational preference at the transition state distance of the addition reaction of triplet methylene to acetylene.¹² So, the absence of indene (2.8) product formation analogous that found from the reaction of diphenylcarbene, is the result of the the planar geometry of fluorenylidene. In addition, Jones et al. have shown that an entirely different course is followed by the reaction of triplet diphenylcarbene with disubstituted acetylenes. The cyclopropene becomes the major product and the corresponding indene appears in only trace amounts (< 2%) or is not observed, findings which these authors also attribute to steric effects.

Since the failures of the self-trapping and intermolecular trapping reaction of the vinylcarbene were due to steric effects, we attempted to get around this problem by using another intramolecular trap in the form of another hydroxy or alkyne group at the tail of the acetylene substrate. It was our hope that the vinylcarbene would be quenched by either O-H insertion or addition to the second alkyne, as shown in Scheme 2.13. It turned out that the rate of cyclopropene ring-closure is still much faster than the rate at which the tail wraps around the secondary carbene produced in the photolyses of 9-diazofluorene in 1,5-hexadiyne or 1,7-octadiyne matrices, as shown in Scheme 2.7. And the O-H insertions found on photolyses of 9-diazofluorene in 5-pentyn-1-ol or 6-hexyn-1-ol matrix were not surprising; triplet arylcarbenes favor O-H insertion in soft matrices like methanol and ethanol,^{4,13} in which the diffusion rate is still faster than the rate of the triplet carbene addition to the alkyne.

In 1984, Gaspar et al. studied the reaction of fluorenylidene with *cis*- and *trans*-1,2-dichloroethylene.¹⁴ With fluorenylidene, they observed three products containing the elements of dichloroethylene: *cis*-cyclopropane, *trans*-cyclopropane and 9-(2,2-dichloroethylidene)fluorene, which was presumably formed via rearrangement of a diradical intermediate, as shown in Scheme 2.14. In the presence of styrene or butadiene, which were believed to be triplet carbene quenchers, the stereoselectivity of cyclopropanation increased, and the yield of chlorine-migration product decreased. An opposite trend was found when the reaction was diluted with hexafluorobenzene. Those workers concluded that the butadiene was efficient in trapping the triplet carbene, while the dilution in hexafluorobenzene was believed to enhance the triplet carbene formation.

So, 9-(2,2-dichloroethylidene)fluorene was generated solely from the diradical intermediate of triplet fluorenylidene addition to 1,2-dichloroethylene.

Scheme 2.14



We modified the dichloroethylene methodology based on the same idea – chlorine migration. Here is the experiment: Photolyze 9-diazo fluorene in a propargyl chloride matrix. If addition of triplet fluorenylidene to propargyl chloride indeed generates a triplet vinylcarbene intermediate (2.27), then the intermediate should be trapped by chlorine migration to give 2-chloro-3,9'-fluorenylidenyl-propene (2.21) (Scheme 2.15). The results are summarized in Scheme 2.9 and

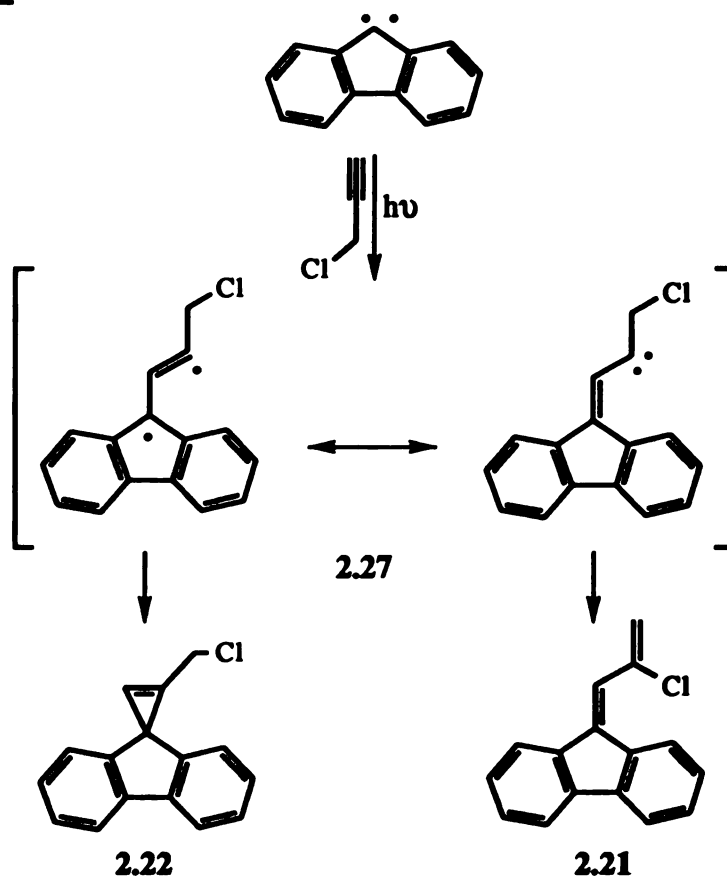
Scheme 2.15

Table 2.1. Three products of the photolyses contained the propargyl chloride fragment: 2-chloro-3,9'-fluorenylidene-propene (2.21), 1-(chloromethyl)-spiro[cyclopropene-3,9'-fluorene] (2.22) and 3-chloro-3,9'-fluorenyl-propyne (2.24). Although 2.22 and 2.24 can be generated from either the singlet or triplet states of fluorenylidene, 2.21 must arise through a stepwise process, in which triplet fluorenylidene adds to propargyl chloride followed by 1,2-chlorine atom shift (see Table 2.1). Further, the ratio (2.22/2.21) is sensitive to temperature and dilution with 1,2-dichloroethane. The yield of 2-chloro-3,9'-fluorenylidene (2.21) increases with increasing concentration of 1,2-dichloroethane or at lower temperature. In both cases the increase in 2.21 yield is because singlet-to-triplet intersystem crossing of fluorenylidene is enhanced relative to

reaction with propargyl chloride. However, only the triplet fluorenylidene ESR spectrum was obtained from irradiation of 9-diazafluorene and propargyl chloride or propargyl bromide at 77 K. It is possible that propargyl chloride or propargyl bromide, like other haloalkenes (i.e. 1,2-dichloroethane) are more inert than the other alkynes we examined at the low temperature.

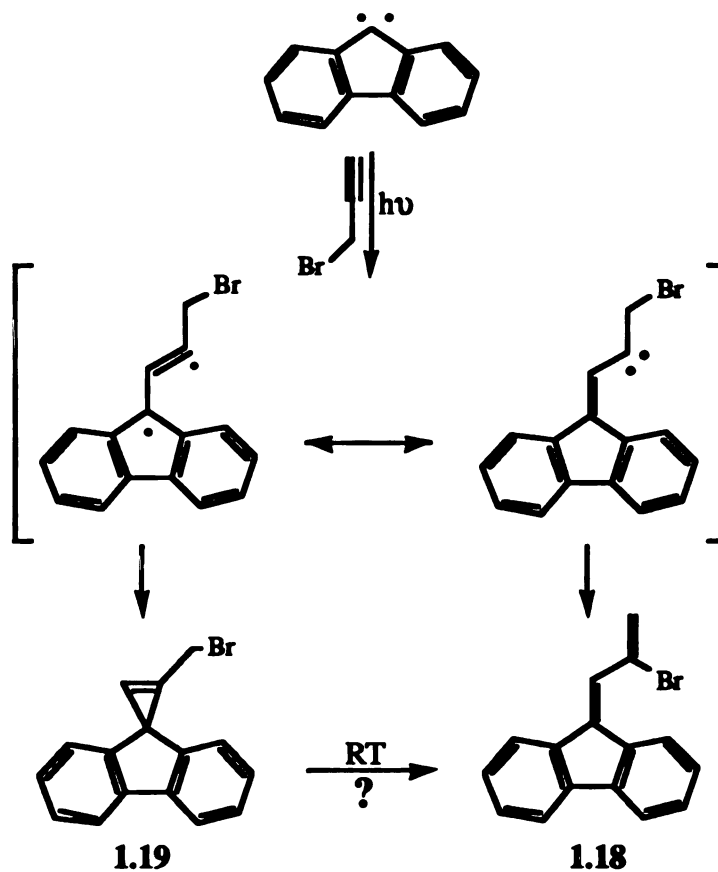
In the reaction of fluorenylidene and propargyl bromide, 2-bromo-3,9'-fluorenylidene-propene (**2.18**) was the only adduct. Apparently, the cyclopropene (**2.19**) was not thermally stable and rearranged to **2.18** (Scheme 2.15). To further test the stability of cyclopropene **2.19**, the corresponding chloride **2.22**, was exposed to LiBr in refluxing methanol. This reaction yielded only **2.18** and unreacted **2.22**; no cyclopropene **2.19** nor rearranged product (**2.21**) from **2.22** was found (Scheme 2.10). We do not quite understand the process of this rearrangement, and also we can not rule out the possibility that the rate of cyclopropene ring closure can not compete with that of bromine migration.

2.4 Conclusion:

As originally suggested by Jones et al., it appears that steric interactions prevent the vinylcarbene intermediate derived from the addition of triplet fluorenylidene to monosubstituted acetylene from being intramolecularly trapped by its aryl ring as in the case of its analogue, triplet diphenylcarbene. We have demonstrated through ESR studies and 1,2-chlorine atom shift that triplet fluorenylidene addition to alkynes

proceeds through the same type of intermediate, vinylcarbene or its resonance 1,3-diradical resonance form.

Scheme 2.16



2.5 Experimental:

General Procedures. All ¹H NMR and ¹³C NMR spectra were obtained by using a 300 MHz Varian Gemini, a 300 MHz Varian VXR-300 or a 500 MHz Varian VXR-500 instrument. UV spectra were recorded on a Shimadzu UV-160 spectrometer kindly shared by the group of Prof. Peter Wagner. Mass spectra were recorded on a Fisons VG Trion-1 mass spectrometer. High resolution mass spectra were recorded

on a JEOL JMS-HX110 high resolution double-focusing mass spectrometer. Gas chromatographic analyses were performed on Perkin-Elmer 8500 equipped with a flame ionization detector. Unless specified, concentration of mixtures after workup was performed using a Büchi rotary evaporator.

Dry solvents, benzene, toluene, tetrahydrofuran, and diethyl ether were distilled from sodium/benzophenone immediately prior to use. Methylene chloride and acetonitrile were heated at reflux over calcium hydride and distilled immediately prior to use.

Photolytic Procedures in Organic Matrices. In the general procedure, a solution of 9-diazofluorene (0.1 M) in the neat appropriate alkyne was placed in an NMR tube (8 in). The sample was then degassed using three freeze-pump-thaw cycles. The sample tube was transferred to a quartz-tailed Dewar flask which contained liquid nitrogen.

Samples were irradiated by placing the tail of the Dewar in front of a 500W mercury arc lamp shielded with a water jacket and a uranium glass filter. Matrices were irradiated for 9-12 hours, with thawing and shaking every 2 hours for 5-10 minutes in order to homogenize them.

After irradiation, samples were brought to room temperature and the tubes were opened. After the alkyne had evaporated, the residue was separated by flash chromatography over silica gel (10 x 100 mm) eluted with hexane. Besides the major product, cyclopropene, unreacted diazofluorene, and trace amounts of fluorenone ketazine and fluorenone were visible in the ^1H NMR spectrum before separation.

Irradiation of 9-Diazafluorene in Phenylacetylene Matrix. The only addition product of fluorenylidene with phenylacetylene is 1-phenylspiro[cyclopropene-3,9'-fluorene] (2.7a): ^1H NMR (300 MHz, acetone- d_6) δ 7.17 (dt, 2 H, $J = 7.5, 1.1$ Hz), 7.26 (td, 2 H, $J = 7.4, 1.1$ Hz), 7.30-7.42 (complex, 7 H), 7.81 (s, 1 H), 7.97 (dt, 2 H, $J = 7.7, 0.8$ Hz); ^{13}C NMR (75.5 MHz, acetone- d_6) δ 148.4, 139.9, 129.7 (doublet), 128.7, 126.4, 126.2, 125.8, 120.7, 119.8, 119.6, 103.1, 36.3; MS (EI) m/e 266 (M^+), 265, 181, 180, 152, 105; UV λ_{max} [nm] (log ϵ) 258.9 (5.78), 221.4 (4.96). The cyclopropene was dimerized at room temperature after a few days. ^1H NMR (300 MHz, CDCl_3) δ 5.28 (d, 2 H, $J = 7.5$ Hz), 6.28 (t, 2 H, $J = 7.5$ Hz), 6.59 (d, 4 H, $J = 7.5$ Hz), 6.75-7.00 (complex, 10 H), 7.10 (d, 2 H, $J = 7.5$ Hz), 7.25-7.41 (m, 4 H), 7.45 (d, 2 H), 8.32 (d, 2 H, $J = 7.5$ Hz); ^{13}C NMR (75.5 MHz, CDCl_3) δ 146.6, 144.5, 143.5, 142.0, 141.0, 140.8, 130.0, 129.2, 128.3, 127.4, 126.7, 126.6, 126.5, 126.4, 126.3, 126.1, 125.9, 125.1, 119.9, 118.1; MS (EI) m/e 532 (M^+), 460, 367, 289, 265, 252, 165, 105.

Irradiation of 9-Diazafluorene in *t*-Butylacetylene Matrix. The only addition product of fluorenylidene with *t*-butylacetylene is 1-*t*-butylspiro[cyclopropene-3,9'-fluorene] (2.7b): ^1H NMR (300 MHz, CDCl_3) δ 1.17 (s, 9 H), 6.79 (s, 1 H), 7.18 (d, 2 H, $J = 7.3$ Hz), 7.28 (tt, 2 H, $J = 7.3, 1.3$ Hz), 7.34 (tt, 2 H, $J = 7.3, 1.3$ Hz), 7.85 (d, 2 H, $J = 7.3$ Hz); ^{13}C NMR (75.5 MHz, CDCl_3) δ 149.8, 139.5, 130.0, 126.8, 126.2, 120.7, 119.9, 97.2, 37.1, 33.6, 29.1; MS (EI) m/e 246 (M^+), 231, 216, 215, 203, 202, 190, 189, 165.

Irradiation of 9-Diazafluorene In 1-Hexyne Matrix. The major products were 1-*n*-butylspiro[cyclopropene-3,9'-fluorene]

(2.7c) and the C-H insertion products (relative ratio < 10% calculated from the integral ratio in NMR spectrum). Data for 1-*n*-butylspiro[cyclopropene-3,9'-fluorene] (2.7c): ¹H NMR (300 MHz, CDCl₃) δ 0.85 (t, 3 H, *J* = 6.8 Hz), 1.25-1.70 (m, 4 H), 2.55 (t, 2 H, *J* = 7.5 Hz), 6.91 (s, 1 H), 7.16 (d, 2 H, *J* = 6.6 Hz), 7.31 (td, 2 H, *J* = 7.3, 1.1 Hz), 7.35 (td, 2 H, *J* = 7.3, 1.1 Hz), 7.85 (d, 2H, *J* = 7.4 Hz); ¹³C NMR (75.5 MHz, CDCl₃) δ 150.4, 139.8, 126.4, 125.9, 122.7, 120.6, 119.8, 114.0, 99.9, 29.3, 24.1, 22.1, 13.4; MS (EI) *m/e* 247 (M⁺⁺¹), 246 (M⁺), 231, 217, 203, 189.

Photolytic Procedures at Room Temperature. Basic procedures are the same as described above except that the sample tube was directly put into the water jacket without using the liquid nitrogen Dewar.

Irradiation of 9-Diazo fluorene in Alkynes (Phenylacetylene, *t*-Butylacetylene and 1-Hexyne) at Room Temperature. The major products are the same as in low temperature matrices, except that the relative ratio for the C-H insertion products is higher for the 1-hexyne (< 10% calculated from the integral ratio in NMR spectrum)

9-Diazo fluorene (9-DAF) was prepared by literature procedures.^{9,15}

1,9'-Fluorenyl-3-Phenylprop-2-yn-1-ol (2.9a). In an oven-dried 300 mL three-neck round-bottom flask equipped with pressure equalizing dropping funnel, reflux condenser, magnetic stirrer, and an argon inlet, a solution of ethylmagnesium bromide in diethyl ether (ca. 15 mL), was generated from magnesium turning (0.66 g, 27.3 mmol) in dry

diethyl ether (5 mL), ethyl bromide (2.95 g, 27.1 mL) in dry diethyl ether (10 mL) and a trace of iodine. A solution of phenylacetylene (2.79 g, 27.3 mmol) in dry diethyl ether (10 mL) was added into the flask slowly through the dropping funnel. The reaction mixture was gently refluxed for 2 hours and then cooled to room temperature. After the stirrer was started, a solution of 9-fluorenone (4.92 g, 27.3 mmol) in dry ether (10 mL) was slowly added; the reaction was stirred at room temperature for 1.5 hours. Finally, it was refluxed for 1 hour and cooled in an ice bath. The reaction was quenched by adding ammonium chloride (8 g) as a saturated aqueous solution. The aqueous layer was extracted with diethyl ether (3 x 30 mL). The combined organic layers were dried over magnesium sulfate and the solvent was removed under vacuum to afford a yellow oil. The yellow oil was crystallized from methanol/hexane (1:1), affording a yellow solid (5.36 g, 69%): ^1H NMR (300 MHz, CDCl_3) δ 2.8 (s, 1 H), 7.15-7.42 (m, 9 H), 7.61 (d, 2 H, $J = 7.5$ Hz), 7.75 (d, 2 H, $J = 7.5$ Hz); ^{13}C NMR (75.5 MHz, CDCl_3) δ 147.5, 139.3, 132.1, 129.9, 129.8, 128.7, 128.4, 124.6, 122.6, 120.4, 89.0, 83.0, 75.1; MS (EI) m/e 282 (M^+), 265, 252.

Preparation of 2.9b. A procedure analogous to that given for 2.9a was followed. Reaction of 9-fluorenone (5.86 g, 32.5 mmol) in dry diethyl ether with 3,3-dimethyl-1-butyneylmagnesium bromide, generated from *t*-butyl acetylene (2.67 g, 32.5 mmol) and ethyl magnesium bromide (32.5 mmol), gave 1b (2.7 g, 32%) after recrystallization from pentane and a few drops of benzene: ^1H NMR (300 MHz, CDCl_3) δ 1.18 (s, 12 H), 2.43 (s, 1 H), 7.26-7.40 (m, 4 H), 7.59 (d, 2 H, $J = 6.9$ Hz), 7.67

(d, 2 H, $J = 6.9$ Hz); ^{13}C NMR (75.5 MHz, CDCl_3) δ 147.7, 139.0, 129.4, 128.4, 124.2, 120.0, 92.4, 78.2, 74.8, 30.8, 27.4.

Preparation of 2.9c. A procedure analogous to that given for **2.9a** was followed. Reaction of 9-fluorenone (6.27 g, 34.8 mmol) in dry diethyl ether with 1-hexynylmagnesium bromide, generated from *n*-butyl acetylene (2.86 g, 34.8 mmol) and ethylmagnesium bromide (34.8 mmol), gave **1c** (8.13 g, 89%) after recrystallization from pentane and a few drops of benzene: ^1H NMR (300 MHz, CDCl_3) δ 0.87 (t, 3 H, $J = 7.5$ Hz), 1.27-1.5 (complex, 4 H), 2.18 (t, 2 H, $J = 7.5$ Hz), 2.43 (s, 1 H), 7.27-7.4 (m, 4 H), 7.58 (d, 2 H, $J = 6.6$ Hz), 7.67 (d, 2 H, $J = 6.6$ Hz); ^{13}C NMR (75.5 MHz, CDCl_3) δ 147.6, 138.9, 134.7, 129.4, 129.1, 128.5, 124.3, 124.2, 120.3, 120.1, 84.4, 79.8, 74.9, 30.5, 21.9, 18.5, 13.6.

Isomerization of 2.9a. A solution of **2.9a** (4.02 g, 14.3 mmol) and dilute sulfuric acid (1 mL, 25% v/v in H_2O) in THF (20 mL) was refluxed for 5 hours. The mixture was cooled to room temperature and quenched by addition of saturated aqueous sodium bicarbonate solution (80 mL). The aqueous layer was extracted with benzene (3 x 30 mL) and the combined organic solution was washed with water, brine, and dried over magnesium sulfate. The solvent was removed under vacuum and the residue was crystallized from THF/benzene (1:1) to give a yellow solid (**2.10a**) was obtained (3.14 g, 78%): ^1H NMR (300 MHz, acetone- d_6) δ 7.26 (tt, 1 H, $J = 7.5, 1.5$ Hz), 7.36 (tt, 1 H, $J = 7.5, 1.5$ Hz), 7.46 (m, 2 H), 7.59 (t, 2 H), 7.69 (t, 1 H), 7.81 (d, 2 H, $J = 7.5$ Hz), 7.97 (s, 1 H), 8.08 (d, 1 H, $J = 7.5$ Hz), 8.20 (dm, 2 H), 8.37 (d, 1 H, $J = 7.5$ Hz); ^{13}C NMR (75.5 MHz, CDCl_3) δ 193.0, 146.4, 142.5, 141.1, 139.0, 138.5, 135.6,

133.5, 131.1, 130.7, 129.3, 129.0, 128.1, 127.9, 127.8, 127.6, 121.3, 120.1, 120.0, 119.9, 119.7, 119.6.

Isomerization of 2.9b. A procedure analogous to that given for **2.9a** was followed. Treatment of **2.9b** (2.33 g, 8.9 mmol) with dilute sulfuric acid (1 mL, 25% v/v in H₂O) in THF (20 mL) gave **2.10b** (1.66 g, 71%) as a yellow solid: ¹H NMR (300 MHz, CDCl₃) δ 1.30 (s, 9 H), 7.25 (t, 2 H, *J* = 7.5 Hz), 7.38 (t, 2 H, *J* = 7.5 Hz), 7.61 (d, 2 H, *J* = 7.5 Hz), 7.68 (d, 1 H, *J* = 7.5 Hz), 8.51 (d, 1 H, *J* = 7.5 Hz). ¹³C NMR (75.5 MHz, CDCl₃) δ 207.1, 145.0, 142.2, 140.8, 139.0, 135.4, 130.7, 130.3, 128.0, 127.8, 127.3, 120.9, 119.8, 119.6, 118.1, 44.7, 26.7.

Isomerization of 2.9c. A procedure analogous to that given for **2.9a** was followed. Treatment of **2.9c** (11.6 g, 14.4 mmol) with dilute sulfuric acid (10 mL, 25% v/v in H₂O) in THF (110 mL) gave **2.10c** (7.88 g, 68%) as a yellow solid: ¹H NMR (300 MHz, CDCl₃) δ 0.93 (t, 3 H, *J* = 7.5 Hz), 1.47 (m, 2 H), 1.69 (m, 2 H), 2.70 (t, 2 H, *J* = 7.5 Hz), 7.01 (s, 1 H), 7.23 (m, 2 H), 7.30-7.40 (m, 2 H), 7.56 (d, 2 H), 7.63 (d, 1 H, *J* = 7.5 Hz), 8.73 (d, 1 H, *J* = 7.5 Hz); ¹³C NMR (75.5 MHz, CDCl₃) δ 201.5, 145.7, 142.3, 141.2, 139.0, 135.4, 131.1, 130.6, 128.4, 127.3, 121.0, 120.8, 119.9, 119.5, 44.7, 26.4, 22.4, 14.0.

Preparation of 2.11a. A mixture of **2.10a** (2.37 g, 8.4 mmol), *p*-toluenesulfonhydrazide (2.36 g, 1.27 mmol) and a few drops of acetic acid in absolute ethyl alcohol (50 mL) was refluxed for 36 hours. The reaction mixture was then poured into methanol (150 mL) and a yellow precipitate formed while the solution cooled. The yellow precipitate was collected by suction filtration, air-dried and recrystallized

from methanol to afford needle-shaped yellow crystals (1.9 g, 50%): ^1H NMR (300 MHz, CDCl_3) δ 2.42 (s, 3 H), 6.70 (td, 1 H, $J = 8.5, 0.6$ Hz), 6.77 (s, 1 H), 6.95 (d, 1 H, $J = 8.5$ Hz), 7.22-7.38 (complex, 7 H), 7.43 (td, $J = 8.5, 0.6$ Hz), 7.61 (d, 1 H, $J = 8.6$ Hz), 7.67 (d, 1 H, $J = 8.6$ Hz), 7.75 (m, 4 H), 8.00 (br, 1 H).

Preparation of 2.11b. A solution of 2.10b (4.87 g, 18.4 mmol), a few drops of acetic acid and *p*-toluenesulfonylhydrazide in absolute ethyl alcohol (60 mL) was refluxed for 2 days. The solvent was evaporated to about 25 mL, and the reaction mixture was diluted with pentane (80 mL) and put in a freezer (~ -20 °C) overnight. A pale yellow solid was precipitated and collected by suction filtration (1.0 g, 13%): ^1H NMR (300 MHz, CDCl_3) δ 1.18 (s, 9 H), 2.48 (s, 3 H), 6.61 (s, 1 H), 6.76 (t, 1 H, $J = 7.5$ Hz), 6.89 (d, 1 H, $J = 7.5$ Hz), 7.31 (d, 2 H, $J = 7.5$ Hz), 7.39 (t, 1 H, $J = 7.5$ Hz), 7.64 (m, 2 H), 7.76 (d, 1 H, $J = 8.6$ Hz); ^{13}C NMR (75.5 MHz, CDCl_3) δ 159.9, 143.8, 141.6, 141.2, 139.8, 137.1, 135.5, 134.6, 129.9, 129.7, 129.6, 129.3, 128.2, 127.9, 127.5, 123.9, 120.8, 119.9, 112.6, 39.7, 28.0, 21.7.

Preparation of 5-Phenyl-3-spirofluorenyl-3H-pyrazole. (2.13a) To a solution of the tosyl hydrazone (2.11a) (1.0 g, 2.22 mmol) in pyridine (10 mL) was slowly added sodium methoxide (0.18 g, 3.33 mmol). After the addition was complete, the dark-red reaction mixture was protected with a drying tube filled with calcium chloride and warmed gently on a water bath to 60-65 °C for 20 min. The reaction was quenched with ice-water (50 mL) and the aqueous layer extracted with pentane (3 x 20 mL). The combined organic layers were washed with aqueous copper(II) sulfate until no more color change was observed, water,

and dried with magnesium sulfate. The solvent was removed under vacuum to give a pale-pink solid, which was recrystallized from methylene chloride and pentane to afford **2.13a** (0.4 g, 61%): ^1H NMR (300 MHz, acetone- d_6) δ 6.85 (d, 2 H, $J = 8.0$ Hz), 7.28 (td, 2 H, $J = 8.0, 1.6$ Hz), 7.36 (s, 1 H), 7.51 (td, 2 H, $J = 8.0, 1.6$ Hz), 7.58 (m, 3 H), 8.00 (d, 2 H, $J = 8.0$ Hz), 8.24 (dm, 2 H, $J = 8.0$ Hz); ^{13}C NMR (75.5 MHz, CDCl_3) δ 159.5, 143.2, 135.6, 130.3, 129.7, 129.6, 129.0, 127.9, 127.4, 123.7, 120.9, 108.1; MS (EI) m/e 293.8 (M^+), 265.3, 239.2, 190.1, 163.2, 132.9; UV (pentane) λ_{max} [nm] (log ϵ) 304.2 (3.69), 235.6 nm (4.58).

Preparation of 5-*t*-Butyl-3-spirofluorenyl-3H-pyrazole (2.13b). The procedure as described above for (**2.13a**) was followed. Treatment of the tosyl hydrazone (**2.11b**) (1.0 g, 2.3 mmol) with sodium methoxide (0.2 g, 3.7 mmol) in pyridine (8 mL) afforded **2.13b** (25 mg, 3.9%): ^1H NMR (300 MHz, CDCl_3) δ 1.52 (s, 9H), 6.28 (s, 1 H), 6.68 (d, 2 H, $J = 7.5$ Hz), 7.20 (t, 2 H, $J = 7.5$ Hz), 7.40 (t, 2 H, $J = 7.5$ Hz), 7.78 (d, 2 H, $J = 7.5$ Hz); ^{13}C NMR (75.5 MHz, CDCl_3) δ 172.0, 143.3, 135.7, 129.4, 127.9, 127.8, 123.3, 120.9, 106.5, 32.5, 29.1; MS (EI) m/e 274.2 (M^+), 259.4, 232.3.

Irradiation of 5-Phenyl-3-spirofluorenyl-3H-pyrazole (2.13a) at Room Temperature. The pyrazole **2.13a** was irradiated in toluene according to the general photolytic procedures described above. The reaction is very clean and the only product found was 1-phenylspiro[cyclopropene-3,9'-fluorene] (**2.7a**).

Irradiation of 5-Phenyl-3-spirofluorenyl-3H-pyrazole (2.13a) in Toluene Matrix at 77 K. The procedures are as described

above in general photolytic procedures; 1-phenylspiro[cyclopropene-3,9'-fluorene] (2.7a) was the only product isolated.

Irradiation of 5-*t*-Butyl-3-spirofluorenyl-3H-pyrazole (2.13b) at Room Temperature. Basically, the procedures are as described above in general photolytic procedures except that the pyrazole was irradiated in toluene. The reaction is very clean and the only product found was 1-*t*-butylspiro[cyclopropene-3,9'-fluorene] (2.7b).

Irradiation of 5-*t*-Butyl-3-spirofluorenyl-3H-pyrazole (2.13b) in Toluene Matrix at 77 K. The procedures are as described above in general photolytic procedures; 1-*t*-butylspiro[cyclopropene-3,9'-fluorene] (2.7b) was the only product.

Irradiation of 5-Phenyl-3-spirofluorenyl-3H-pyrazole (2.13a) in a Mixture of Cyclohexene and Toluene at Room Temperature or 77 K. A solution of 5-phenyl-3-spirofluorenyl-3H-pyrazole (2.13a) (0.1 M) was prepared in a mixture of cyclohexene and toluene (7:3, v/v). The solution was degassed, irradiated and worked up as described above. The reaction was very clean and the only product found is 1-phenylspiro[cyclopropene-3,9'-fluorene] (2.7a).

Irradiation of 5-Phenyl-3-spirofluorenyl-3H-pyrazole (2.13a) in a Mixture of Methanol and Toluene at Room Temperature or 77 K. A solution of 5-phenyl-3-spirofluorenyl-3H-pyrazole (2.13a) (0.1 M) was prepared in a mixture of methanol and toluene (7:3, v/v). The solution was degassed, irradiated and worked up as described above. The reaction is clean and the only product found was 1-Phenylspiro[cyclopropene-3,9'-Fluorene] (2.7a).

Irradiation of 5-Phenyl-3-spirofluorenyl-3H-pyrazole (2.13a) in a Mixture of 2-Propanol and Toluene at Room Temperature or 77 K. A solution of 5-phenyl-3-spirofluorenyl-3H-pyrazole (2.13a) (0.1 M) was prepared in a mixture of 2-propanol and toluene (7:3, v/v). The solution was degassed, irradiated and worked up as described above. The reaction is clean and the only product found is 1-Phenylspiro[cyclopropene-3,9'-Fluorene] (2.7a).

Irradiation of 5-Phenyl-3-spirofluorenyl-3H-pyrazole (2.13a) in a Mixture of Acetic Acid, Methanol and Toluene at Room Temperature or 77 K. A solution of 5-phenyl-3-spirofluorenyl-3H-pyrazole (2.13a) (0.1 M) in a mixture of acetic acid, methanol and toluene (0.5:8:2, v/v) was degassed, irradiated and worked up as described above. The reaction is clean and the only product found was 1-Phenylspiro[cyclopropene-3,9'-Fluorene] (2.7a).

Thermolysis of 5-Phenyl-3-spirofluorenyl-3H-pyrazole (2.13a) in Acetic Acid. A solution of 5-phenyl-3-spirofluorenyl-3H-pyrazole (2.13a) (14.7 mg, 0.05 mmol) in acetic acid (4 mL) was refluxed for 1.5 hours until all starting material was gone, as shown by TLC. The solution was poured into benzene (100 mL). The benzene solution was washed with aqueous saturated sodium bicarbonate solution three times and dried over magnesium sulfate. After removal of solvent, the residue was directly subjected to NMR analysis. Only 1-phenylspiro[cyclopropene-3,9'-fluorene] (2.7a) was detected.

Electron Spin Resonance Studies. Irradiation of a dilute degassed solution ($\sim 5 \times 10^{-3}$ M) of 9-diazo fluorene in polycrystalline

phenylacetylene cooled to 77 K in the microwave cavity of an ESR spectrometer gave rise not to the well-known ESR spectrum of triplet fluorenylidene formed in other matrices but to the triplet spectrum shown in Figure 2.1. The lifetime of the triplet species was at least several hours in the low temperature matrix. A similar triplet ESR spectrum was obtained from irradiation of a dilute degassed solution ($\sim 5 \times 10^{-3}$ M) of 5-phenyl-3-spirofluorenyl-3H-pyrazole (2.13a) in toluene/pentane (1:1) or phenylacetylene matrices at 77 K, as shown in Figure 2.1.

The similar procedures described above for irradiation of 9-diazafluorene in 1-hexyne and hex-1-yne-6-ol were carried out in the neat alkyne or in dry toluene/pentane (1:1). The ESR spectrum for 9-diazafluorene reacting with 1-hexyne was shown in Figure 2.2 and a similar spectrum was obtained for 9-diazafluorene reacting with 5-hexyn-1-ol under the same condition.

Procedures similar to those described above for irradiation of 9-diazafluorene in 3,3-dimethylbutyne were carried out in the neat alkyne or in dry toluene/pentane (1:1). A triplet ESR spectrum was obtained but was not considered very successful due to significant radical contamination; however, this spectrum, judged from the non-free-radical region, was still different from the ESR spectrum of triplet fluorenylidene.

A procedure analogous to that given for irradiation of 5-*t*-butyl-3-spirofluorenyl-3H-pyrazole (2.13b) was carried out in toluene/pentane (1:1) or 3,3-dimethyl-1-butyne matrices at 77 K and the ESR spectrum was shown in Figure 2.3.

Irradiation of 1-phenyl-spiro[cyclopropene-3,9'-fluorene] (2.7a) in phenylacetylene or dry toluene/pentane (1:1) matrices at 77 K gave only a featureless free-radical signal.

Only the triplet fluorenylidene ESR spectrum was obtained from the irradiation of 9-diazo fluorene in neat propargyl chloride or propargyl bromide (80% w/w in toluene) at 77 K followed the above similar procedures.

Irradiation of 9-Diazo fluorene in 1,5-Hexadiyne at Room Temperature or 77 K. The procedures were as described above in general photolytic procedures. Only one major product, 1-(3-butynyl)spiro[cyclopropene-3,9'-fluorene] (2.14), was found for both photolysis at room temperature and at 77 K: ^1H NMR (300 MHz, CDCl_3) δ 1.98 (t, 1 H, $J = 2.5$ Hz), 2.43 (td, 2 H, $J = 7.5, 2.5$ Hz), 2.82 (td, 2 H, $J = 7.5$ Hz), 7.08 (s, 1 H), 7.19 (d, 2 H, $J = 7.6$ Hz), 7.30 (td, 2 H, $J = 7.6, 1.5$ Hz), 7.37 (td, 2 H, $J = 7.6, 1.5$ Hz), 7.84 (d, 2 H, $J = 7.6$ Hz); ^{13}C NMR (75.5 MHz, CDCl_3) δ 149.3, 139.7, 126.3, 126.0, 120.8, 120.5, 119.7, 102.1, 82.7, 69.3, 36.2, 24.4, 17.4, 17.2; MS (EI) m/e 242 (M^+), 241, 203, 202.

Irradiation of 9-Diazo fluorene in 1,7-Octadiyne at Room Temperature or 77 K. The procedures were the same as described above in general photolytic procedures. Only one major product, 1-(5-hexynyl)-spiro[cyclopropene-3,9'-fluorene] (2.15), was found for both photolysis in solution and in 1,7-hexadiyne matrix at 77 K: ^1H NMR (75.5 MHz, CDCl_3) δ 1.5-1.78 (complex, 4 H), 1.92 (t, 1 H, $J = 3.0$ Hz), 2.15 (td, 2 H, $J = 6.7, 3.0$ Hz), 2.60 (td, 2 H, $J = 7.5$ Hz), 6.95 (s,

1 H), 7.14 (d, 2 H, $J = 7.0$ Hz), 7.29 (td, 2 H, $J = 7.0, 1.7$ Hz), 7.35 (td, 2 H, $J = 7.0, 1.7$ Hz), 7.84 (d, 2 H, $J = 7.0$ Hz); ^{13}C NMR (75.5 MHz, CDCl_3) δ 149.6, 139.6, 126.3, 125.8, 122.2, 120.4, 119.7, 100.4, 84.0, 68.5, 36.2, 27.8, 26.5, 24.1, 18.0; MS (EI) m/e 270 (M^+), 269, 242, 241, 216, 215, 203, 202, 189, 178, 165.

Irradiation of 9-Diazofluorene in 5-Hexyn-1-ol at Room Temperature or 77 K. The procedures were as described above in general photolytic procedures. Only one major product, 9-fluorenyl 5-hexynyl ether (**2.16**) was found: ^1H NMR (300 MHz, CDCl_3) δ 1.60 (m, 4 H), 1.89 (t, 1 H, $J = 2.6$ Hz), 2.12 (m, 2 H), 3.16 (t, 2 H, $J = 6.0$ Hz), 5.61 (s, 1 H), 7.31 (dd, 2 H, $J = 7.3, 1.2$ Hz), 7.38 (tm, 2 H, $J = 7.3$ Hz), 7.60 (d, 2 H, $J = 7.3$ Hz), 7.66 (d, 2 H, $J = 7.3$ Hz); ^{13}C NMR (75.5 MHz, CDCl_3) δ 143.0, 140.8, 128.9, 127.5, 125.4, 119.9, 84.3, 80.6, 68.3, 63.9, 29.1, 25.1, 18.1; IR cm^{-1} 3299 (s), 2941(s), 2869(s), 2050(w); MS (EI) m/e 262 (M^+), 182, 181, 180, 165, 152, 139.

Irradiation of 9-Diazofluorene in Propargyl Bromide at 77 K. A solution of 9-diazofluorene (16.3 mg, 0.085 mmol) in propargyl bromide (0.5 mL, 80% w/w in toluene) was prepared in an NMR tube. The solution was deaerated by three freeze-pump-thaw cycles. The setup of irradiation was same as described above. The solution was irradiated for 11 h, while the solution was warmed to room temperature for every 1.5 h. After removal of solvent, the residue was separated by flash column chromatography over silica gel eluting with methylene chloride/hexane (20%). Besides trace amount of fluorenone, 2-bromo-3,9'-fluorenylidenyl-propene (**2.18**) was the only major product: ^1H NMR (300 MHz, CDCl_3) δ 5.98 (t, 1 H, $J = 1.5$ Hz), 6.15 (t, 1 H, $J = 1.9$

Hz), 7.00 (s, 1 H), 7.18-7.25 (m, 2 H), 7.35 (t, 2 H, $J = 7.6$ Hz), 7.58 (m, 3 H), 8.22 (d, 1 H, $J = 7.7$ Hz); Selected decoupling ^1H NMR δ 5.98, 6.15 and 7.00 were coupling each other; ^{13}C NMR (75.5 MHz, CDCl_3) δ 157.0, 138.3, 129.4, 127.8, 127.2, 127.1, 125.6, 125.3, 124.4, 121.8, 120.7, 119.8, 119.7; MS (EI) m/e 284 (M^{++2}), 282 (M^+), 204, 203, 202, 200, 101.

Irradiation of 9-Diazofluorene in Propargyl Bromide at Room Temperature. A solution of 9-diazofluorene (101.2 mg, 0.53 mmol) in propargyl bromide (5 mL, 80% w/w in toluene) was prepared in an NMR tube. The solution was deaerated by three freeze-pump-thaw cycles. The setup of irradiation was the same as described above and the solution was irradiated for 2 h. After removal of solvent, the residue was separated with flash chromatography eluting over silica gel with methylene chloride/hexane (20%). Only 2-bromo-3,9'-fluorenylidenyl-propene (2.18) has been isolated.

Irradiation of 9-Diazofluorene in Propargyl Chloride at 77 K. A solution of 9-diazofluorene (19.0 mg, 0.099 mmol) in propargyl chloride (0.5 mL) was prepared in an NMR tube. The solution was deaerated by three freeze-pump-thaw cycles. The setup of irradiation was the same described as above. The solution was irradiated for 11 h, with warming to room temperature and mixing every 1.5 h. After removal of solvent, the residue was separated by flash chromatography over silica gel eluting with methylene chloride/hexane (20%). Five compounds were isolated: 2-chloro-3,9'-fluorenylidenyl-propene (2.21): ^1H NMR (300 MHz, CDCl_3) δ 5.76 (s, 1 H), 5.79 (s, 1 H), 6.91 (s, 1 H), 7.21 (d, 1 H, $J = 7.8$ Hz), 7.24-7.46 (m, 3 H), 7.68 (m, 3 H), 8.23 (d, 1 H, J

= 7.8 Hz); ^{13}C NMR (75.5 MHz, CDCl_3) δ 143.8, 140.0, 139.5, 138.5, 137.7, 135.7, 135.3, 129.3, 129.2, 128.0, 127.2, 127.1, 125.8, 125.5, 122.5, 120.6, 120.1, 119.8, 119.7, 117.9; MS (EI) m/e 240 (M^{++2}), 238 (M^+), 236, 204, 203, 202, 200, 101. 1-(chloromethyl)-spiro[cyclopropene-3,9'-fluorene] (2.22) ^1H NMR (300 MHz, CDCl_3) δ 4.55 (d, 2 H, $J = 1.5$ Hz), 7.22 (d, 2 H, $J = 7.2$ Hz), 7.34 (td, 2 H, $J = 7.3, 1.1$ Hz), 7.42 (m, 3 H), 7.87 (d, 2 H, $J = 8.7$ Hz); ^{13}C NMR (75.5 MHz, CDCl_3) δ 147.8, 139.9, 126.7, 126.6, 120.8, 119.9, 119.1, 106.1, 39.1, 36.1; MS (EI) m/e 240 (M^{++2}), 238 (M^+), 204, 203, 202, 200, 101. 9-chloro-fluorene (2.23): ^1H NMR (300 MHz, CDCl_3) δ 5.75 (s, 1 H), 7.33 (td, 2 H, $J = 7.8, 1.5$ Hz), 7.46 (td, 2 H, $J = 7.8, 1.5$ Hz), 7.66 (d, 2 H, $J = 7.8$ Hz), 7.82 (d, 2 H, $J = 7.8$ Hz); ^{13}C NMR (75.5 MHz, CDCl_3) δ 157.0, 140.0, 129.3, 128.0, 125.8, 120.1, 57.5; MS (EI) m/e 202 (M^{++2}), 200 (M^+), 180, 166, 165, 163, 83, 82. bifluorenylidene (2.5): ^1H NMR (300 MHz, CDCl_3) δ 7.19 (t, 2 H, $J = 7.1$ Hz), 7.31 (t, 2 H, $J = 7.1$ Hz), 7.68 (d, 2 H, $J = 8.1$ Hz), 8.38 (d, 2 H, 8.1 Hz); ^{13}C NMR (75.5 MHz, CDCl_3) δ 141.3, 138.2, 129.1, 126.8, 126.7, 119.9; MS (EI) m/e 329 (M^{++1}), 328 (M^+), 327, 326, 324, 164, 163, 162, 150, 149. And there was trace amount of 9-fluorenone (2.4).

Irradiation of 9-Diazo fluorene in Propargyl Chloride at Room Temperature. A solution of 9-diazo fluorene (56.1 mg, 0.29 mmol) in propargyl chloride (5 mL) was prepared in an NMR tube. The solution was deaerated by three freeze-pump thaw cycles. The solution was irradiated as described above for 2 h. After removal of solvent, the residue was separated by flash chromatography over silica gel eluting with methylene chloride/hexane (20%). Besides the same five products as

above, there was another product: 3-chloro-3,9'-fluorenyl-propyne (**2.24**): ^1H NMR (300 MHz, CDCl_3) δ 2.49 (d, 1 H, $J = 2.4$ Hz), 4.39 (d, 1 H, $J = 4.1$ Hz), 5.20 (dd, 1 H, $J = 4.0, 2.4$ Hz), 7.38 (t, 2 H, $J = 7.5$ Hz), 7.43 (t, 2 H, $J = 7.5$ Hz), 7.72-7.82 (m, 4 H); ^{13}C NMR (75.5 MHz, CDCl_3) δ 141.8, 138.6, 128.6, 128.3 (doublet), 127.2 (doublet), 125.1, 119.9 (doublet), 80.0, 75.5, 52.8, 49.8; MS (EI) m/e 240 (M^{++2}), 238(M^+), 203, 202, 200, 166, 165. IR cm^{-1} 3291 (m), 1450 (s).

Bromide Exchange of 1-(Chloromethyl)-spiro[cyclopropene-3,9'-fluorene] (2.22**).** A solution of the cyclopropene (**2.22**) (9.6 mg, 0.04 mmol) and lithium bromide (86.9 mg, 1 mmol) in methanol (10 mL) was refluxed for 10 hours. After removal of the solvent, the residue was directly subjected to NMR. Only 1-(chloromethyl)-spiro[cyclopropene-3,9'-fluorene] (**2.22**) and 2-bromo-3,9'-fluorenylidenyl-propene (**2.18**) were found.

Yield Studies. A solution of 9-diazafluorene (14.6 g, 0.076 mmol), propargyl chloride (3 mL) and 1,2-dichloroethane (3 mL) was prepared. The degassing and irradiation procedures were the same as described above for 77 K studies. After removal of the solvent, the residue was transferred to an NMR tube and toluene (2 μL) was injected into the tube prior to analysis. The yields were determined by ^1H NMR integration relative to toluene (δ 2.36 ppm) in CDCl_3 . The results are summarized in Table 2.1.

A solution of 9-diazafluorene (11.2 g, 0.058 mmol) with various ratios of propargyl chloride and 1,2-dichloroethane were prepared. The degassing and irradiation procedures were the same as described above

for room temperature studies. After removal of the solvent, the residue was transferred to an NMR tube and toluene (2 μ L) was injected into the tube prior to analysis. The yields were determined by ^1H NMR integration relative to toluene (δ 2.36 ppm) in CDCl_3 . The results are summarized in Table 2.1.

2.6 References and Notes:

- (1) Baron, W. J.; Hendrick, M. E.; Jones, M., Jr. *J. Am. Chem. Soc.* **1973**, *95*, 6286-6294.
- (2) Baron, W. J.; DeCamp, M. R.; Hendrick, M. E.; Jones, M., Jr.; Levin, R. H.; Sohn, M. B. In *Carbenes*; M. Jones Jr. and R. A. Moss, Ed.; Wiley: New York, 1973; Vol. I; pp 73-84.
- (3) Griller, D.; Nazran, A. S.; Scaiano, J. C. *Acc. Chem. Res.* **1984**, *17*, 283-289.
- (4) Platz, M. S. In *Kinetics and Spectroscopy of Carbenes and Biradicals*; M. S. Platz, Ed.; Plenum: New York, 1990; pp 143.
- (5) Savino, T. G.; Senthilnathan, V. P.; Platz, M. S. *Tetrahedron* **1986**, *42*, 2167-2180.
- (6) Wright, B. B.; Platz, M. S. *J. Am. Chem. Soc.* **1984**, *106*, 4175-4180.
- (7) Turro, N. J. *Tetrahedron* **1982**, *38*, 809.

- (8) Grasse, P. B.; Brauer, B.-E.; Zupancic, J. J.; Kaufmann, K. J.; Schuster, G. B. *J. Am. Chem. Soc.* **1983**, *105*, 6833-6845.
- (9) Moss, R. A.; Joyce, M. A. *J. Am. Chem. Soc.* **1978**, *100*, 4475-4480.
- (10) Ruzicka, J.; Leyva, E.; Platz, M. S. *J. Am. Chem. Soc.* **1992**, *114*, 897-905.
- (11) We have obtained the crystal structure for compound **2.13a** which is quite similar to the optimized structure by the MNDO method but, we were unable to crystallize the 3,3-diphenyl-5-phenyl-3H-pyrazole. In order to make a fair comparison, both geometries shown in Figure 2.4 are optimized by MNDO method.
- (12) Jackson, J. E.; O'Brien, T., Jr. *J. Phys. Chem.* **1988**, *92*, 2686-2696.
- (13) Leyva, E.; Barcus, R. L.; Platz, M. S. *J. Am. Chem. Soc.* **1986**, *108*, 7786-7788.
- (14) Gaspar, P. P.; Lin, C.-T.; Dunbar, W.; Mack, D. P.; Balasubramanian, P. *J. Am. Chem. Soc.* **1984**, *106*, 2128-2139.
- (15) Moss, R. A.; Dolling, U.-H. *J. Am. Chem. Soc.* **1971**, *93*, 954.

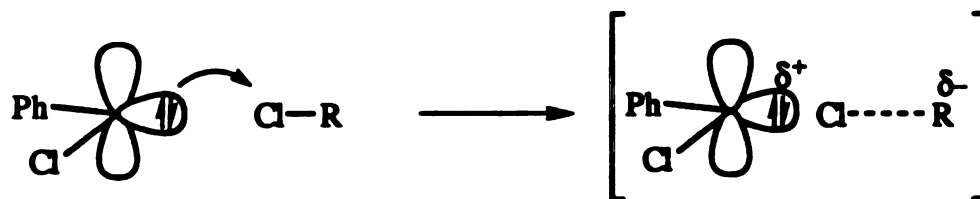
CHAPTER 3

Carbene-to-Carbene Oxygen Transfer Reactions

Abstract: Our initial work on oxygen atom transfers to fluorenylidene from various donors is described. Product studies in benzene and acetonitrile have established that fluorenylidene reacts with pyridine-N-oxide to make 9-fluorenone in high yield. Competition experiments using methanol in acetonitrile over a wide concentration range have shown that the rate constant for oxygen atom transfer to fluorenylidene from pyridine-N-oxide (PNO) exceeds that for O-H insertion into methanol ($k_{\text{PNO}}/k_{\text{MeOH}}$) by a factor of 1.7 ± 0.4 ; together with the literature value for k_{MeOH} , this result yields an absolute rate constant of $k_{\text{PNO}} = 1.5 \pm 0.5 \times 10^9 \text{ M}^{-1}\text{s}^{-1}$. Fluorenylidene is also oxygenated by other substrates: N-methyl morpholine-N-oxide, sulfolane, trimethyl phosphate, and dimethyl carbonate. Unlike the first three, dimethyl carbonate (DMC) should yield not a stable deoxygenated product, but rather dimethoxycarbene. Competition with methanol yields a rate ratio of $k_{\text{DMC}}/k_{\text{MeOH}} = 1.1 \pm 0.3 \times 10^{-3}$ in dimethyl carbonate solvent. We have not yet demonstrated the presence of products from the stabilized carbene, but the new observations are consistent with the known reactivity of fluorenylidene with carbonyl compounds to form ylides, and with the strong stabilizing effects of donor groups such as methoxy on carbene stability. The net oxygen atom-transfer from one carbene to another represents a new mode of carbene reactivity.

3.1 Introduction:

Atom abstraction is an important type of carbene reaction,¹ with hydrogen and chlorine atom-transfer being the two most familiar examples. It is well accepted that a triplet carbene is responsible for the hydrogen atom-transfer,¹⁻³ but this is not always true for chlorine atom-transfer. By using CIDNP to study the reactions of many types of carbenes with chloroform, Roth clearly showed that hydrogen abstraction is due to a triplet precursor, whereas the corresponding singlet carbenes preferentially abstract chlorine.⁴ Roth also demonstrated that both singlet and triplet states of methylene can abstract chlorine atoms from suitable donors. More recently, Platz et al. have examined the reactions of singlet phenylchlorocarbene and triplet diphenylcarbene with carbon-chlorine bonds using laser flash photolysis techniques.¹ These workers indicated that the transition states of both reactions have considerable carbene-chlorine bond formation and charge development. They also showed that the rate

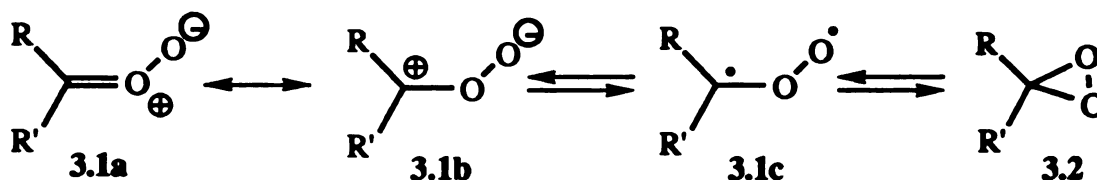


constants for triplet diphenylcarbene reacting with chlorine donors are roughly one order of magnitude faster than those for singlet phenylchlorocarbene.

Extensive reviews have been written about ylide formation resulting from the interaction of a carbene with the lone-pair electrons of heteroatoms such as oxygen, nitrogen, phosphorus, and sulfur. However, there are few cases in which a carbene abstracts a divalent atom or group,

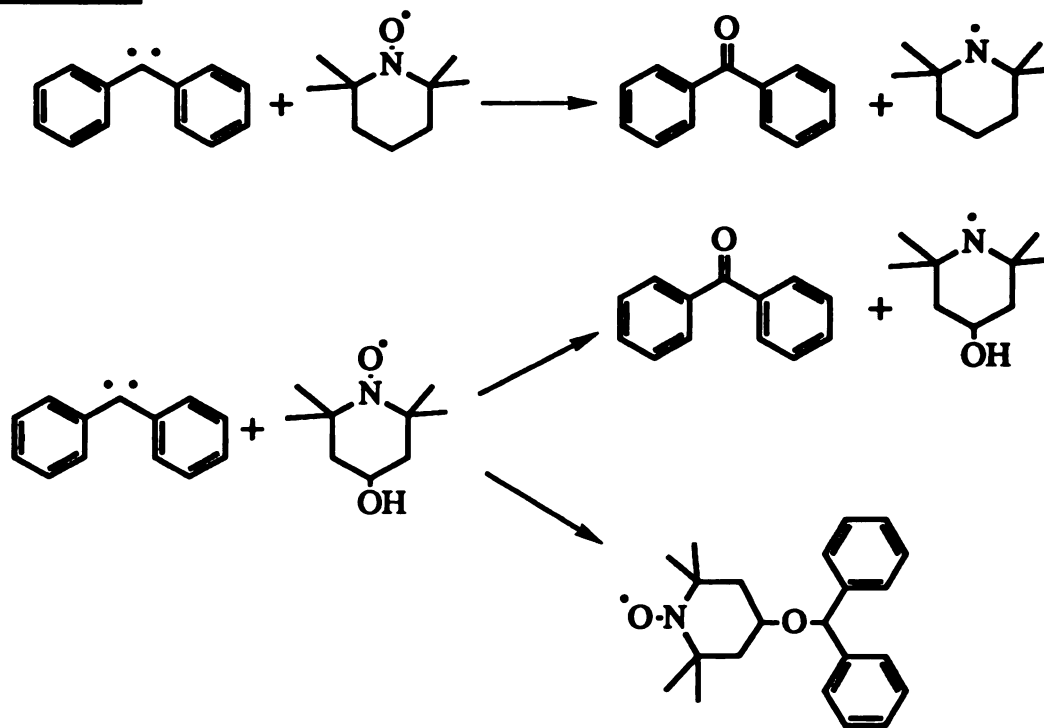
such as oxygen, to produce a closed-shell species having a double bond between the former carbenic center and the transferred fragment.^{5,6}

Reactions of carbenes with molecular oxygen have been well studied owing to interest in the intermediate carbonyl oxide (3.1), which plays a role in the mechanism of ozonolysis, and in its isomeric form, the dioxirane (3.2).⁷ It has also been known for some time that carbon atoms

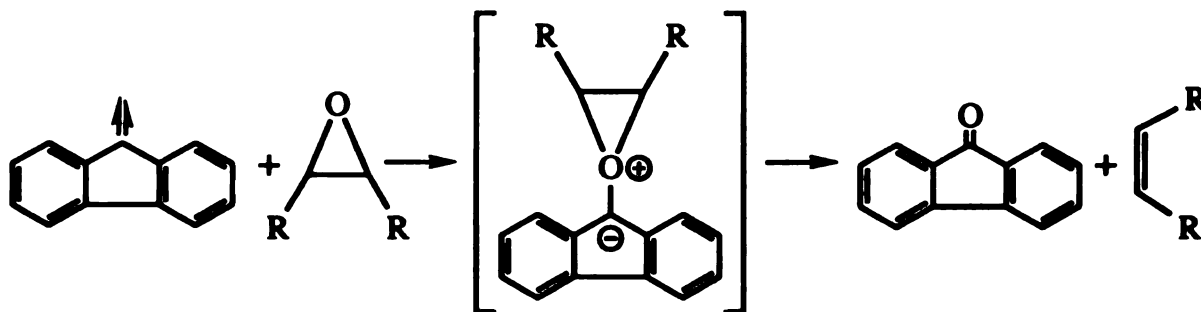


abstract oxygen from a wide variety of carbonyl compounds to produce carbon monoxide and carbenes.⁸ These reactions are not understood in full detail but they are enormously exothermic, producing "hot" carbenes which can undergo a variety of thermally activated processes.⁹ However, there are just a few reported cases in which a free carbene abstracts oxygen from a donor other than molecular oxygen.

In 1984, Scaiano and co-workers studied the reactions of triplet diphenylcarbene with nitroxides¹⁰ (Scheme 3.1). These reactions involve oxygen-transfer, leading to quantitative yields of benzophenone. In the case of 4-hydroxy-2,2,6,6-tetramethylpiperidine-N-oxide, the triplet diphenylcarbene deoxygenates the nitroxide center instead of inserting into the O-H bond. Field and Schuster later showed that triplet anthronylidene is oxidized by molecular oxygen at a nearly diffusion-controlled rate which is two orders of magnitude faster than oxidation of the same carbene by pyridine-N-oxide.¹¹ In a study of the reactions of epoxides with fluorenylidene, Shields and Schuster observed equimolar amounts of

Scheme 3.1

9-fluorenone and the respective alkene resulting from the stereospecific deoxygenation of the epoxide.¹² These workers also found that diphenylcarbene does not efficiently abstract oxygen from epoxides. They concluded that the deoxygenation of epoxides was proceeding by addition of the singlet state of the carbene to the epoxides to form an oxonium ylide which rearranges to give a carbonyl compound and an olefin with retained stereochemistry (Scheme 3.2).

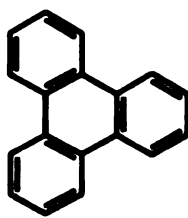
Scheme 3.2

In this work, other oxygen donors were sought which could be deoxygenated by fluorenylidene. As shown in earlier studies, different spin states of carbenes show different preferences for oxygen donors. For example, triplet diphenylcarbene abstracts an oxygen atom from doublet TEMPO or triplet molecular oxygen, whereas singlet fluorenylidene reacts with closed-shell oxygen-donors such as epoxides. This bias suggests that oxygen atom-transfer could be used to determine singlet versus triplet pathways in reactions of arylcarbenes which have small singlet-triplet energy gaps.

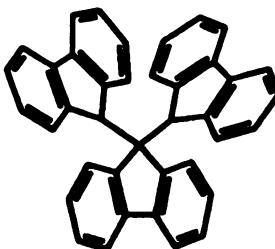
3.2 Results:

Product Studies. Photolyses of 9-diazo fluorene with pyridine-N-oxide or 4-picoline-N-oxide in dry, degassed acetonitrile afforded 9-fluorenone as the major product (> 70%), and bifluorenyl and bifluorenylidene as minor byproducts.

Similar results were obtained with other oxygen donors, such as sulfolane and N-methyl morpholine-N-oxide, examined similarly or used neat as solvents (sulfolane and trimethyl phosphate). Reactions carried out in dry benzene gave two additional minor byproducts (< 5%): triphenylene (3.3)¹³ and 9,9':9,9''-terfluorene (3.4).¹⁴⁻¹⁶



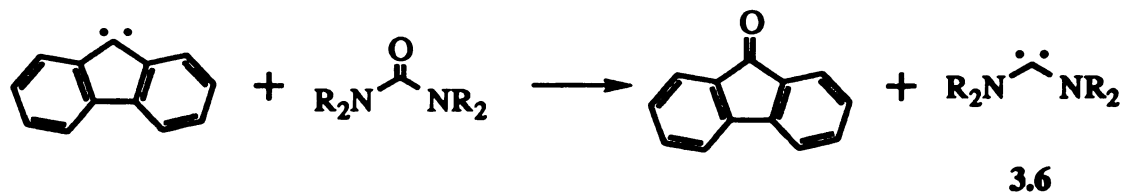
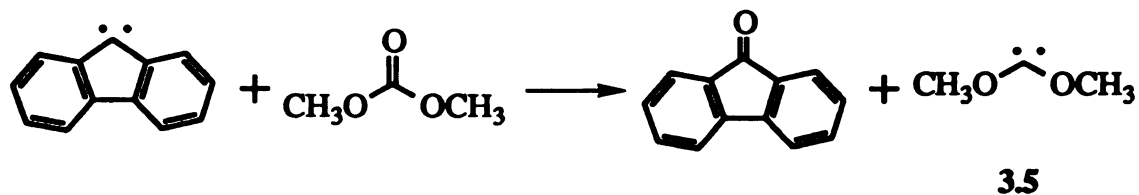
3.3



3.4

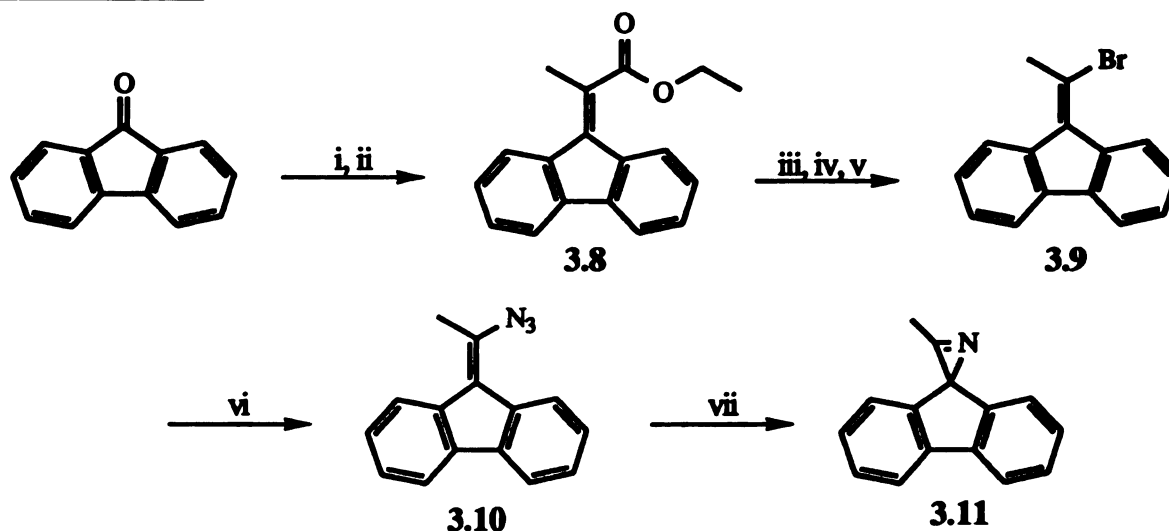
In light of the stability of dialkoxy- (3.5) and diamino- (3.6) carbenes, we extended our study to include dimethyl carbonate, tetramethylurea, and 1,3-dimethylimidazolin-2-one. As with the more traditional oxidants, fluorenylidene reacted with these substrates to give 9-fluorenone; the corresponding stabilized carbenes are implied as by-products.

Scheme 3.3

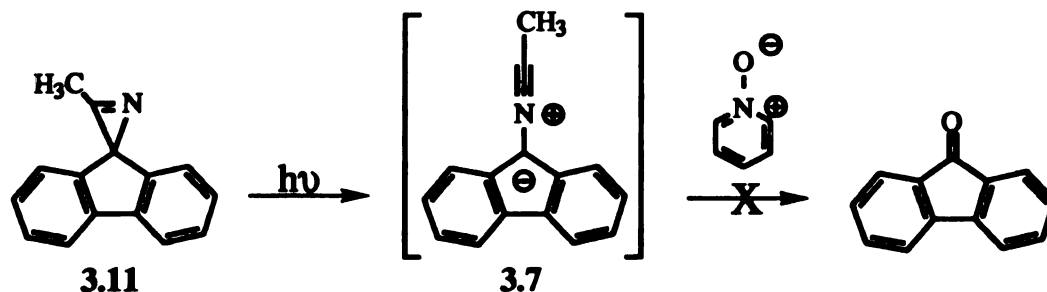


Control Experiments. To show that pyridine-N-oxide does not oxidize the fluorenylidene - acetonitrile ylide (3.7) to give 9-fluorenone, we independently synthesized 2,2-(2,2'-biphenylene)-3-methyl-2H-azirine (3.11),¹⁷ a direct photolytic precursor to 3.7, by the route shown in Scheme 3.4. No 9-fluorenone was detected from photolysis of the azirine in acetonitrile in the presence of pyridine-N-oxide¹⁸ (Scheme 3.5).

Rate Studies. Estimates of the absolute rates of reaction of fluorenylidene with all oxygen-donors were made using the competition method with methanol and the literature value for the methanol quenching

Scheme 3.4

- i. $\text{CH}_3\text{CH}(\text{Br})\text{CO}_2\text{C}_2\text{H}_5$, Zn, benzene-ether (4:1). ii. TsOH, benzene.
 iii. KOH, H_2O -EtOH (1:1). iv. Br_2 , CCl_4 . v. KOH (0.2 N). vi. NaN_3 , DMF.
 vii. benzene, reflux.

Scheme 3.5

rate of fluorenylidene in acetonitrile ($k_{\text{MeOH}} = 8.95 \times 10^8 \text{ M}^{-1} \text{ s}^{-1}$).¹⁹ Ratios of 9-fluorenone to 9-methoxyfluorene products were determined either by NMR or GC analysis. For all oxygen-donors, except dimethyl carbonate and trimethyl phosphate, the studies were run in dry acetonitrile solvent. A range of absolute concentrations and concentration ratios of oxygen-donor to methanol were examined to ensure that the observed product ratios reflected only direct reactions of fluorenylidene with the substrates and not the same products formed via indirect pathways. The results are summarized in Table 3.1.

Table 3.1 Rate Constants for Oxygen Transfer to Fluorenylidene

| Substrate | $k_{\text{sub}}/k_{\text{MeOH}}$ (# of evaluations) | $k_{\text{sub}}(\text{M}^{-1} \text{s}^{-1})$ |
|---|---|---|
| methanol | (1.0) | 8.95×10^8 |
| pyridine-N-oxide | 1.7 ± 0.4 (30) | 1.5×10^9 |
| 4-picoline-N-oxide | 1.7 ± 0.1 (3) | 1.5×10^9 |
| 1,3-dimethylimidazolin-2-one | $5.2 \pm 0.2 \times 10^{-1}$ (9) | 4.7×10^8 |
| tetramethylurea | $4.9 \pm 0.2 \times 10^{-1}$ (9) | 4.4×10^8 |
| trimethyl phosphate | $1.4 \pm 0.1 \times 10^{-2}$ (3) | 1.3×10^7 |
| dimethyl carbonate | $1.2 \pm 0.2 \times 10^{-3}$ (3) | 1.0×10^6 |
| <i>cis</i> -2,3-epoxybutane ¹² | | 3.1×10^8 |
| <i>trans</i> -2,3-epoxybutane ¹² | | 9.3×10^8 |

Photolyses of diphenyldiazomethane with pyridine-N-oxide in acetonitrile were carried out similarly, and the rate constant of oxygen transfer to diphenylcarbene was estimated from the ketone/ether product ratio (or oxygen transfer over O-H insertion) obtained from the ^1H NMR spectra, along with the literature value for the methanol quenching rate of diphenylcarbene in acetonitrile ($k_{\text{MeOH}} = 2.4 \times 10^7 \text{ M}^{-1} \text{ s}^{-1}$).²⁰ The rate constant for oxygen transfer from pyridine-N-oxide to diphenylcarbene is essentially the same as that for O-H insertion ($k = 2.4 \times 10^7 \text{ M}^{-1} \text{ s}^{-1}$).

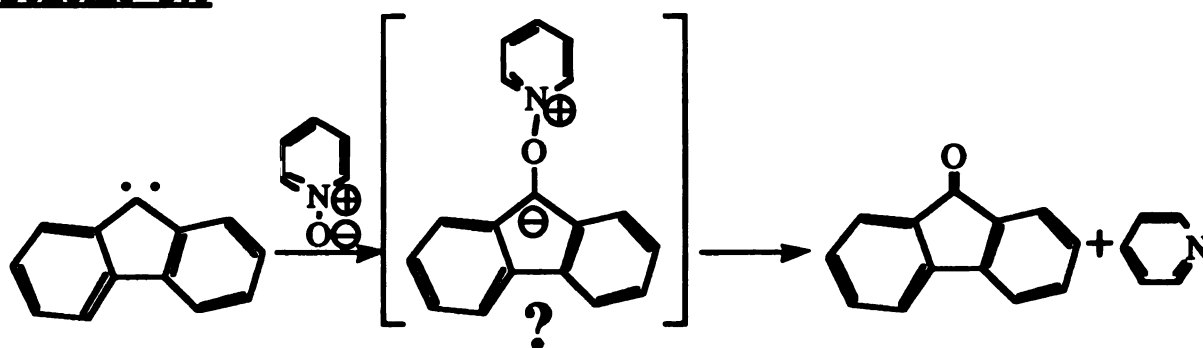
3.3 Discussion:

Despite the fact that the ground state of fluorenylidene is a triplet, it exhibits significant singlet reactivity under most experimental conditions at room temperature due to a small singlet-triplet energy gap

(~1.1 kcal/mol in CH₃CN).^{18,21-23} Therefore, it is assumed that the singlet fluorenylidene is responsible in the spin-allowed deoxygenation reactions described here. Although it is well-known that singlet carbenes often react with non-bonding electron pairs to form ylide,^{24,25} none of these ylide species are known to undergo the atom-transfer process.

Oxygen atom abstraction from pyridine-N-oxide, which is believed to be an extraordinary singlet carbene quencher,^{26,27} has been known for years. In this work, a rate constant of $1.5 \times 10^9 \text{ M}^{-1}\text{s}^{-1}$ was obtained for the reaction between fluorenylidene and pyridine-N-oxide. This was the only substrate studied that was found to be faster than methanol in reaction with fluorenylidene. As shown in Table 3.2, the oxygen atom-transfer from pyridine-N-oxide to fluorenylidene is quite exothermic (ca. 124 kcal/mol) (Scheme 3.6). This is not surprising, since the C=O double bond in 9-fluorenone is much stronger than the N⁺-O-bond in pyridine-N-oxide. Since it is known that pyridine-N-oxide can also

Scheme 3.6



function as an oxidizing agent, we have photolyzed azirine (3.7) with pyridine-N-oxide in acetonitrile in order to rule out oxidation of the acetonitrile ylide 3.8 as a source of 9-fluorenone. No 9-fluorenone was found in these reactions (Scheme 3.5). So, there is no

**Table 3.2: Heats of Formation of X=O and X: Species
(AM1 Calculated Values in Parentheses)**

| X: | $\Delta H_f(X:)^a$ | $\Delta H_f(XO)^a$ | Difference ^b | ΔH_{rxn} |
|-------------------------------------|----------------------------|----------------------|----------------------------|------------------|
| ¹ Fl: | 156 ^c (154) | 13 ^d (34) | 143,121 ^d (120) | 0.0 |
| C ₅ H ₅ N: | 33 (32) | 14 (40) | 19 (-8) | -124 (-128) |
| (MeO) ₂ C: | -55,-61 ^e (-53) | -139 (-137) | 80 (84) | -63 (-36) |
| (Me ₂ N) ₂ C: | (40.0) | (-24) | (64) | (-56) |
| (MeO) ₃ P: | -167 (-189) | -265 (-259) | 98 (70) | -45 (-50) |

^a Unless otherwise noted, these are ΔH_f values at 298 K, taken from Lias, S. G.; Bartmess, J. E.; Liebman, J. F.; Holmes, J. L.; Levin, R. D.; Mallard, W. G.; "Gas Phase Ion and Neutral Thermochemistry" *J. Phys. Chem. Ref. Data* **1988**, *17*, Suppl. 1. We thank Professor J. A. Allison for generously sharing his copy of this essential document with us.

^b Note that the ΔH_f of oxygen atom is 59.6 kcal/mol at 298 K; the C=O bond strengths can then be calculated by adding this quantity + 3/2RT to the values listed in the difference column. Thus, for example, the C=O bond strength in CH₂O is 128 + 60 + 1 = 189 kcal/mol.

^c Li, Y.; Schuster, G. B. *J. Org. Chem.* **1988**, *53*, 1273. This number is based on computational estimates, so it cannot be consider an independent experimental value.

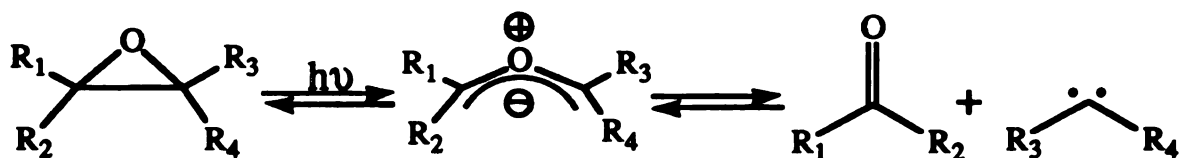
^d Sabbah, R.; Watik, L. E.; Minadakis, C. *Comptes Rendus de l'Academie des Sciences de Paris*, **307**, Serie II, 239 (1988).

^e El-Saidi, M.; Kassam, K.; Pole, D. L.; Tadey, T.; Warkentin, J. *J. Am. Chem. Soc.* **1992**, *114*, 8751.

doubt that the atom-transfer from pyridine-N-oxide to fluorenylidene is the major source of 9-fluorenone.

Although carbonyl ylides have been known for some time,²⁵ no one has reported the formation of a secondary carbene by fragmentation of a carbonyl ylide intermediate generated by carbene addition to a carbonyl compound. However, fragmentations of oxiranes through carbonyl ylide intermediates, as depicted in Scheme 3.7, have been extensively studied experimentally²⁸⁻³² and theoretically.³³⁻³⁷ Contradictions are found between experimental results³² obtained for C-O bond cleavage pathways in substituted oxiranes and predictions based on theoretical calculations.³⁴ The calculations suggest that the

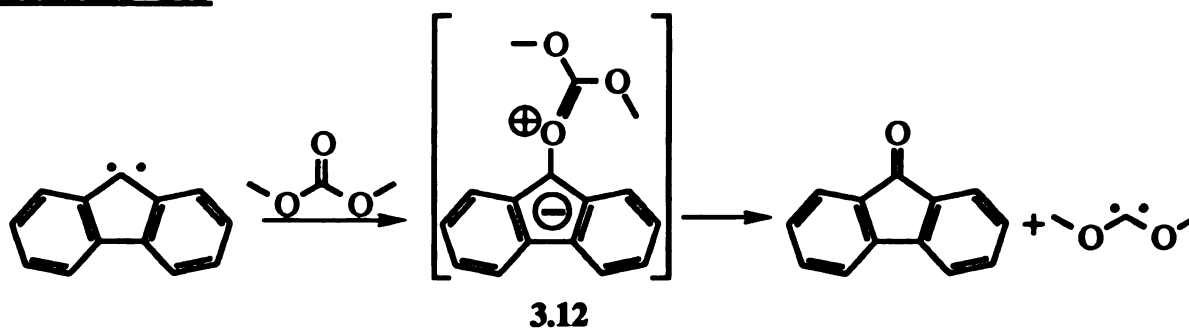
Scheme 3.7



thermochemically preferred mode of fragmentation should be between oxygen and the more electron-rich substituted terminus (i.e. R₃ & R₄ = π electron-donors), which is opposite to the direction observed experimentally by Griffin and co-workers under photolytic conditions (i.e. R₁ & R₂ = π electron-donors).³² Houk et al. conclude that the difference between the thermochemical predictions and experimental results supports the notion that the fragmentation is an excited-state, rather than a ground state process. This conclusion is based on the calculated product stabilities and does not examine the actual preferred pathways of cleavage. Another way to look at it is that if the carbonyl ylides were generated in ground

states before fragmentation, then the regioselectivity of their fragmentation would follow the computational suggestion that the thermochemically preferred mode of fragmentation is between oxygen and the π -electron-donor substituted terminus.

Scheme 3.8

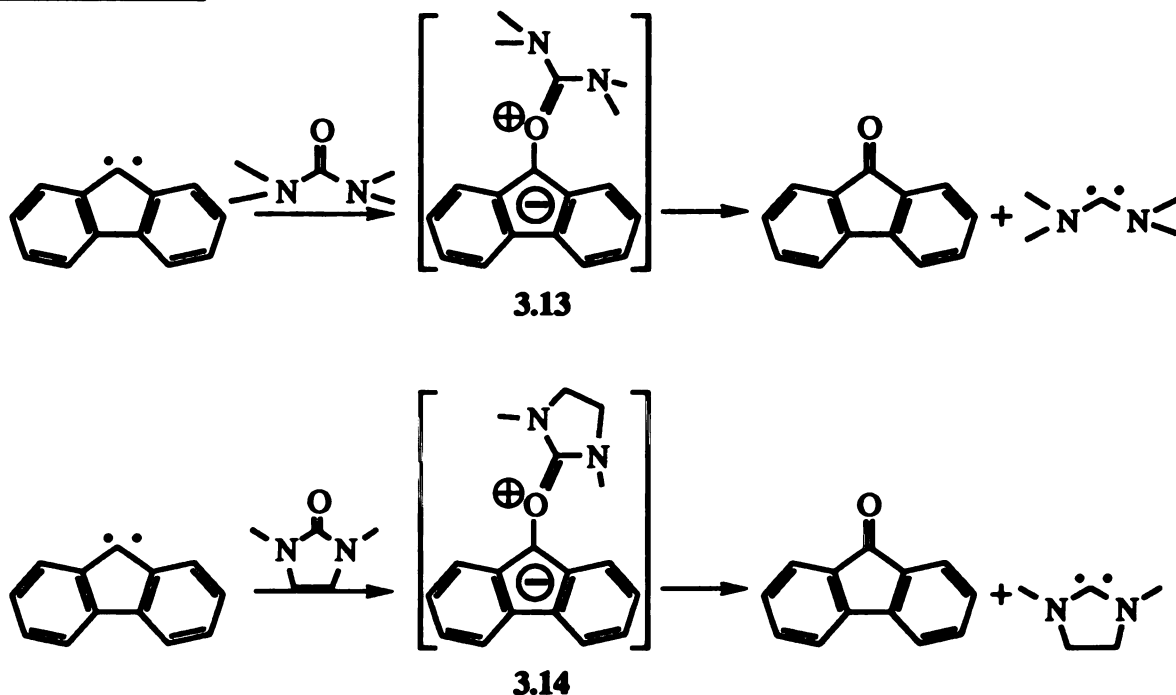


As mentioned previously, fluorenylidene forms a carbonyl ylide with acetone. There is no reason to believe that fluorenylidene would not react with the more electron-rich carbonyl group on dimethyl carbonate to form the carbonyl ylide 3.12 shown in Scheme 3.8. This ylide is similar to those, generated by photolysis of tetra-substituted oxiranes, that can fragment further to a secondary carbene, but the mode of fragmentation of the carbonyl ylides is different from the previous experiments. The simple interpretation is that it is singlet fluorenylidene that reacts with dimethyl carbonate. An alternative interpretation is that the ylide 3.12 may be generated in an excited state but prefers to relax to the ground state before further fragmentation because the anion in ylide 3.12 is stabilized by the 9-fluorenyl system and the cation is significantly stabilized by three alkoxy groups; bond cleavage between oxygen and the more electron-rich substituted side would then occur according to the prediction of Houk et al.

Similar reactions to dimethyl carbonate reacting with fluorenylidene were observed with other oxygen donors like tetramethyl urea and 1,3-dimethyl-2-imidazolinone. Fluorenylidene presumably reacts with ureas to generate carbonyl ylides, followed by C-O bond cleavage from the diamino terminus to give diaminocarbenes and 9-fluorenone, as shown in Scheme 3.9. Unfortunately, so far, we have been unable to trap the secondary carbenes in the reactions.

Trimethyl phosphate was the poorest oxygen-donor examined (Table 3.2). Trimethyl phosphate presumably reacts with fluorenylidene to

Scheme 3.9



afford 9-fluorenone and trimethyl phosphite. Even though we are not sure of the reaction mechanism, the oxygen atom-transfer from trimethyl phosphate to fluorenylidene is worthy of further investigation. We also examined the reactions of fluorenylidene with sulfolane and 4-

methylmorpholine N-oxide. Both reactions form 9-fluorenone but the rate constants have not been determined yet.

3.4 Conclusion:

We have investigated a new type carbene reaction—the oxygen atom-transfer from a carbonyl to fluorenylidene—to give the more stable secondary dimethoxy and diamino carbenes which are not easily generated by a photolytic process. We have not confirmed the presence of products expected from the dimethoxy- and diamino-carbenes, but control experiments in which the oxygen donors are left out show little or no 9-fluorenone product. An ylide intermediate seems likely, but product studies are uninformative on this issue. Nevertheless, the reaction is worthy of further studies by isotopic labeling, laser flash kinetics, and ab initio calculations to check the proposed oxygen transfer pathway and its rates, activation parameters, and thermochemistry.

3.5 Experimental:

General Methods. Dimethyl carbonate was predried over 4 Å molecular sieves overnight and then distilled from calcium hydride. Tetramethylurea and 1,3-dimethyl-2-imidazolidinone were distilled from barium oxide. Trimethyl phosphate was distilled from calcium hydride. Acetonitrile was refluxed over calcium hydride for a minimum of 12 h and then distilled prior to use. Anhydrous methanol was obtained from

Aldrich Chemical Co. and used without further purification. Other general experimental procedures are the same as described in Chapter 2.

General Procedure for Irradiations. A Pyrex tube (1 cm x 10 cm) containing a solution of 9-diazofluorene ($\sim 5 \times 10^{-3}$ M) in and oxygen-donor (0.1 to 1 M) in dry acetonitrile was placed in a water-cooled jacket. After being purged with dry nitrogen gas for 10 mins, the solution was irradiated for 1 h with a 500W high-pressure mercury arc lamp shielded with a uranium glass filter; the nitrogen purge was continued throughout the process of irradiation. After removal of solvent, the mixture was separated by flash chromatography over silica gel.

General Procedure for Measuring Relative Rates of Deoxygenation. A solution of 9-diazofluorene solution was prepared as described above at various oxygen-donor/methanol ratio (0.1:0.1, 0.3:0.1 and 0.3:0.3); the irradiation process was the same as that described above in the general procedure for irradiations.

After removal of solvent, the reaction mixture was directly subjected to ^1H NMR or GC analysis. The relative rates were calculated from either the NMR or GC integral ratio between 9-methoxyfluorene and 9-fluorenone based on the known rate constant for reaction of fluorenylidene with methanol in acetonitrile ($8.95 \times 10^8 \text{ M}^{-1} \text{ sec}^{-1}$).¹⁹ The GC integral ratio was corrected by time a response factor which was calculated from the GC integral ratio from a standard solution of 9-methoxyfluorene and 9-fluorenone in acetonitrile (1:1 mole ratio).

Ethyl α -Fluorenylidene propionate (3.8).¹⁷ A mixture of fluorenone (6.81 g, 37.8 mmol), ethyl- α -bromopropionate (5.78 g, 32.0

mmol) and zinc dust (2.35 g, 36.1 mmol) in benzene-ether (1:1, 50 mL) was refluxed overnight (the reaction was initiated by adding a piece of iodine). The reaction was cooled to room temperature and added to saturated aqueous ammonium chloride solution (80 mL). The aqueous layer was extracted with methylene chloride (3 x 30 mL). The combined organic layers were dried over magnesium sulfate and the solvent was removed by vacuum. The residue was purified by flash chromatography over silica gel using CH₂Cl₂/hexane (1:5) as eluent: ¹H NMR (300 MHz, CDCl₃) δ 0.80 (d, 3 H, *J* = 9.4 Hz), 1.23 (t, 3 H, *J* = 8.1 Hz), 3.28 (q, 1 H, *J* = 9.4 Hz), 4.23 (q, 2 H, *J* = 8.1 Hz), 4.45 (s, 1 H), 7.20-7.40 (m, 4 H), 7.47 (d, 1 H, *J* = 9.4 Hz), 7.50-7.65 (m, 3 H); ¹³C NMR (75.5 MHz, CDCl₃) δ 175.4, 147.5, 146.0, 140.3, 139.9, 129.1, 129.0, 128.0, 127.7, 124.8, 123.2, 119.9, 119.8, 83.2, 61.0, 47.3, 14.1, 12.3; MS (EI) *m/e* 282 (M⁺), 237, 181, 152.

The yellow condensation product was dissolved in dry benzene (180 mL) and a catalytic amount of *p*-toluenesulfonic acid was added. The solution was refluxed overnight using a Dean-Stark trap. The mixture was cooled to room temperature, additional benzene (100 mL) was added and the solution washed with saturated NaHCO₃ solution. The organic layer was dried over magnesium sulfate and the solvent was removed under pressure: ¹H NMR (300 MHz, CDCl₃) δ 1.49 (t, 3 H, *J* = 7.3 Hz), 2.58 (s, 3 H), 4.43 (q, 2 H, *J* = 7.3 Hz), 7.22 (t, 1 H, *J* = 7.7 Hz), 7.25-7.40 (m, 2 H), 7.48 (d, 1 H, *J* = 7.7 Hz), 7.57 (m, 2 H), 7.79 (d, 1 H, *J* = 8.1 Hz); ¹³C NMR (75.5 MHz, CDCl₃) δ 171.3, 140.9, 137.9, 136.4, 134.6, 129.4, 128.5, 128.3, 127.1, 125.8, 123.1, 119.7, 119.5, 61.5, 19.2, 14.0; MS (EI) *m/e* 264 (M⁺), 235, 219, 192, 191, 190, 189, 165.

9-(1-Bromoethylidene)fluorene (3.9) The fluorenylidenepropionate (3.8) was saponified by refluxing an aqueous ethanolic potassium hydroxide solution (0.2 N, 30 mL) for 20 min under argon. The acid was precipitated by the addition of dilute hydrochloric acid, collected, and dried overnight under vacuum. The crude acid was pulverized, suspended in carbon tetrachloride, and stirred for 48 h under argon in the dark with 1 equiv of bromine. The solvent was removed under reduced pressure, and the resulting residue boiled for 2 h with slight excess of 0.5 N KOH. The mixture was extracted with benzene, the organic layer was separated, and evaporation of the solvent afforded the product as a pink solid (86%): ^1H NMR (300 MHz, CDCl_3) δ 3.14 (s, 3 H), 7.25-7.41 (m, 4 H), 7.65-7.80 (m, 3 H), 7.82 (d, 1 H, $J = 7.5$ Hz); ^{13}C NMR (75.5 MHz, CDCl_3) δ 157.0, 140.3, 138.3, 135.4, 128.3, 127.8, 127.3, 126.9, 125.8, 125.3, 124.9, 119.6, 119.3, 31.6; MS (EI) m/e 273 ($M+3$), 272($M+2$), 271($M+1$), 270(M^+), 192, 191, 190, 189, 165, 95.

9-(1-Azidoethylidene)fluorene (3.10). Sodium azide (3.11 g, 47.8 mmol) was added to an ice-cold solution of 3.9 (5.89 g, 21.7 mmol) in dimethylformamide (150 mL). The resulting mixture was stirred under argon, cooled in an ice bath for 3 h, and then placed in a freezer at $-20\text{ }^\circ\text{C}$ for 70 h and swirled occasionally. The mixture was poured onto ice, diluted with ice-water, and extracted with methylene chloride (4 x 100 mL). The organic layer was washed with ice-water (6 x 80 mL), dried over magnesium sulfate, and evaporated under reduced pressure. The pale yellow solid showed strong absorptions of $-\text{N}=\text{N}^+=\text{N}-$ at 2102 cm^{-1} and 2150 cm^{-1} .

2,2-(2,2'-Biphenylene)-3-methyl-2H-azirine (3.11). A solution of **3.10** in benzene (150 mL) was refluxed for 2 h under argon. The solvent was evaporated and the residue separated by column chromatography over silica gel using CH₂Cl₂/hexane (1:5) as eluent. Recrystallization from methanol afforded a reddish solid (1.76 g, 40% from **3.10**): ¹H NMR (300 MHz, CDCl₃) δ 2.66 (s, 3 H), 7.03 (d, 2 H, *J* = 7.8 Hz), 7.27 (t, 2 H, *J* = 7.8 Hz), 7.40 (t, 2 H, *J* = 7.8 Hz), 7.83 (d, 2 H, *J* = 7.8 Hz); ¹³C NMR (75.5 MHz, CDCl₃) δ 168.0, 144.5, 127.6, 126.9, 121.0, 120.2, 12.7; MS (EI) *m/e* 205 (M⁺), 190, 164, 163, 102, 82.

Irradiation of 2,2-(2,2'-Biphenylene)-3-methyl-2H-azirine (3.11) with Pyridine N-oxide. A solution of 2,2-(2,2'-biphenylene)-3-methyl-2H-azirine (**3.11**) (14.3 mg, 0.07 mmol) and pyridine N-oxide (0.44 g, 4.64 mmol) in acetonitrile (6 mL) was placed in a Pyrex tube, degassed, and irradiated as described above. After removal of solvent, the reaction mixture was directly subjected to NMR; only 2,2-(2,2'-biphenylene)-3-methyl-2H-azirine (**3.11**) and pyridine N-oxide were found.

Irradiation of 2,2-(2,2'-Biphenylene)-3-methyl-2H-azirine (3.11) with Methanol. A solution of 2,2-(2,2'-biphenylene)-3-methyl-2H-azirine (**3.11**) (11.7 mg, 0.057 mmol) and methanol (1.98 g, 6.18 mmol) in acetonitrile (6 mL) was placed in a Pyrex tube, degassed, and irradiated as described above. After removal of solvent, the reaction mixture was directly subjected to NMR; only 2,2-(2,2'-biphenylene)-3-methyl-2H-azirine (**3.11**) was found—no 9-methoxyfluorene was detected.

3.6 References and Notes:

- (1) Platz, M. S.; Maloney, V. M. In *Kinetics and Spectroscopy of Carbenes and Biradicals*; M. S. Platz, Ed.; Plenum Press: New York, 1990; Chap. 8.
- (2) Platz, M. S. *Acc. Chem. Res.* **1988**, *21*, 236-242.
- (3) Platz, M. S. In *Kinetics and Spectroscopy of Carbenes and Biradicals*; M. S. Platz, Ed.; Plenum Press: New York, 1990; Chap. 6.
- (4) Roth, H. D. *Acc. Chem. Res.* **1977**, *10*, 85-91.
- (5) Kirmse, W. *Carbene Chemistry*; 2nd ed.; Academic Press: New York, 1971.
- (6) Nikolaev, V. A.; Korobitsyna, I. K. *Mendeleev Chem. J.* **1979**, *24*, 88.
- (7) Sander, W. *Angew. Chem., Int. Ed. Engl.* **1990**, *29*, 344-354.
- (8) Rahman, M.; Shevlin, P. B. *Tetrahedron Lett.* **1985**, *26*, 2959.
- (9) Ahmed, S. N.; Shevlin, P. B. *J. Am. Chem. Soc.* **1983**, *92*, 6488.
- (10) Casal, H. L.; Werstiuk, N. H.; Scaiano, J. C. *J. Org. Chem.* **1984**, *49*, 5214-5217.
- (11) Field, K. W.; Schuster, G. B. *J. Org. Chem.* **1988**, *53*, 4000-4006.
- (12) Shields, C. J.; Schuster, G. B. *Tetrahedron Lett.* **1987**, *28*, 853-856.
- (13) Dürr, H.; Kober, H. *Tetrahedron Lett.* **1972**, *13*, 1255-1258.

(14) Compound 3.4 was quite a surprising product. Because this molecule is conformationally locked and contains a C_2 axis which bisects the middle fluorenyl group, 1H and ^{13}C NMR do not give enough information to identify the product. Also, since the molecule is so crowded with three fluorenyl groups, the highest m/e value in the mass spectrum is just 330 — the fluorenyl radical dimer. Ultimately, we identified the product by X-ray crystallography, only to discover that its structure had already been reported from studies in a different context (see ref. 16)

(15) Filipescu, N.; DeMember, J. R. *Tetrahedron* **1968**, *24*, 5181-5191.

(16) Kuo, C.-H.; Luh, T.-Y.; Cheng, M.-C.; Peng, S.-M. *J. Chin. Chem. Soc. Taipei* **1991**, *38*, 35-38.

(17) Smolinsky, G.; Pryde, C. A. *J. Org. Chem.* **1968**, *6*, 2411-2416.

(18) Griller, D.; Hadel, L.; Nazran, A. S.; Platz, M. S.; Wong, P. C.; Savino, T. G.; Scaiano, J. C. *J. Am. Chem. Soc.* **1984**, *106*, 2227-2235.

(19) Zupancic, J. J.; Schuster, G. B. *J. Am. Chem. Soc.* **1980**, *102*, 5958-5960.

(20) Griller, D.; Nazran, A. S.; Scaiano, J. C. *J. Am. Chem. Soc.* **1984**, *106*, 198-202.

(21) Gaspar, P. P.; Lin, C.-T.; Dunbar, W.; Mack, D. P.; Balasubramanian, P. *J. Am. Chem. Soc.* **1984**, *106*, 2128-2139.

(22) Griller, D.; Nazran, A. S.; Scaiano, J. C. *Acc. Chem. Res.* **1984**, *17*, 283-289.

- (23) Grasse, P. B.; Brauer, B.-E.; Zupancic, J. J.; Kaufmann, K. J.; Schuster, G. B. *J. Am. Chem. Soc.* **1983**, *105*, 6833-6845.
- (24) Schuster, G. B. *Adv. Phys. Org. Chem.* **1986**, *22*, 313.
- (25) Jackson, J. E.; Platz, M. S. In *Advances in Carbene Chemistry*; U. Brinker, Ed.; JAI Press: Greenwich, CT, in press.
- (26) Cauquis, G.; Reverdy, G. *Tetrahedron Lett.* **1972**, 3491-3494.
- (27) Cauquis, G.; Reverdy, G. *Tetrahedron Lett.* **1971**, 3771-3774.
- (28) Chiba, T.; Okimoto, M. *J. Org. Chem.* **1992**, *57*, 1375-1379.
- (29) Shimizu, N.; Bartlett, P. D. *J. Am. Chem. Soc.* **1978**, *100*, 4260-4267.
- (30) Trozzolo, A. M.; Leslie, T. M.; Sarpotdar, A. S.; Small, R. D.; Ferraudi, G. J. *Pure Appl. Chem.* **1979**, *51*, 261-270.
- (31) Zoghbi, M.; Warkentin, J. *J. Org. Chem.* **1991**, *56*, 3214-3215.
- (32) Griffin, G. W. *Angew. Chem., Int. Ed. Engl.* **1971**, *10*, 537-547.
- (33) Volatron, F.; Anh, N. T.; Jean, Y. *J. Am. Chem. Soc.* **1983**, *105*, 2364-2368.
- (34) Houk, K. N.; Rondan, N. G.; Santiago, C.; Gallo, C. J.; Gandour, R. W.; Griffin, G. W. *J. Am. Chem. Soc.* **1980**, *102*, 1504-1512.
- (35) Bigot, B.; Sevin, A.; Devaquet, A. *J. Am. Chem. Soc.* **1979**, *101*, 1095-1100.

(36) Bigot, B.; Sevin, A.; Devaquet, A. *J. Am. Chem. Soc.* **1979**, *101*, 1101-1106.

(37) Clark, K. B.; Bhattacharyya, K.; Das, P. K.; Scaiano, J. C.; Schaap, A. P. *J. Org. Chem.* **1992**, *57*, 3706-3712.

CHAPTER 4

On the Symmetry of Carbene-Alkene Cyclopropanations: Computational and Experimental Studies

Abstract: The carbene-alkene cycloaddition has been described as simultaneous electrophilic and nucleophilic attacks on opposite ends of the alkene. Previous theoretical studies have addressed the effects of carbene substitution on carbene-olefin reactivities, but relatively little is known about how alkene substituents modify the characteristics of the transition structures. We therefore examined singlet carbenes reacting with a set of donor, acceptor (D, A) 1,2 disubstituted alkenes; the D- or A-monosubstituted alkenes are also studied by the MNDO method.

The MNDO results show that the "inward" approach of singlet carbenes to the electron-donor substituted carbon atom of the alkene are favored by ~5 kcal/mol. Also, steric effects can make distinctions between two rotamers of the transition structures for a unsymmetric carbene adding to the alkene by more than 0.5 kcal/mol.

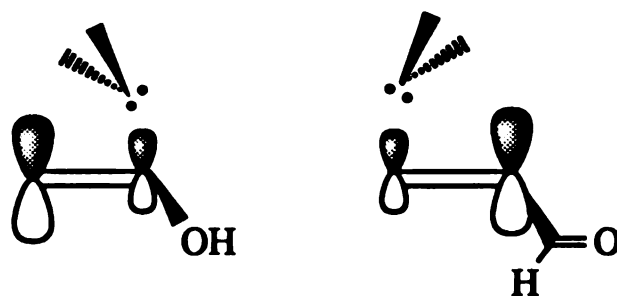
A parallel experimental effort seeks evidence for the asymmetric path (C_s) as opposed to a symmetrical approach (C_2). We have built a push-pull substituted alkene that should electronically prefer one carbene approach path ("forward") over the other ("backward"). Steric interaction would favor anti-substituted cyclopropane products, so study of the reaction of the alkene with an unsymmetrical carbene :CXY should reveal the electronic orientation preference in the regiochemistry of the carbenes's addition, making a clear distinction between the path. Unfortunately, the unsubstituted alkene (i.e. D = A = H) is completely unreactive toward carbenes at the double bond, despite its easy epoxidation by MCPBA. Thus, our original strategy has been blocked.

4.1 Introduction:

Transition states of singlet carbenes reacting with olefins have been studied through a variety of theoretical¹⁻⁹ and experimental^{2,10,11} efforts. In general, the widely accepted reaction path for the singlet carbene adding to an olefin begins with the "electrophilic phase" as the carbene's empty 2p orbital (LUMO) interacts with the filled π orbital (HOMO) of the olefin; during this first stage of the interaction, electron density is transferred from olefin to carbene. In the second stage, when the two reactants become closer, the sp^2 HOMO of the carbene overlaps with the vacant π^* orbital ("nucleophilic phase"), electron density is transferred from the lone pair of the carbene to the π^* orbital of the olefin, and the carbene rotates. Finally, the plane of the carbene is perpendicular to and intersecting the center of the C-C bond of the olefin; then cyclopropane is formed.

From the above theoretical studies, it is believed that the reaction is smooth and concerted, and that depending on carbene stability the transition state is located around or before the beginning of the "nucleophilic" phase when the lone pair of the carbene becomes involved in bonding. The geometrical parameters of the transition state, and more important, the activation barrier, depend on the substituents' stabilization of the carbene and the olefin.^{2,6,7,9,12} More precisely speaking, they are related to the timing of the transition from the carbene LUMO - olefin HOMO interaction to the carbene HOMO - olefin LUMO interaction. Overall, the geometric nature of the predicted addition pathway varies just slightly from the "early" to the "late" transition states.

For the cycloaddition of methylene to ethylene, the influence of the introduction of substituents in methylene has been extensively investigated by Hoffmann et al.,⁵ Houk et al.^{7,8,12} and Moss^{13,14} and co-workers. However, in only a few cases have substituent effects in the alkene been studied.^{5,6,10} In 1972, Hoffmann, Hayes and Skell examined methylene addition to isobutene using extended Hückel theory (EHT) calculation. They found that methylene prefers addition to the unsubstituted carbon atom of the alkene. Thirteen years later, Moreno and co-workers investigated the addition of singlet methylene to the polarized olefins, hydroxyethylene and formylethylene, using the MINDO/3 method. They concluded that the "inward" approach of methylene to the unsubstituted carbon atom of the alkene is the most favorable one, in both cases. However, according to FMO theory,¹⁵ attack of the methylene should preferentially occur at the atom with the largest orbital coefficient in the π orbital of the polarized olefin; thus the methylene addition to hydroxyethylene and formylethylene should attack opposite ends of the olefins. From this orbital perspective the carbene center of methylene should move closer (or "add to") to the unsubstituted carbon atom of

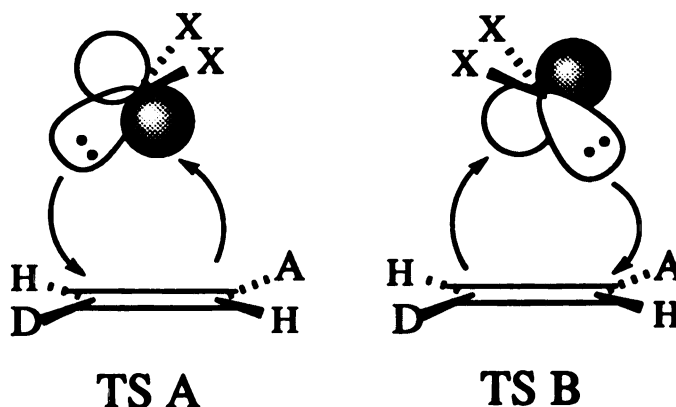


hydroxyethylene and to the substituted carbon atom of formylethylene than the other end. In a related study, Fox et al. were unsuccessful in matching experimental with theoretical results for the addition of alkylidene to

polarized olefins such as styrene and ethyl vinyl ether; this failure was attributed to underestimation of steric effects by the MNDO method used.

Here, we try to expand the understanding of polarizing effects in the cycloaddition of singlet carbenes to olefins by adding electron-donating or electron-withdrawing groups on the olefins. The two paths for cycloaddition to the different ends of the olefin should then be energetically differentiated due to olefin polarization by the donor and the acceptor substituents, as shown in Figure 4.1. The substitution pattern electronically

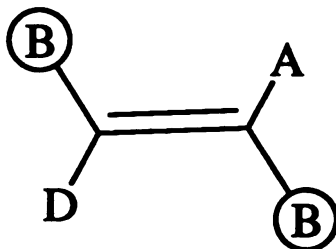
Figure 4.1



Two possible transition states for carbene addition to a substituted olefin. (A = π -Acceptor, D = π -Donor)

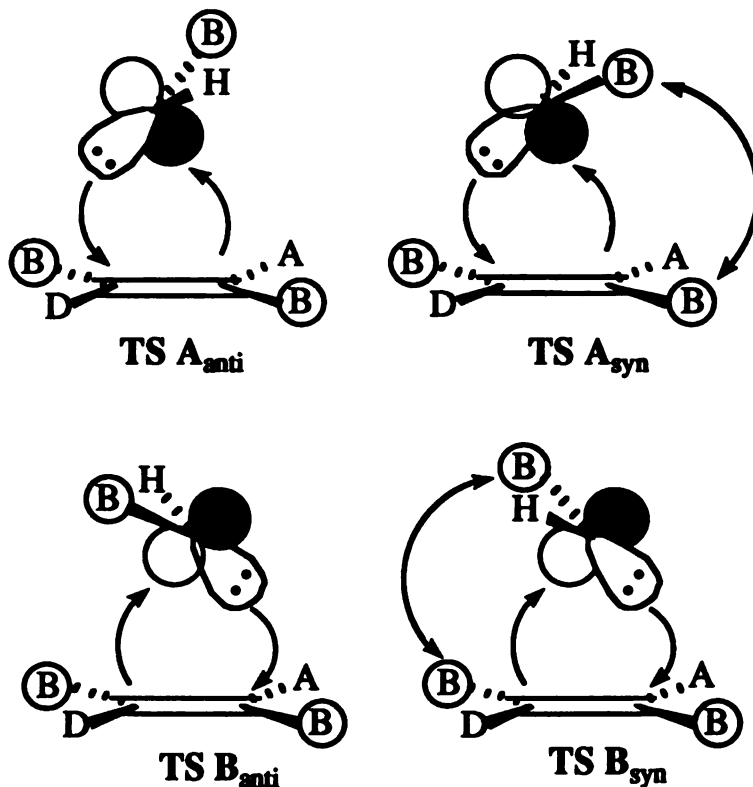
perturbs the olefin, making the π HOMO coefficient largest on the acceptor-bearing carbon, and the π^* LUMO coefficient largest on the donor-bearing carbon. The carbene orientation in TS A can best take advantage of having both better carbene LUMO (empty p orbital) - olefin HOMO and carbene HOMO (filled sp² orbital) - olefin LUMO interactions than in TS B, so that TS A should be electronically preferred over TS B. The polarized olefin, additionally substituted with *trans* related bulky

groups as shown below, is a substrate which may allow the distinction between these two reaction paths to be made.



With two different substituents on the carbene, TS A and TS B will be further divided into TS A_{syn}, TS A_{anti}, and TS B_{syn}, and TS B_{anti}, as shown in Figure 4.2. Because the two TSs B are electronically

Figure 4.2



TS A is electronically preferred over TS B
Anti TSs are sterically preferred over syn

disfavored, the product stereochemistry should be largely determined by the choice between TS A_{syn} and TS A_{anti} . In other words, the "standard" picture of singlet carbene addition to ethylene appears to predict that the steric environment at the acceptor end of the olefin should control product stereochemistry.

Since there is limited information available concerning substituent effects on the carbene orientation at transition state, we have investigated the above hypothesis by using the MNDO method. It is our hope that we can adapt the calculation results to design a suitable model to ultimately direct and predict "real" experimental results.

Part I. Computational:

As mentioned above, previous calculations on the effects of olefin polarization on cycloadditions of singlet carbenes were either limited to methylene, for which it is known that there is no barrier for the cycloaddition to ethylene^{7,9}, or were unsuccessful matching experimental results. In order to refine our understanding of the polarization effects, we report here calculations using the MNDO method to study the cycloaddition of several different electrophilic carbenes :CH₂, :CHBr, :CHCH₃, :CHCl, and :CFCH₃ to polarized olefins.

4.2 Procedure:

MNDO calculations were carried out using the MOPAC package (QCPE No. 455). All stationary points were characterized by vibrational analysis. All transition structures were fully optimized by

gradient minimization to confirm the presence of only one negative eigenvalue. The calculated activation energies represent the difference between the heats of formation for reactants (carbene and olefin) and the corresponding transition structures. All computations were run on the M.S.U. Chemistry Department's VAX Cluster.

4.3 Results:

First, we examine how cycloaddition of various singlet carbenes is affected by π -polarization in the monosubstituted alkenes, hydroxyethylene and cyanoethylene.¹⁶ Monosubstitution changes the character of the olefin to electron-poor with the CN group or electron-rich with the OH group, resulting in increased or decreased activation energies, but we can get some idea about the carbenes' preferences between the two ends of the polarized olefins. Then, we the push-pull disubstituted olefins, mentioned previously, in which the LUMO and HOMO orbitals energies are not much different from these in a simple ethylene itself. So, we can neglect the gross effects of changing the electronegativity of the olefins and focus on the effects of polarization.

In order to remain consistent in naming transition structures in the following text, we designate the electronically favored transition structures as TS A and the disfavored ones as TS B as defined in the introduction; the sterically disfavored transition structures are then TS A' and TS B' for TS A_{syn} and TS B_{syn}, respectively (see Figure 4.2). We also use the term that a carbene "adds to" a given carbon atom of an olefin to mean that this is the closer of the olefin carbons to the carbene center.

4.3.1 Cycloaddition of Carbenes to the Electron-Rich Olefin, Hydroxyethylene.

We calculated paths for four different carbenes of decreasing electrophilicity—methylene, methylcarbene, chlorocarbene, and methyl fluorocarbene—adding to hydroxyethylene. Selected geometry parameters and activation energies for the cycloaddition transition structures are given in Tables 4.1-4.4, along the above carbenes' sequence.

Methylene. There are two transition structures for methylene, the most electrophilic carbene, adding to hydroxyethylene as shown in Table 4.1. The activation energies of these two transition structures are basically the same, 5.2 and 5.3 kcal/mol for methylene addition to the substituted (4.1A) and unsubstituted carbon atoms (4.1B), respectively, and about 0.6 kcal/mol lower than the barrier for methylene addition to plain ethylene. The shortest C-C bond distance(a) between methylene and ethylene is 2.355 Å, which is between 2.371 Å for 4.1A and 2.318 Å for 4.1B. The tilt angle (β) for the plane of methylene is 111.5°, 108.6°, and 103.5° for 4.1A, transition structure of addition to ethylene, and 4.1B, respectively. The position of methylene for 4.1A almost sits on the center above of the olefin ($\alpha = 82^\circ$). However, methylene in 4.1B sits more toward the top of the unsubstituted carbon ($\alpha = 67^\circ$).

Chlorocarbene. For chlorocarbene addition to hydroxyethylene, four transition structures have been located, as shown in Table 4.2. The activation energies for the carbene adding to the substituted carbon are 1.2 and 1.1 kcal/mol for 4.2A and 4.2A', respectively, higher

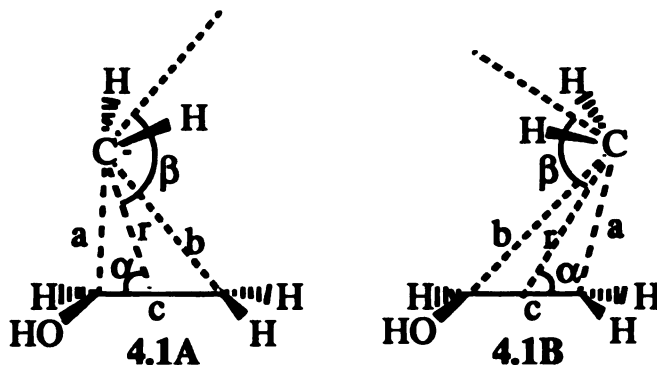
than that of the unsubstituted parent system. In contrast, the barrier for **4.2B** and **4.2B'** is 0.8 and 0.6 kcal/mole, respectively, lower than the barrier of the parent system. Similar to previous systems, the carbene centers of **4.2A** and **4.2A'** also almost sit on the top of the mid-point of the olefin ($\alpha = 87.8^\circ$ and 80.7° for **4.2A** and **4.2A'**, respectively) and the carbene centers of **4.2B** and **4.2B'** sit over the end of the olefin ($\alpha = 62.3^\circ$ and 63.2° for **4.2B** and **4.2B'**, respectively). But the tilt angles (β) for the plane of the chlorocarbene are quite different. The angle for **4.2A** is 120.5° which is more than 10° larger than the angle of **4.2A'**, **4.2B**, and **4.2B'** ($\beta = 102.4^\circ$, 107.5° and 109.7° , respectively).

Methylcarbene. As with chlorocarbene addition to hydroxyethylene, there are four transition structures for the cycloaddition of chlorocarbene to hydroxyethylene. Two transition structures are the methylcarbene addition to the substituted carbon atom (**4.3A** and **4.3A'**) and the other two are the methylcarbene addition to the unsubstituted carbon atom (**4.3B** and **4.3B'**). The barriers for all four transition structures are increased by 1.1, 0.3, 0.4, and 0.6 kcal/mol for **4.3A**, **4.3A'**, **4.3B**, and **4.3B'**, respectively, relative to the parent system--methylcarbene addition to unsubstituted ethylene. The geometries for **4.3A** and **4.3A'** are very similar. The shortest C-C bond distances (a) are both around 2.3 Å and the carbene centers almost sit on the top of mid-point of the olefin ($\alpha = 83.6^\circ$ and 77.6° for **4.3A** and **4.3A'**, respectively). The tilt angles (β) of the carbene planes are 124.5° and 122.0° for **4.3A** and **4.3A'**, respectively. The geometries for transition structures **4.3B** and **4.3B'** are also quite similar. The shortest C-C bond distances (a) are around 2.25 Å and both the carbene centers sit on the top

and just outside the edge of the olefin ($\alpha = 65.4^\circ$ and 66.0° for **4.3B** and **4.3B'**, respectively). The tilt angle (β) of the carbene plane is 117.9° and 118.5° for **4.3B** and **4.3B'**, respectively. Interestingly, the geometry parameters in Table 4.3 for the transition structure for the addition of methylcarbene to ethylene are all around the average between the parameters of **4.3As** and **4.3Bs**.

Methyl Fluorocarbene. Methyl fluorocarbene, the most nucleophilic carbene we have examined here, is quite interesting. Unlike the previous carbenes, methyl fluorocarbene has barriers for the four transition structures that are all higher than of the parent system by 2.6 kcal/mol for **4.4A** to 0.7 kcal/mol for **4.4B'**. Except for the orientations of the carbene center, the geometrical parameters for the transition structures are quite similar to those seen in the parent system. The shortest C-C bond distances (a) from the carbene center to hydroxyethylene are all around 2.0 Å, which is more than 0.2 Å shorter than in the transition structures for other carbenes above. Although transition structures **4.4A** and **4.4A'** for the carbene addition to substituted carbon atom sit above and between the olefin carbons as in the other carbene systems, the methyl fluorocarbenes in **4.4A** and **4.4A'** lean farther over the carbon atom rather than sitting at the middle of the olefins as with the other carbenes. For **4.4B** and **4.4B'**, the angles α are like the previous carbene additions to the unsubstituted carbon atom, which means that the carbene center of **4.4B** and **4.4B'** is also sitting above and outside the edge of the olefin.

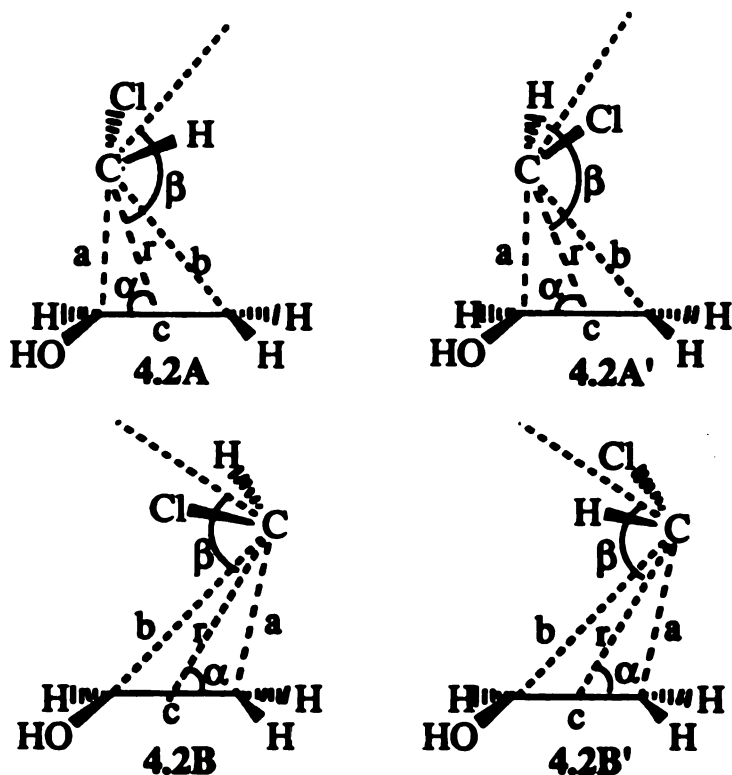
Table 4.1. Selected Geometry Parameters and Activation Energies for Transition Structures for the Addition of Methylene to Hydroxyethylene



| parameters | Transition Structures | | |
|-------------------------------|-----------------------|-------|-------|
| | ethylene | 4.1A | 4.1B |
| a (Å) | 2.355 | 2.371 | 2.318 |
| b (Å) | 2.692 | 2.547 | 2.836 |
| c (Å) | 1.344 | 1.361 | 1.360 |
| r (Å) | 2.438 | 2.365 | 2.500 |
| α (degree) | 75.0 | 82.3 | 66.9 |
| β (degree) | 108.6 | 111.5 | 103.5 |
| $\Delta E(\text{kcal/mol})^*$ | 5.9 | 5.2 | 5.3 |

* ΔE is the energy difference between carbene + alkene and transition structure.

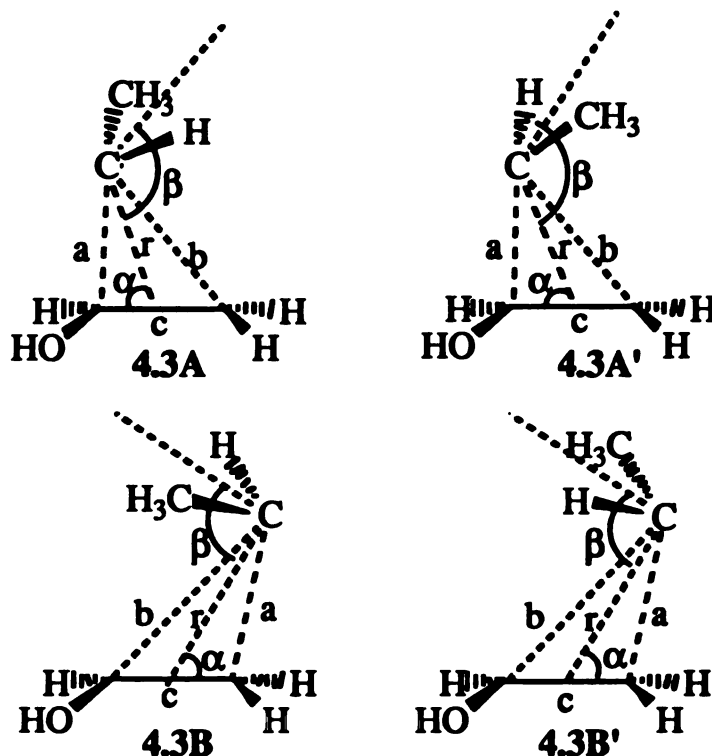
Table 4.2. Selected Geometry Parameters and Activation Energies for Transition Structures for the Addition of Chlorocarbene to Hydroxyethylene



| parameters | Transition Structures | | | | |
|--------------------------|-----------------------|-------|-------|-------|-------|
| | ethylene | 4.2A | 4.2A' | 4.2B | 4.2B' |
| a (Å) | 2.205 | 2.267 | 2.219 | 2.214 | 2.209 |
| b (Å) | 2.664 | 2.317 | 2.430 | 2.831 | 2.805 |
| c (Å) | 1.350 | 1.372 | 1.369 | 1.366 | 1.365 |
| r (Å) | 2.339 | 2.187 | 2.224 | 2.448 | 2.430 |
| α (degree) | 70.3 | 87.8 | 80.7 | 62.3 | 63.2 |
| β (degree) | 114.5 | 120.5 | 102.4 | 107.5 | 109.7 |
| ΔE_a (kcal/mol)* | 8.4 | 9.6 | 9.5 | 7.6 | 7.8 |

* ΔE is the energy difference between carbene + alkene and transition structure.

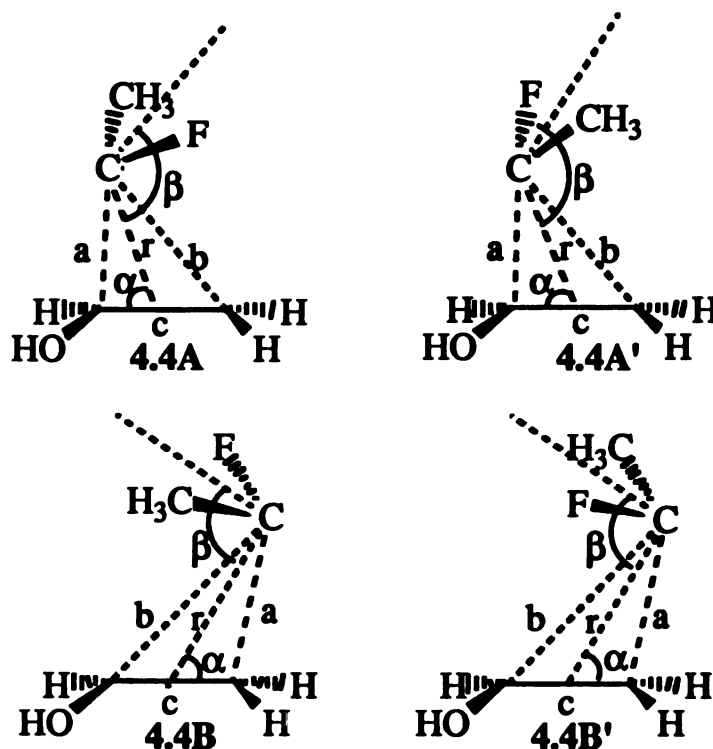
Table 4.3. Selected Geometry Parameters and Activation Energies for Transition Structures for the Addition of Methylcarbene to Hydroxyethylene



| parameters | Transition Structures | | | | |
|--------------------------|-----------------------|-------|--------|-------|--------|
| | ethylene | 4.3 A | 4.3 A' | 4.3 B | 4.3 B' |
| a (Å) | 2.266 | 2.300 | 2.265 | 2.245 | 2.254 |
| b (Å) | 2.683 | 2.468 | 2.546 | 2.794 | 2.790 |
| c (Å) | 1.348 | 1.367 | 1.365 | 1.363 | 1.362 |
| r (Å) | 2.390 | 2.286 | 2.331 | 2.441 | 2.443 |
| α (degree) | 71.3 | 82.6 | 77.6 | 65.4 | 66.0 |
| β (degree) | 120.8 | 124.5 | 122.0 | 117.9 | 118.5 |
| ΔE_a (kcal/mol)* | 8.5 | 9.6 | 8.8 | 8.9 | 9.1 |

* ΔE is the energy difference between carbene + alkene and transition structure.

Table 4.4. Selected Geometry Parameters and Activation Energies for Transition Structures for the Addition of Methyl Fluorocarbene to Hydroxyethylene



| parameters | Transition Structures | | | | |
|--------------------------|-----------------------|-------|-------|-------|-------|
| | ethylene | 4.4A | 4.4A' | 4.4B | 4.4B' |
| a (Å) | 2.048 | 2.045 | 2.035 | 2.052 | 2.065 |
| b (Å) | 2.603 | 2.457 | 2.475 | 2.719 | 2.697 |
| c (Å) | 1.360 | 1.381 | 1.379 | 1.375 | 1.374 |
| r (Å) | 2.241 | 2.152 | 2.159 | 2.309 | 2.302 |
| α (degree) | 65.0 | 71.8 | 70.5 | 59.9 | 61.6 |
| β (degree) | 126.0 | 129.9 | 127.5 | 122.7 | 122.9 |
| ΔE_a (kcal/mol)* | 15.4 | 18.2 | 17.9 | 16.1 | 16.1 |

* ΔE is the energy difference between carbene + alkene and transition structure.

Generally speaking, following the sequence of the carbenes, :CH_2 , :CHCl , :CHCH_3 , and :CFCH_3 , the differences between the activation energies for the carbenes' addition to hydroxyethylene and the corresponding parent system are increased from no energy barrier for the :CH_2 system to around +3 kcal/mole for :CFCH_3 . Second, the carbenes center in the transition structures for addition to the substituted carbon atom (TS A) progress from being centered above the olefin as with :CH_2 to leaning over the carbon atom as with :CFCH_3 ; resulting in smaller angles α . The angles α in the transition structures for addition to the unsubstituted carbon atoms (TS B) do not change much, but there is still a trend getting smaller from 66.9° for 4.1B to 59.0° for 4.4B. The OH group does not cause much steric effects and, in most cases, it stays almost on the plane of olefin.

4.3.2 Cycloaddition of Carbenes to the Electron-Poor Olefin, Cyanoethylene.

We have also calculated transition structures of cycloaddition of the above four different carbenes to cyanoethylene. Selected geometry parameters and activation energies for the transition structures of the cycloaddition of the four different carbenes to cyanoethylene are given in Table 4.5-4.8.

Methylene. For the addition of methylene to cyanoethylene, the methylene shows significant bias between the two ends of the olefin. The activation energy for methylene adding to the unsubstituted carbon atom (4.5A) is 8.5 kcal/mol, which is 3.5 kcal/mol higher than the barrier for methylene addition to the substituted carbon atom (4.5B) and also 2.6

kcal/mol higher than the barrier for the parent system, methylene addition to plain ethylene. Nevertheless, the geometries of **4.5A** and the parent system are quite similar, as shown in Table 4.5. However, the geometry of **4.5B** is unlike that of **4.5A**, with the carbene center in **4.5B** leaning more outside over olefin, while the carbene in **4.5A** is sitting on the top and middle of the olefin and a little toward to the unsubstituted carbon center.

Chlorocarbene. The activation energies for chlorocarbene adding to the unsubstituted carbon atom (TSs A in Table 4.6) are almost the same as the ethylene barriers, 8.4 kcal/mol. However, the energy barriers for the transition structures the carbene adding to the substituted carbon atom (TSs B in Table 4.6) are about 4 kcal/mol higher than those of TSs A.

Basically, the distances (a, b, c, and r) of all four transition structures do not vary much, as shown in Table 4.6. The locations of the carbene centers of the transition structures are pretty much the same; they sit right on top of the closer carbon atom of the olefin, though for the carbene centers of TSs A, they are a bit more outside the olefin than in TSs B. The tilt angles (β) of the carbene planes for TSs A are around 8° larger than for TSs B, but the angles for all **4.6s** are larger than for the corresponding parent system.

Methylcarbene. The four different transition structures are described in Table 4.7. The activation energies for **4.7A** and **4.7A'** are the same: 6.7 kcal/mol, which is 1.7 kcal/mol lower than the parent system, 8.5 kcal/mol; however, the activation energies for **4.7B** and **4.7B'**

are 11.5 and 11.3 kcal/mol, respectively, which is around 3 kcal/mol higher than for the parent system.

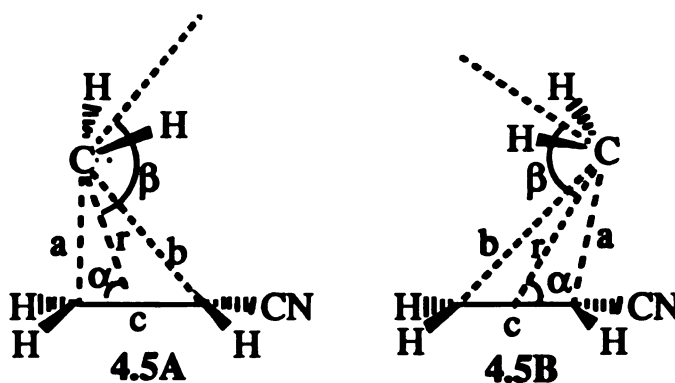
The locations of the carbene centers of transition structures 4.7 are pretty much the same as in 4.6. The carbene in 4.7A and 4.7A' just lies more outside the olefin than in 4.7B and 4.7B'. The tilt angles (β) of the carbene planes of the carbene for TSs A are around 10° larger than for TSs B, but the angles for all 4.7s are larger than in the corresponding parent system.

Methyl Fluorocarbene. The transition structures of the carbene adding to the unsubstituted carbon atom (TSs A) are about 7 kcal/mol favored over those for the carbene adding to the substituted carbon atom (TSs B). This is the largest energy gap between TS A and TS B among the carbenes we have examined so far. The barriers for TSs B are even about 5 kcal/mol higher than the barrier of the corresponding parent system, 15.4 kcal/mol.

Interestingly enough, the geometries of all four transition structures are similar except for the tilt angle (β). The tilt angles (β) of the carbene planes for TSs A are around 8° larger than for TSs B, but the angles for all 4.8s are larger than in the corresponding parent system.

Generally speaking, as carbene electrophilicity decreases in the order :CH₂, :CHCl, :CHCH₃, and :CFCH₃ the additions of the carbenes to cyanoethylene increasingly favor addition to the unsubstituted carbon atom. There is not much steric effects resulting from the CN group. Especially for the TSs A, the energy barriers between two rotators are less than 0.3 kcal/mol. The shortest C-C distances (a) are also getting shorter from

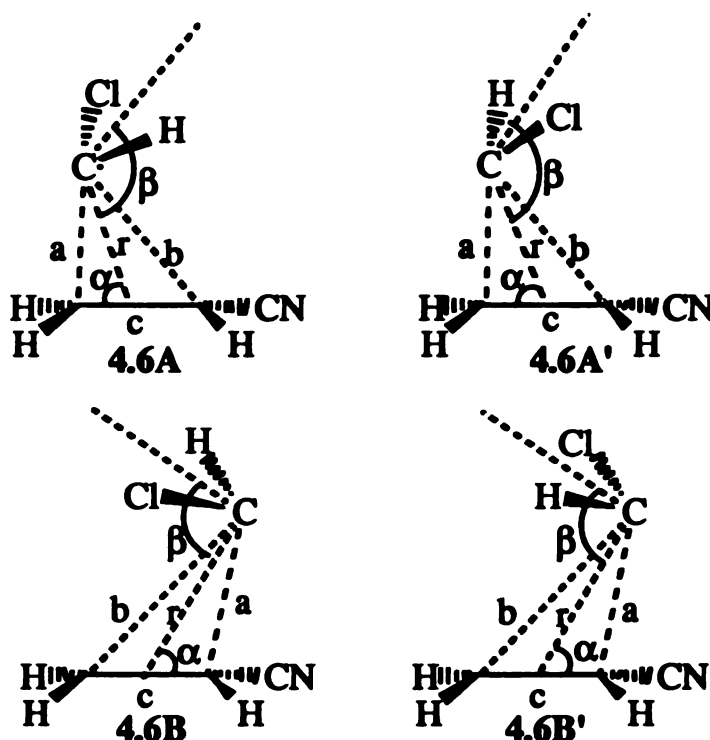
Table 4.5. Selected Geometry Parameters and Activation Energies for Transition Structures for the Addition of Methylene to Cyanoethylene



| parameters | Transition Structures | | |
|-----------------------|-----------------------|-------|-------|
| | ethylene | 4.5A | 4.5B |
| a (Å) | 2.355 | 2.282 | 2.335 |
| b (Å) | 2.692 | 2.624 | 2.810 |
| c (Å) | 1.344 | 1.356 | 1.355 |
| r (Å) | 2.438 | 2.364 | 2.493 |
| α (degree) | 75.0 | 74.8 | 68.8 |
| β (degree) | 108.6 | 111.8 | 124.0 |
| ΔE (kcal/mol) | 5.9 | 8.5 | 5.2 |

* ΔE is the energy difference between carbene + alkene and transition structure.

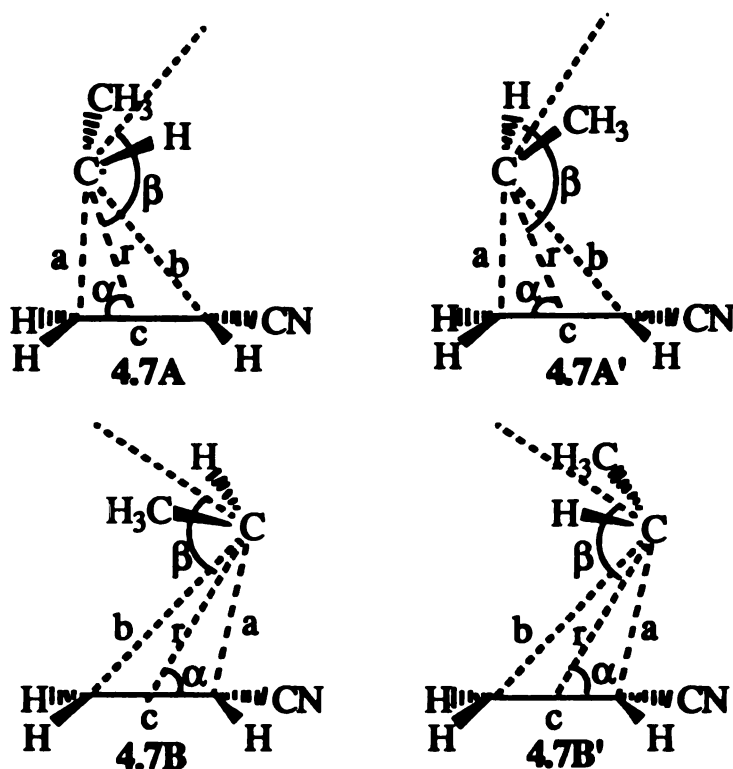
Table 4.6. Selected Geometry Parameters and Activation Energies for Transition Structures for the Addition of Chlorocarbene to Cyanoethylene



| parameters | Transition Structures | | | | |
|--------------------------|-----------------------|-------|-------|-------|-------|
| | ethylene | 4.6A | 4.6A' | 4.6B | 4.6B' |
| a (Å) | 2.205 | 2.194 | 2.200 | 2.130 | 2.127 |
| b (Å) | 2.664 | 2.720 | 2.718 | 2.570 | 2.564 |
| c (Å) | 1.350 | 1.361 | 1.360 | 1.363 | 1.363 |
| r (Å) | 2.339 | 2.376 | 2.377 | 2.260 | 2.255 |
| α (degree) | 70.3 | 66.4 | 66.8 | 70.4 | 70.0 |
| β (degree) | 114.5 | 125.7 | 125.0 | 116.8 | 116.9 |
| ΔE_a (kcal/mol)* | 8.4 | 8.6 | 8.3 | 12.4 | 13.0 |

* ΔE is the energy difference between carbene + alkene and transition structure.

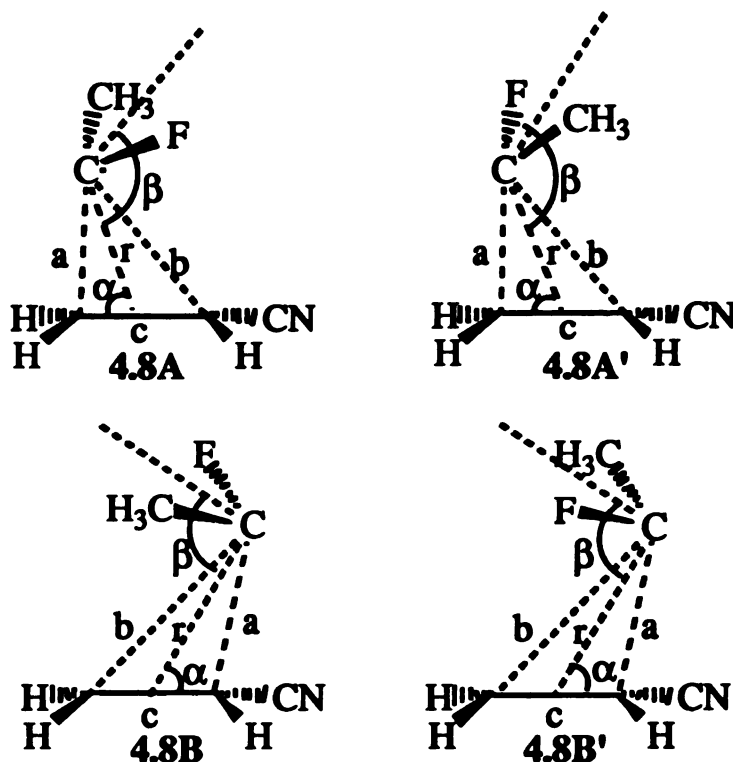
Table 4.7. Selected Geometry Parameters and Activation Energies for Transition Structures for the Addition of Methylcarbene to Cyanoethylene



| parameters | Transition Structures | | | | |
|-----------------------------|-----------------------|-------|-------|-------|-------|
| | ethylene | 4.7A | 4.7A' | 4.7B | 4.7B' |
| a (Å) | 2.266 | 2.262 | 2.267 | 2.200 | 2.206 |
| b (Å) | 2.683 | 2.812 | 2.812 | 2.632 | 2.629 |
| c (Å) | 1.348 | 1.359 | 1.359 | 1.359 | 1.359 |
| r (Å) | 2.390 | 2.460 | 2.462 | 2.323 | 2.330 |
| α (degree) | 71.3 | 65.3 | 65.6 | 71.2 | 71.2 |
| β (degree) | 120.8 | 136.3 | 134.0 | 124.0 | 123.9 |
| ΔE _a (kcal/mol)* | 8.5 | 6.7 | 6.7 | 11.5 | 11.3 |

* ΔE is the energy difference between carbene + alkene and transition structure.

Table 4.8. Selected Geometry Parameters and Activation Energies for Transition Structures for the Addition of Methyl Fluorocarbene to Cyanoethylene



Transition Structures

| parameters | ethylene | 4.8A | 4.8A' | 4.8B | 4.8B' |
|--------------------------|----------|-------|-------|-------|-------|
| a (Å) | 2.048 | 2.068 | 2.068 | 1.996 | 1.995 |
| b (Å) | 2.603 | 2.697 | 2.693 | 2.542 | 2.544 |
| c (Å) | 1.360 | 1.370 | 1.370 | 1.373 | 1.373 |
| r (Å) | 2.241 | 2.304 | 2.300 | 2.180 | 2.181 |
| α (degree) | 65.0 | 61.6 | 61.8 | 65.6 | 65.4 |
| β (degree) | 126.0 | 136.9 | 136.2 | 128.2 | 128.0 |
| ΔE_a (kcal/mol)* | 15.4 | 12.9 | 13.1 | 20.4 | 20.3 |

* ΔE is the energy difference between carbene + alkene and transition structure.

around 2.3 Å in 4.5s to around 2.0 Å in 4.8s. The rotation the carbene planes do not appear to make any difference. The energy barriers and geometries for transition structures A or B are almost the same as for their corresponding transition structures A' or B'. In most cases, except for transition structures 4.5s, the tilt angles β of the planes of those carbenes in TSs A are always around 10° larger than the angles for the corresponding TSs B, which are also 2-3° larger than the angles for the corresponding parent system.

4.3.3 Cycloaddition of Carbenes to Various Push-Pull Olefins.

In order to examine the steric and electronic effects on carbenes - olefin cycloaddition reactions as mentioned in the introduction and in Figure 4.2, we have selected three different monosubstituted carbenes, :CHCl, :CHCH₃, and CHBr, and two disubstituted carbenes, CFCH₃ and CCl₂. Also, three different size "bulky" groups (B in Figure 4.2), H (4.10a), CH₃ (4.10b), and Br (4.10c), have been studied on the push-pull olefins.

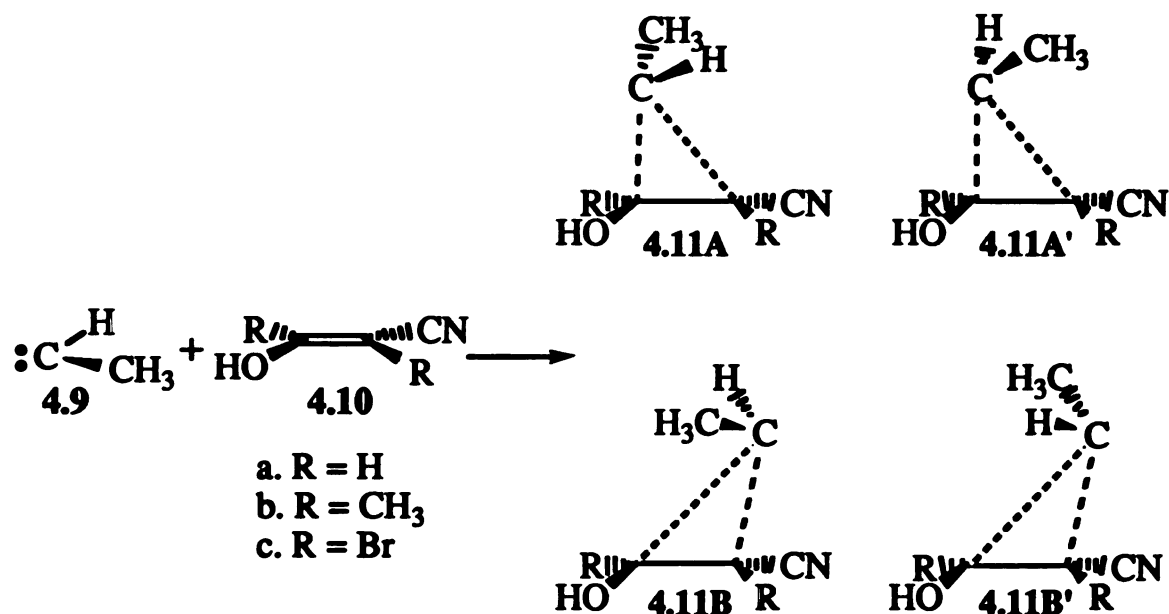
Activation Energies. The heats of formation and activation energies for the transition structures of cycloadditions of various carbenes to push-pull olefins are summarized in Tables 4.9-4.13.

For the monosubstituted carbenes, the transition structures for the carbenes adding toward the hydroxy substituted carbon atom (TS A) have lower barriers than the transition structures for the carbenes adding toward the cyano substituted carbon atom (TS B); thus, the electronic orientation preference of predicted in the introduction holds for these

cases. For the transition structures of methylcarbene, the barriers favor **4.11A** over **4.11B** by about 5 kcal/mol. The energy barrier differences for chlorocarbene and bromocarbene increase with the size of bulky groups (R) on the olefins. For chlorocarbene addition to olefins **4.10a**, **4.10b**, and **4.10c**, respectively, **4.13A** is 2.9, 3.5, and 4.7 kcal/mol favored over **4.13B**. Similar energy gaps are found in favor of transition structures **4.15A** over **4.15B** for bromocarbene cycloaddition to **4.10s**.

Although carbene orientation does show electronic control, transition structures for monosubstituted carbenes do not show strong steric effects. We do observe some steric effects between pairs of transition structures, but, in most cases, the steric effects are opposite to the predictions shown in Figure 2.1 and the barrier differences are less than 1 kcal/mol. For **4.11A** and **4.11A'**, the barriers are almost the same. However, when R = Br, we observe the "reverse" steric effect in which **4.11B'c** is favored by 1.5 kcal/mol over **4.11Bc**. This "reverse" steric effects where R = Br also appears in **4.13**, where **4.13A'c** and **4.13B'c** is favored by 0.7 and 0.6 kcal/mol over **4.13Ac** and **4.13Bc**, respectively. The transition structures for bromocarbene addition to **4.10s** also show the same phenomenon. The **4.15A's** are favored over **4.15As** by 0.4, 0.5, and 0.9 kcal/mol for R = H, CH₃, and Br, respectively. Overall, the steric effects are not nearly as strong as the electronic effects shown previously.

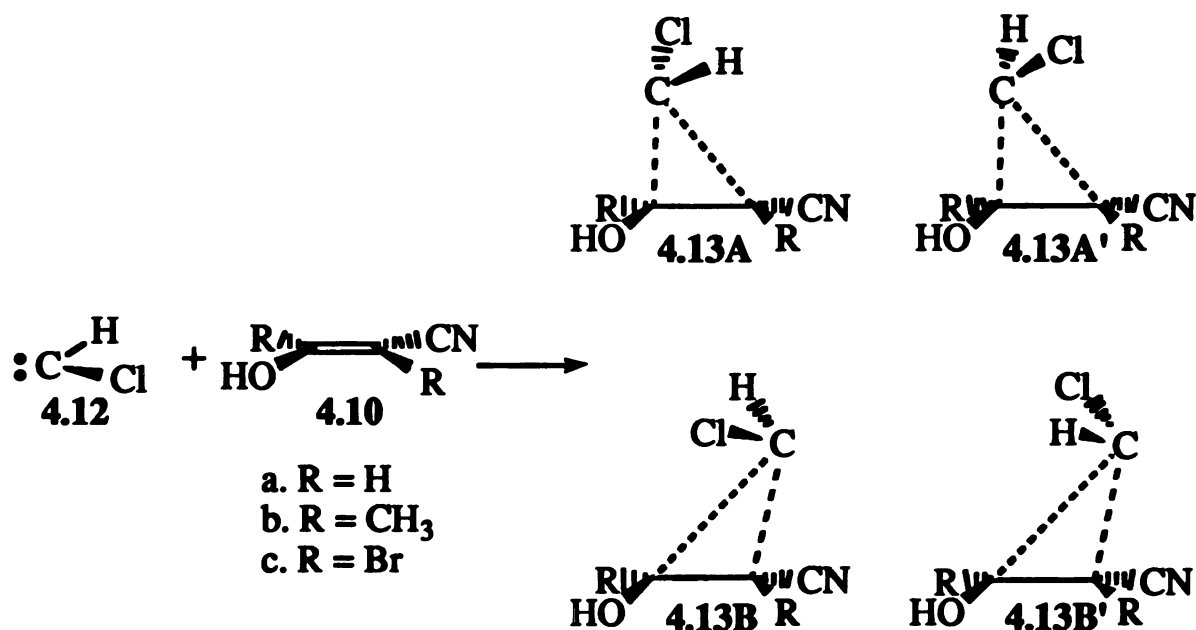
Table 4.9. Heats of Formation* and Activation Energies* of Transition Structures of Methylcarbene Addition to Various Push-Pull Olefins



| olefins | 4.9+4.10 ΔH_f | Transition Structures | | | | | | | |
|----------|---------------------------------------|---------------------------|---------------------------|---------------------------|---------------------------|---------------------------|---------------------------|---------------------------|---------------------------|
| | | 4.11A | | 4.11A' | | 4.11B | | 4.11B' | |
| | | ΔH_f | ΔE_a | ΔH_f | ΔE_a | ΔH_f | ΔE_a | ΔH_f | ΔE_a |
| ethylene | 103.8 | 112.3 | 8.5 | | | | | | |
| 4.10a | 81.7 | 89.6 | 7.9 | 89.4 | 7.7 | 94.2 | 12.5 | 94.0 | 12.3 |
| 4.10b | 68.7 | 82.1 | 13.4 | 82.0 | 13.3 | 87.2 | 18.5 | 87.3 | 18.6 |
| 4.10c | 93.3 | 102.2 | 8.9 | 102.3 | 9.0 | 107.6 | 14.3 | 109.1 | 15.8 |

* All values are in kcal/mol.

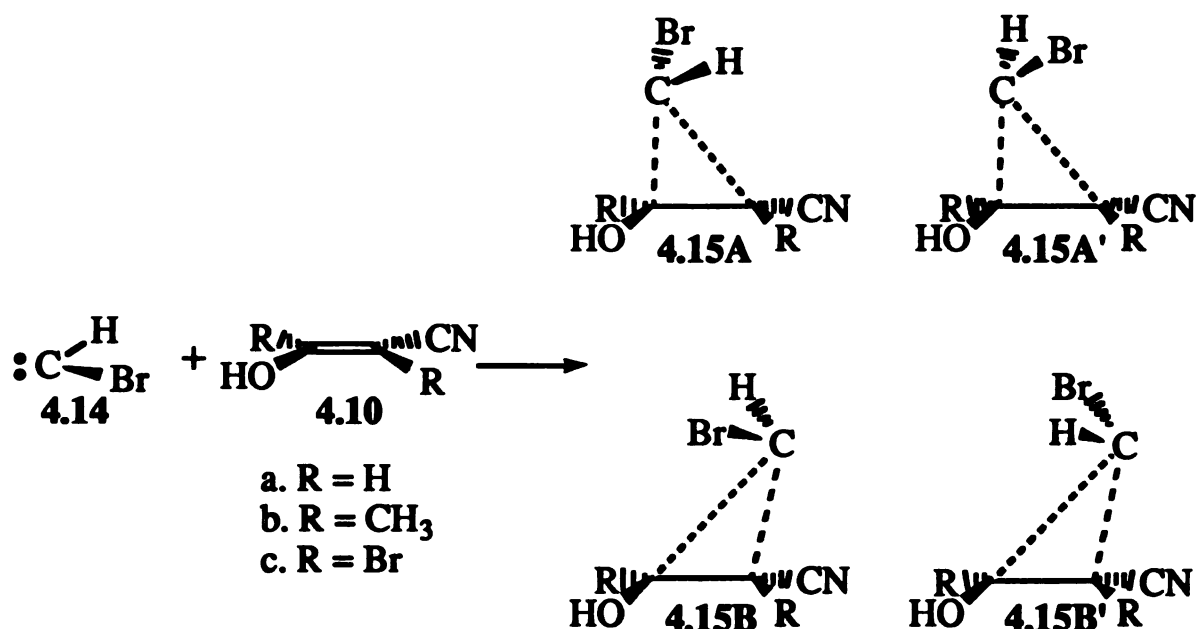
Table 4.10. Heats of Formation* and Activation Energies* of Transition Structures of Chlorocarbene Addition to Various Push-Pull Olefins



| | | Transition Structures | | | | | | | |
|------------------|--------------|-----------------------|--------------|---------------|--------------|--------------|--------------|---------------|--------------|
| <u>4.12+4.10</u> | | <u>4.13A</u> | | <u>4.13A'</u> | | <u>4.13B</u> | | <u>4.13B'</u> | |
| olefins | ΔH_f | ΔH_f | ΔE_a | ΔH_f | ΔE_a | ΔH_f | ΔE_a | ΔH_f | ΔE_a |
| ethylene | 96.4 | 104.8 | 8.4 | | | | | | |
| 4.10a | 74.0 | 84.0 | 10.0 | 84.2 | 10.2 | 86.9 | 12.9 | 86.8 | 12.8 |
| 4.10b | 61.7 | 76.3 | 14.6 | 76.2 | 14.5 | 79.8 | 18.1 | 79.6 | 17.9 |
| 4.10c | 85.6 | 98.9 | 13.3 | 98.2 | 12.6 | 103.6 | 18.0 | 103.0 | 17.4 |

* All values are in kcal/mol.

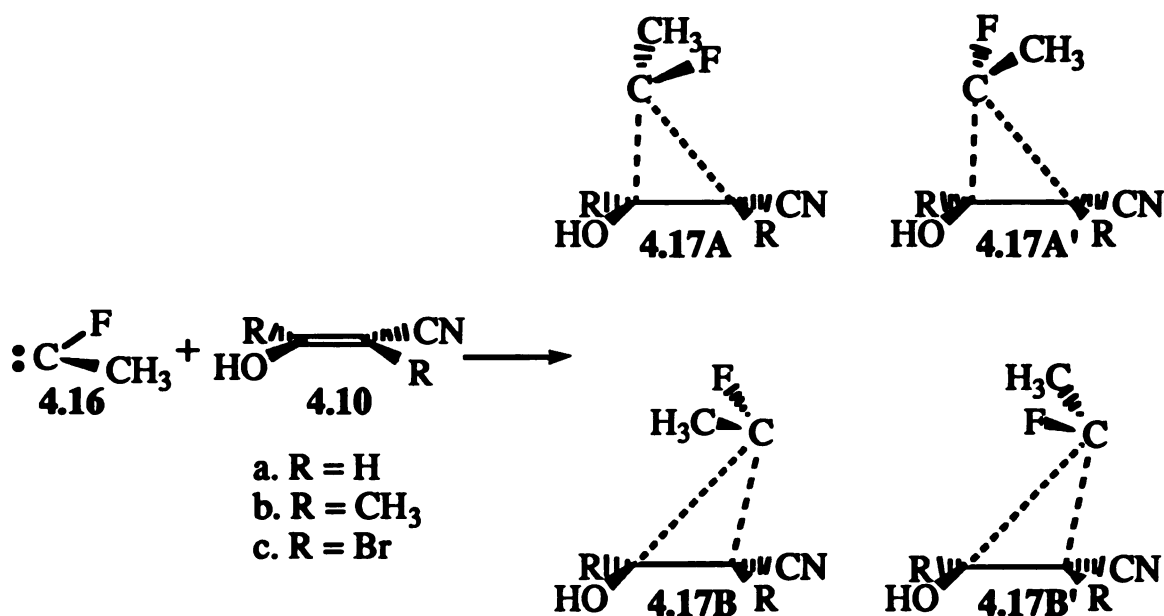
Table 4.11. Heats of Formation* and Activation Energies* of Transition Structures of Bromocarbene Addition to Various Push-Pull Olefins



| | | Transition Structures | | | | | | | |
|------------------|------------|-----------------------|-----------------------|---------------|-----------------------|--------------|-----------------------|---------------|-----------------------|
| <u>4.14+4.10</u> | | <u>4.15A</u> | | <u>4.15A'</u> | | <u>4.15B</u> | | <u>4.15B'</u> | |
| <u>olefins</u> | <u>ΔHf</u> | <u>ΔHf</u> | <u>ΔE_a</u> | <u>ΔHf</u> | <u>ΔE_a</u> | <u>ΔHf</u> | <u>ΔE_a</u> | <u>ΔHf</u> | <u>ΔE_a</u> |
| ethylene | 113.4 | 121.2 | 7.8 | | | | | | |
| 4.10a | 90.7 | 100.7 | 10.0 | 100.4 | 9.6 | 103.0 | 12.3 | 103.7 | 13.0 |
| 4.10b | 78.3 | 92.8 | 14.5 | 92.3 | 14.0 | 96.2 | 17.9 | 96.0 | 17.7 |
| 4.10c | 102.3 | 114.7 | 12.4 | 113.8 | 11.5 | 119.3 | 17.0 | 118.8 | 16.5 |

* All values are in kcal/mol.

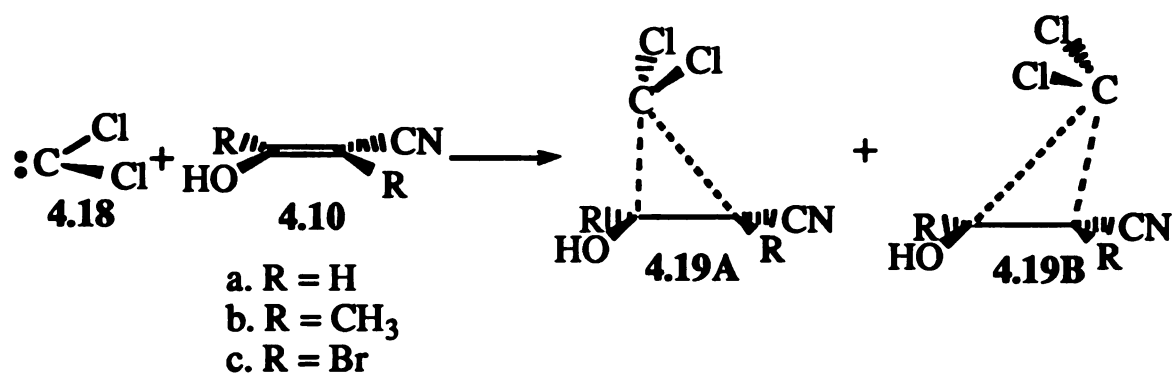
Table 4.12. Heats of Formation* and Activation Energies* of Transition Structures of Methyl Fluorocarbene Addition to Various Push-Pull Olefins



| olefins | 4.16+4.10 ΔH_f | Transition Structures | | | | | | | |
|----------|---------------------------------|-----------------------------|--------------------|------------------------------|--------------------|-----------------------------|--------------------|------------------------------|--------------------|
| | | 4.17A ΔH_f | ΔE_a | 4.17A' ΔH_f | ΔE_a | 4.17B ΔH_f | ΔE_a | 4.17B' ΔH_f | ΔE_a |
| ethylene | 23.6 | 39.0 | 15.4 | | | | | | |
| 4.10a. | 1.6 | 16.6 | 15.0 | 17.6 | 16.0 | 22.6 | 21.0 | 22.7 | 21.2 |
| 4.10b | -11.5 | 11.0 | 22.5 | 12.5 | 24.0 | 21.2 | 32.7 | 18.1 | 29.6 |
| 4.10c | 13.1 | 29.8 | 16.7 | 32.3 | 19.2 | 39.3 | 26.2 | 39.6 | 26.3 |

* All values are in kcal/mol.

Table 4.13. Heats of Formation* and Activation Energies* of Transition Structures of Dichlorocarbene Addition to Various Push-Pull Olefins



| olefins | 4.16+4.18 ΔH_f | Transition Structures | | ΔH_f | ΔE_a |
|----------|---------------------------|-----------------------|-----------------------|--------------|--------------|
| | | 4.19A ΔH_f | 4.19B ΔH_f | | |
| ethylene | 73.0 | 85.7 | 12.7 | | |
| 4.10a | 50.3 | 68.4 | 16.1 | 68.2 | 15.9 |
| 4.10b | 38.7 | 62.6 | 25.9 | 63.3 | 24.6 |
| 4.10c | 62.0 | 84.2 | 22.2 | 87.5 | 24.5 |

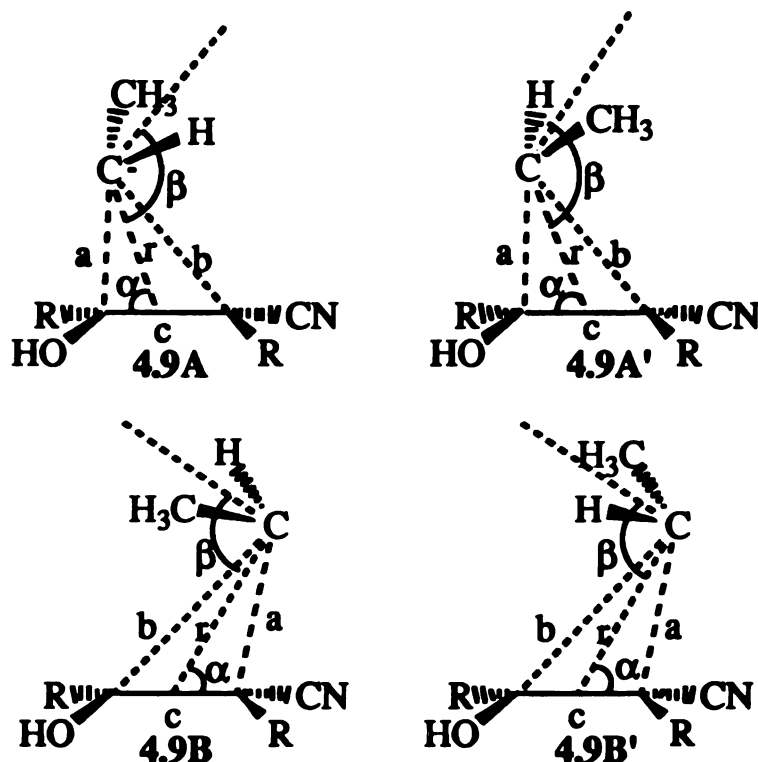
* All values are in kcal/mol

For the addition of methyl fluorocarbene to various olefins (see Table 4.12), energy differences between carbene attacks on the two ends of the olefins exceed those for the above monosubstituted carbenes. **4.17A** is preferred by 6.0, 9.8, and 9.5 kcal/mol over **4.17B** for **4.10a**, **4.10b**, and **4.10c**, respectively. Sterically, the energy gaps between **4.17A** and **4.17A'** increase with alkene bulky group size, yielding barrier differences of 1.0, 1.5, and 2.5 kcal/mol for R = H (**4.10a**), CH₃ (**4.10b**), and Br (**4.10c**), respectively, in favor of **4.17A** over **4.17A'**.

In contrast to all previous carbenes, dichlorocarbene does not show a significant preference between the two ends of olefins (see Table 4.13). This behavior is similar to that found for :CH₂; this similarity is sensible, as these two carbenes are the most electrophilic of those studied.

Transition Structure Geometries. The selected geometric parameters for transition structures for the addition of methylcarbene, chlorocarbene, bromocarbene, methyl fluorocarbene, and dichlorocarbene are listed in Tables 4.14–4.18, respectively. For each carbene addition to the different olefins we examine here, transition structures A and A' are almost identical; likewise B and B' are also very similar. The shortest C–C bond distances from carbene center to olefin in all transition structures (parameter a in the Tables) decrease generally along the series :CHCH₃ > :CHBr > :CHCl > :CFCH₃, from 2.23Å down to 2.03Å. Along the same series, the distance from the carbene center to the middle point of olefin (parameter r in the Tables) also decreases from 2.38Å to 2.22Å. For a given carbene, the distances also gradually decrease with increasing size of the bulky groups on the olefins.

Table 4.14. Selected Geometry Parameters for Transition Structures for the Addition of Methylcarbene to the Various Push-Pull Olefins

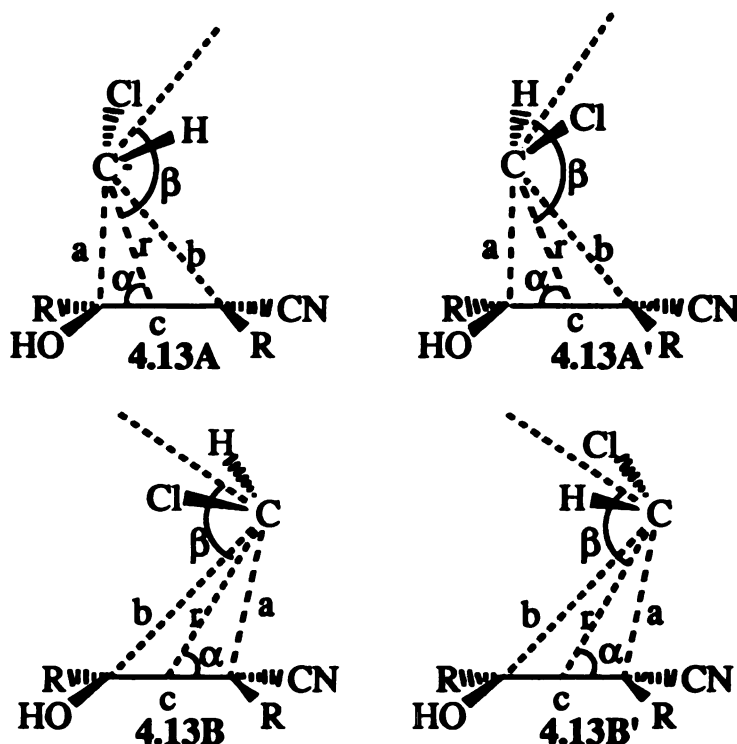


| parameters | ethylene | Push-pull olefin 4.10a (R = H) | | | |
|-------------------|----------|----------------------------------|--------|-------|--------|
| | | 4.9 A | 4.9 A' | 4.9 B | 4.9 B' |
| a (Å) | 2.266 | 2.233 | 2.229 | 2.175 | 2.183 |
| b (Å) | 2.683 | 2.694 | 2.680 | 2.725 | 2.725 |
| c (Å) | 1.348 | 1.383 | 1.379 | 1.376 | 1.376 |
| r (Å) | 2.390 | 2.376 | 2.366 | 2.367 | 2.371 |
| α (degree) | 71.3 | 69.8 | 70.2 | 65.6 | 65.9 |
| β (degree) | 120.8 | 138.8 | 129.4 | 122.7 | 121.3 |

| parameters | ethylene | Push-pull olefin 4.10b (R = CH ₃) | | | |
|-------------------|----------|--|--------|-------|--------|
| | | 4.9 A | 4.9 A' | 4.9 B | 4.9 B' |
| a (Å) | 2.266 | 2.210 | 2.208 | 2.172 | 2.169 |
| b (Å) | 2.683 | 2.604 | 2.618 | 2.646 | 2.654 |
| c (Å) | 1.348 | 1.405 | 1.406 | 1.397 | 1.397 |
| r (Å) | 2.390 | 2.310 | 2.317 | 2.318 | 2.321 |
| α (degree) | 71.3 | 73.0 | 72.4 | 69.4 | 68.9 |
| β (degree) | 120.8 | 137.0 | 137.5 | 123.7 | 124.5 |

| parameters | ethylene | Push-pull olefin 4.10c (R = Br) | | | |
|-------------------|----------|-----------------------------------|-------|-------|-------|
| | | 4.9A | 4.9A' | 4.9B | 4.9B' |
| a (Å) | 2.266 | 2.219 | 2.227 | 2.173 | 2.171 |
| b (Å) | 2.683 | 2.745 | 2.713 | 2.711 | 2.695 |
| c (Å) | 1.348 | 1.386 | 1.381 | 1.376 | 1.379 |
| r (Å) | 2.390 | 2.398 | 2.384 | 2.358 | 2.348 |
| α (degree) | 71.3 | 66.8 | 68.6 | 66.0 | 66.8 |
| β (degree) | 120.8 | 150.2 | 137.6 | 137.4 | 129.9 |

Table 4.15. Selected Geometry Parameters for Transition Structures for the Addition of Chlorocarbene to the Various Push-Pull Olefins

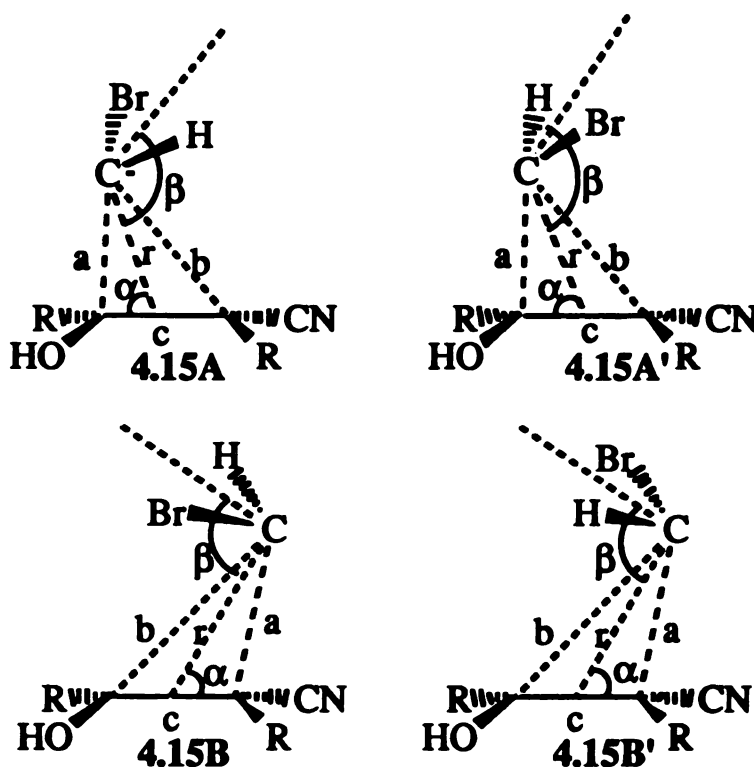


| parameters | ethylene | Push-pull olefin 4.10a (R = H) | | | |
|------------|----------|----------------------------------|--------|-------|--------|
| | | 4.13A | 4.13A' | 4.13B | 4.13B' |
| a (Å) | 2.205 | 2.162 | 2.166 | 2.126 | 2.111 |
| b (Å) | 2.644 | 2.592 | 2.572 | 2.708 | 2.722 |
| c (Å) | 1.350 | 1.382 | 1.382 | 1.381 | 1.382 |
| r (Å) | 2.339 | 2.284 | 2.275 | 2.335 | 2.336 |
| α (degree) | 70.3 | 71.0 | 72.2 | 64.0 | 62.8 |
| β (degree) | 114.5 | 127.0 | 125.9 | 116.7 | 113.0 |

| parameters | ethylene | Push-pull olefin 4.10b (R = CH ₃) | | | |
|------------|----------|--|--------|-------|--------|
| | | 4.13A | 4.13A' | 4.13B | 4.13B' |
| a (Å) | 2.205 | 2.145 | 2.143 | 2.104 | 2.100 |
| b (Å) | 2.644 | 2.516 | 2.524 | 2.634 | 2.646 |
| c (Å) | 1.350 | 1.404 | 1.404 | 1.403 | 1.403 |
| r (Å) | 2.339 | 2.230 | 2.233 | 2.278 | 2.283 |
| α (degree) | 70.3 | 74.0 | 73.6 | 66.9 | 66.0 |
| β (degree) | 114.5 | 127.5 | 128.0 | 116.2 | 115.9 |

| parameters | ethylene | Push-pull olefin 4.10c (R = Br) | | | |
|-------------------|----------|-----------------------------------|--------|-------|--------|
| | | 4.13A | 4.13A' | 4.13B | 4.13B' |
| a (Å) | 2.205 | 2.142 | 2.140 | 2.096 | 2.097 |
| b (Å) | 2.644 | 2.596 | 2.615 | 2.624 | 2.643 |
| c (Å) | 1.350 | 1.386 | 1.386 | 1.382 | 1.381 |
| r (Å) | 2.339 | 2.276 | 2.287 | 2.272 | 2.283 |
| α (degree) | 70.3 | 70.0 | 69.0 | 66.6 | 65.8 |
| β (degree) | 114.5 | 132.8 | 134.8 | 130.5 | 128.6 |

Table 4.16. Selected Geometry Parameters for Transition Structures for the Addition of Bromocarbene to the Various Push-Pull Olefins

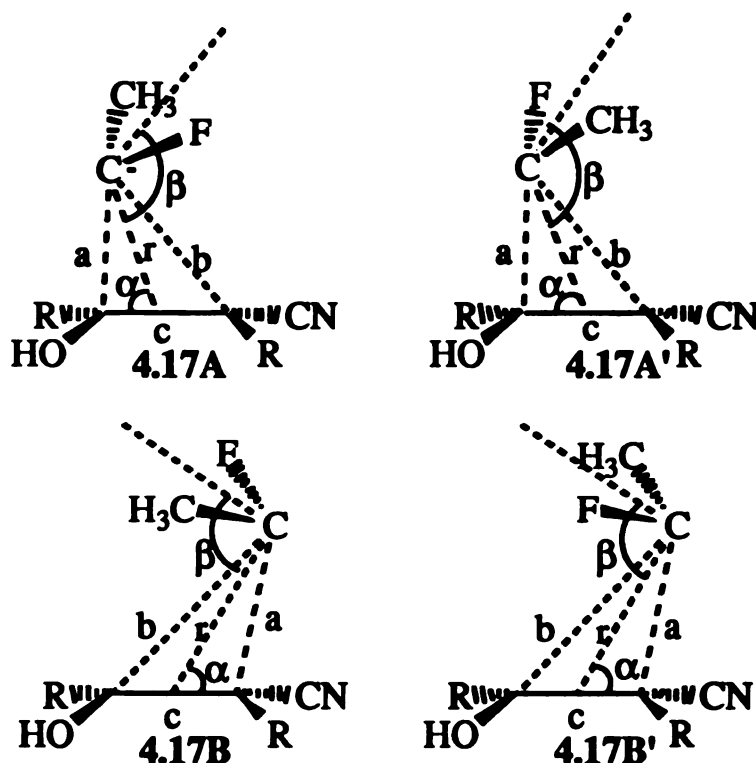


| parameters | ethylene | Push-pull olefin 4.10a (R = H) | | | |
|-------------------|----------|----------------------------------|--------|-------|--------|
| | | 4.15A | 4.15A' | 4.15B | 4.15B' |
| a (Å) | 2.244 | 2.207 | 2.209 | 2.155 | 2.153 |
| b (Å) | 2.637 | 2.585 | 2.572 | 2.751 | 2.735 |
| c (Å) | 1.348 | 1.384 | 1.384 | 1.382 | 1.381 |
| r (Å) | 2.374 | 2.302 | 2.295 | 2.372 | 2.362 |
| α (degree) | 70.7 | 73.5 | 74.2 | 63.5 | 64.2 |
| β (degree) | 115.2 | 130.9 | 128.8 | 111.6 | 112.2 |

| parameters | ethylene | Push-pull olefin 4.10b (R = CH ₃) | | | |
|-------------------|----------|--|--------|-------|--------|
| | | 4.15A | 4.15A' | 4.15B | 4.15B' |
| a (Å) | 2.244 | 2.186 | 2.181 | 2.136 | 2.140 |
| b (Å) | 2.637 | 2.520 | 2.539 | 2.659 | 2.648 |
| c (Å) | 1.348 | 1.406 | 1.406 | 1.400 | 1.400 |
| r (Å) | 2.374 | 2.251 | 2.260 | 2.308 | 2.303 |
| α (degree) | 70.7 | 75.6 | 74.6 | 67.2 | 67.9 |
| β (degree) | 115.2 | 131.7 | 131.6 | 116.0 | 115.4 |

| parameters | ethylene | Push-pull olefin 4.10c (R = Br) | | | |
|-------------------|----------|-----------------------------------|--------|-------|--------|
| | | 4.15A | 4.15A' | 4.15B | 4.15B' |
| a (Å) | 2.244 | 2.174 | 2.168 | 2.130 | 2.132 |
| b (Å) | 2.637 | 2.637 | 2.644 | 2.649 | 2.663 |
| c (Å) | 1.348 | 1.388 | 1.387 | 1.379 | 1.379 |
| r (Å) | 2.374 | 2.315 | 2.316 | 2.303 | 2.312 |
| α (degree) | 70.7 | 69.7 | 69.0 | 67.0 | 66.4 |
| β (degree) | 115.2 | 139.7 | 139.7 | 129.8 | 129.9 |

Table 4.17. Selected Geometry Parameters for Transition Structures for the Addition of Methyl Fluorocarbene to the Various Push-Pull Olefins

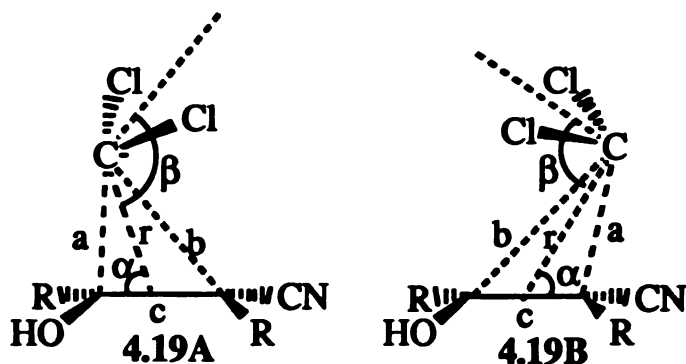


| parameters | ethylene | Push-pull olefin 4.10a (R = H) | | | |
|-------------------|----------|----------------------------------|--------|-------|--------|
| | | 4.17A | 4.17A' | 4.17B | 4.17B' |
| a (Å) | 2.048 | 2.032 | 2.029 | 1.991 | 2.000 |
| b (Å) | 2.603 | 2.594 | 2.573 | 2.657 | 2.634 |
| c (Å) | 1.360 | 1.396 | 1.393 | 1.391 | 1.390 |
| r (Å) | 2.241 | 2.223 | 2.210 | 2.242 | 2.233 |
| α (degree) | 65.0 | 65.2 | 66.0 | 60.2 | 61.7 |
| β (degree) | 126.0 | 140.0 | 134.8 | 125.4 | 126.0 |

| parameters | ethylene | Push-pull olefin 4.10b (R = CH ₃) | | | |
|-------------------|----------|--|--------|-------|--------|
| | | 4.17A | 4.17A' | 4.17B | 4.17B' |
| a (Å) | 2.048 | 2.017 | 2.014 | 1.906 | 1.993 |
| b (Å) | 2.603 | 2.542 | 2.541 | 2.657 | 2.584 |
| c (Å) | 1.360 | 1.421 | 1.421 | 1.431 | 1.412 |
| r (Å) | 2.241 | 2.182 | 2.180 | 2.200 | 2.197 |
| α (degree) | 65.0 | 67.3 | 67.2 | 57.0 | 64.2 |
| β (degree) | 126.0 | 139.8 | 140.3 | 130.2 | 127.3 |

| parameters | ethylene | Push-pull olefin 4.10c (R = Br) | | | |
|-------------------|----------|-----------------------------------|--------|-------|--------|
| | | 4.17A | 4.17A' | 4.17B | 4.17B' |
| a (Å) | 2.048 | 2.025 | 2.030 | 1.981 | 1.995 |
| b (Å) | 2.603 | 2.663 | 2.603 | 2.643 | 2.611 |
| c (Å) | 1.360 | 1.397 | 1.395 | 1.392 | 1.392 |
| r (Å) | 2.241 | 2.260 | 2.227 | 2.224 | 2.217 |
| α (degree) | 65.0 | 61.7 | 64.7 | 60.9 | 62.6 |
| β (degree) | 126.0 | 151.2 | 140.6 | 135.7 | 132.6 |

Table 4.18. Selected Geometry Parameters for Transition Structures for the Addition of Dichlorocarbene to the Various Push-Pull Olefins.



| parameters | ethylene | Push-pull olefin 4.10a (R = H) | |
|-------------------|----------|--------------------------------|--------|
| | | 4.19 A | 4.19 B |
| a (Å) | 2.040 | 2.004 | 2.008 |
| b (Å) | 2.640 | 2.509 | 2.756 |
| c (Å) | 1.360 | 1.397 | 1.400 |
| r (Å) | 2.259 | 2.161 | 2.307 |
| α (degree) | 62.8 | 67.8 | 56.5 |
| β (degree) | 120.2 | 133.7 | 113.0 |

| parameters | ethylene | Push-pull olefin 4.10b (R = CH ₃) | |
|-------------------|----------|---|--------|
| | | 4.19 A | 4.19 B |
| a (Å) | 2.040 | 2.003 | 1.980 |
| b (Å) | 2.640 | 2.516 | 2.669 |
| c (Å) | 1.360 | 1.414 | 1.420 |
| r (Å) | 2.259 | 2.161 | 2.240 |
| α (degree) | 62.8 | 67.7 | 59.8 |
| β (degree) | 120.2 | 132.3 | 117.5 |

| parameters | ethylene | Push-pull olefin 4.10c (R = Br) | |
|-------------------|----------|---------------------------------|--------|
| | | 4.19 A | 4.19 B |
| a (Å) | 2.040 | 1.993 | 1.964 |
| b (Å) | 2.640 | 2.546 | 2.683 |
| c (Å) | 1.360 | 1.400 | 1.404 |
| r (Å) | 2.259 | 2.177 | 2.244 |
| α (degree) | 62.8 | 65.7 | 58.0 |
| β (degree) | 120.2 | 140.0 | 120.0 |

The positions of the carbene centers in the transition structures are (angle α) all off-center by 15-30°. For monosubstituted carbenes, the angles α for transition structures A and A' are always 4-10° larger than those for the corresponding transition structures B and B'; however, the difference decreases as the size of the R groups on the olefins increases. For disubstituted carbenes, the carbene centers are still off-center by 25-30°, but the angles are generally more acute than for the monosubstituted carbenes, and the differences between transition structures A and A' and transition structures B and B' are also general by 2-3° less than those of transition structures of monosubstituted carbenes.

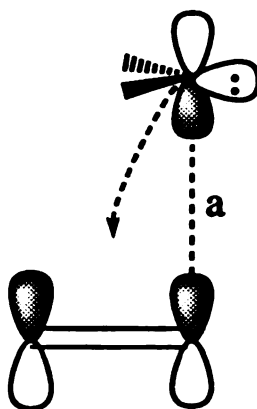
For the transition structures of the carbenes adding to the hydroxy substituted carbon atom of 4.10 (TS A), the tilt angles (β) of the carbene planes, in general, are around 10-20° larger than the β for the carbenes adding to the cyano substituted carbon atom (TS B), and the angle also slowly increases along the series of carbenes $\text{:CHCl} < \text{:CHBr} < \text{:CCl}_2 < \text{:CHCH}_3 < \text{:CFCH}_3$. For the transition structures of each carbene, the angle β also increases with the size of the R group on the olefins $\text{H} < \text{CH}_3 < \text{Br}$. For the TSs B of carbene addition to olefins 4.10a and 4.10b, the angles β are quite similar to the corresponding parent unsubstituted olefin system, however, the angles for addition to 4.10c increase by 10-15°.

4.4 Discussion:

The reported theoretical investigations of carbene cycloaddition to ethylene all agree that the reaction path is nonsymmetric,

only C_s symmetry (or pseudo symmetry in e.g. propene rxn) is preserved, and the reaction starts with an electrophilic phase and ends with a nucleophilic phase. The energy maximum occurs around the transition between the two phases. A monosubstituted olefin with electron-donor or electron-acceptor, which will increase the energy of HOMO or decrease the energy of LUMO of the olefin, respectively, may influence the reaction path of the carbene cycloaddition to the olefin differently. That is the initial reason why we set out to examine the transition structures of cycloaddition of carbenes to cyanoethylene and hydroxyethylene first.

Not surprisingly, the barrier for methylene, the most electrophilic carbene, adding to hydroxyethylene, the electron-rich olefin, is lower than the barrier for addition to plain ethylene for both orientations (4.1A and 4.1B). But for the cycloaddition of other carbenes to the olefin, the orientation of carbenes in transition structures either have no effect, as in the case of $:CHCl$, or are opposite to our expectation, which is that the carbene should add to the substituted carbon atom, allowing its empty p orbital to interact with the larger π -orbital coefficient on the unsubstituted end. Rondan and Houk have also found that the interaction between the LUMO of donor-substituted olefin and the HOMO of a carbene has no influence on the orientation of the carbene at the transition structure.⁸ They conclude that the LUMO of an unsymmetrically substituted alkene is polarized insignificantly by donors. In other words, as mentioned previously, the semiempirical reaction path starts with pure carbene LUMO - olefin HOMO interaction at large α , as shown in Figure 4.3, in which the p orbital of the carbene sits right above one of orbitals of

Figure 4.3

the olefin's π system; then the carbene center begins to slide toward the center of olefin as the reaction progresses.³⁻⁵ So, for hydroxyethylene, in which the unsubstituted carbon atom has the larger HOMO coefficient, the early carbene LUMO - olefin HOMO interaction already determines the favored reaction path and orientation at the transition structures. Another way to illustrate this idea is to note that the geometries of the favored transition structures, in this case TSs B, are quite similar to the geometry of the corresponding transition structure of the carbene addition to plain ethylene; moreover, the more nucleophilic the carbene is, the smaller is the energy gap between TSs A and TSs B, as shown in Tables 4.1- 4.4 (i.e. the alkene's LUMO may begin to participate a little).

If the olefin's HOMO polarization does not determine the orientation of a carbene at the transition structure, it must be controlled by the different coefficients between the two ends in the olefin's LUMO. Except for the transition structures for methylene addition to cyanoethylene, the orientation of the carbene in transition structures of all other carbenes adding to cyanoethylene follows our predictions, by which the carbene adds toward the unsubstituted carbon atom. Obviously, the

carbene LUMO - olefin HOMO interaction still has some influence on the orientation of carbene in the transition structures. The more electrophilic the carbene is, the smaller is the gap between TSs A and TSs B, as shown in Tables 4.5 - 4.8: Nevertheless, the transition structures of methylene addition to cyanoethylene are still affected by the interaction: TS B is favored over TS A by 3.3 kcal/mol, as shown in Table 4.5. Another interesting feature should be noted: All the carbenes examined here are electrophilic carbenes, yet the barriers for almost all favored transition structures, TSs A, of carbenes adding to cyanoethylene, an electron-poor olefin, are lower than the corresponding barriers for carbene addition to plain ethylene. Meanwhile, the transition structures for those carbenes adding to hydroxyethylene, an electron-rich olefin, do not show much lowering relative to the ethylene barriers. It is clear that the carbene HOMO - olefin LUMO interaction, or the energy gap between these two orbitals, is a more important factor in determining the location of the transition structure (includes the barrier and the orientation of a carbene) than is the carbene LUMO - olefin HOMO interaction, at least for the electrophilic carbenes examined here.

We have shown that individual electron-donor and electron-acceptor substituents on an olefin have different effects on the transition structure of cycloaddition of a carbene to the olefin. But such monosubstitution also changes the character of ethylene to electron-rich or electron-poor, plus, they do not polarize the HOMO and LUMO of ethylene to equal extents. So, we further investigated the transition structures of cycloadditions of carbenes to donor, acceptor di-substituted or "push-pull" olefins, as shown in Figures 4.1 and 4.2. In order to test the

"size" effect, we also examined three different size bulky groups, H, CH₃, and Br, on the olefin. For the same reason, we added another monosubstituted carbene, :CHBr, besides those carbenes discussed above. Obviously, it would be meaningless to further pursue the reaction of methylene, which is extremely electrophilic and so dominated by the carbene LUMO - olefin HOMO interaction.

For transition structures for all carbenes, strong electronic preferences are clearly seen, as shown in Tables 4.9 - 4.13. The differences of energy barriers between TS As and TS Bs increase as the electrophilicity of the carbenes decreases due to the reduced influence of carbene LUMO - olefin HOMO interactions, as discussed previously. This is the same reason why the energy barriers for transition structures of these carbenes adding to the olefin are extraordinarily high when R = CH₃, which is almost the same size as Br. The methyl groups (4.10b), which are weak electron-donors, raise the energy of the olefin's HOMO, whereas bromine (4.10c), a weak electron acceptor, decreases the LUMO energy of the olefin, as shown in Table 4.13. Even though CH₃ and Br have roughly the same size, electronically, they change the character of the olefin in opposite directions. It is also well known that the addition of singlet carbenes to olefins is sensitive to steric effects.^{17,18} That is why both bulky substituents increase the energy barriers in comparison with the corresponding parent system.

Table 4.19. Frontier Orbital Energies (eV) for Olefins

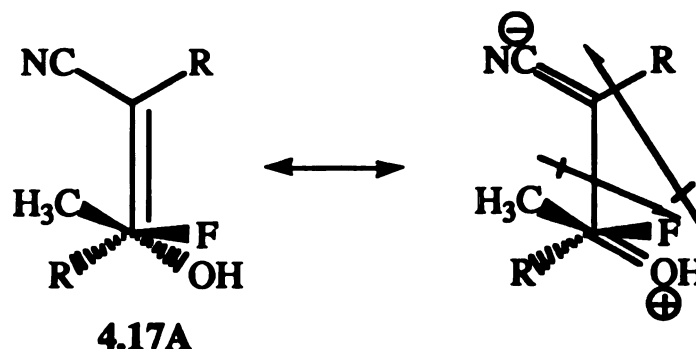
| | C=C | C=COH | C=CCN | 4.10a | 4.10b | 4.10c |
|------|---------|--------|---------|--------|--------|---------|
| LUMO | +1.318 | +1.288 | +0.022 | +0.049 | -0.110 | -0.996 |
| HOMO | -10.176 | -9.298 | -10.612 | -9.785 | -9.509 | -10.083 |

However, the steric effects between TS A_{anti} (or A in Tables) and the corresponding TS A_{syn} (or A' in Tables) are weak or actually opposite to our prediction as shown in Figure 4.2. Nevertheless, for the transition structures of bromocarbene, the carbene with the largest size difference between its two substituents among those calculated, the energy barriers do show the steric effects and the energy difference between 4.15A and 4.15A' increases along the size of the R groups, H, CH₃, and Br, on the olefins, but in the direction opposite to that predicted. Further, in examining the geometries of all transition structures, the distance b is always seen to be more than 0.4 Å longer than distance a. In addition, the angles β, specially for TSs A, are larger than 130°. In other words, the substituents on the carbene at the transition structure experience more steric effects from the bulky group on the near carbon atom of an olefin than from the bulky group on the other end of the olefin. The substituent on chlorocarbene and methylcarbene may not be big enough to show this steric hindrance. However, this interpretation is difficult to apply on transition structures of :CFCH₃, 4.17A and 4.17A', which agree with the prediction shown in Figure 4.2. The size difference between F and CH₃ is not as large as the difference between H and Br or H and CH₃, but the transition structures of neither of the latter carbenes show the same phenomenon as between 4.17A and 4.17A'. There must be another effect involving in the transition structures of cycloaddition of :CFCH₃ to push-pull olefins.

It is not very difficult to imagine that the source of the problem must come from the fluorine on the carbene. One possible explanation is that the 4.17A gain extra stabilization from the dipole -

dipole interaction between the methyl fluorocarbene and the push-pull olefin, as shown in Scheme 4.1. Since fluoride is the most electronegative atom, it can polarize the carbene to form a significant dipole which is in the opposite direction to the dipole generated in the resonance structure of the push-pull olefin. Plus, when $R = \text{Br}$, an electron-withdrawing group, it also enhances the dipole moment of the olefin. This interpretation is just a postulate which needs more detailed investigation; however, examination of though the individual pieces does show that the direction of their dipole moments are the same as shown in Scheme 4.1.

Scheme 4.1



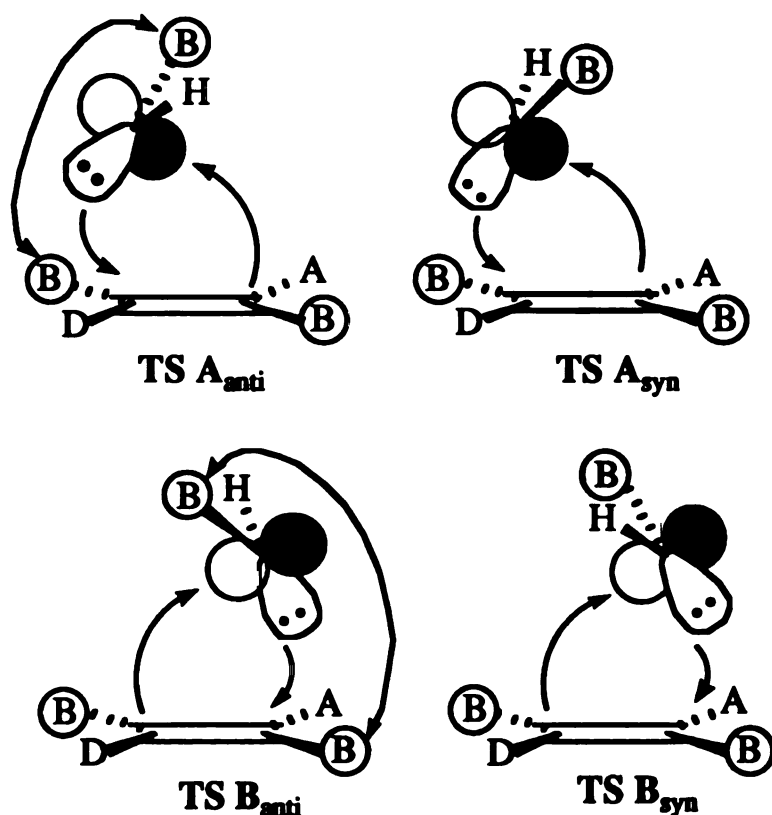
Dichlorocarbene, which is the most electrophilic carbene we have examined here at the MNDO level, is not sensitive to the polarization effect, but does show an electronic effect resulting from the R groups on the olefins which change them into relatively electron-rich ($R = \text{CH}_3$) or electron-poor ($R = \text{Br}$) π -systems.

4.5 Conclusion:

The MNDO results suggest that a carbene, especially an electrophilic carbene except for methylene, shows an orientational bias in

adding between the two ends of a polarized olefin. For a push-pull olefin, a carbene prefers adding to the electron-donor end over the electron-acceptor end of the olefin. The intention to use steric effects to separate between the two polarization favored transition structures (A and A') shows some promise but the prediction needs to be reversed. Overall the picture of the four TSs appears to need revision to Figure 4.4 from Figure 4.2.

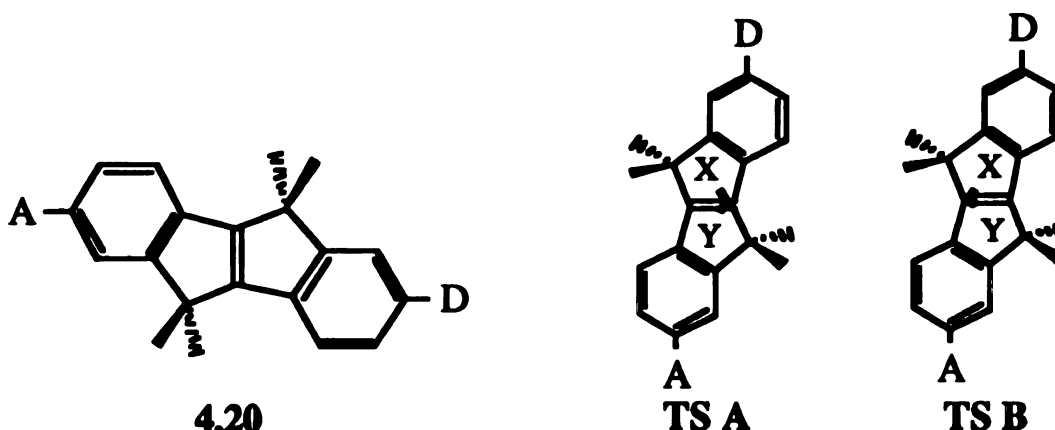
Figure 4.4



TS A is electronically preferred over TS B
Syn TSs are sterically preferred over anti

Part II. Experimental:

The previous calculation results suggested that an experiment which make use of a preference for one of the four possible cyclopropanation reaction paths should be possible: the calculated differences of energy barriers between TS A and TS B, as shown in Figure 4.4, are enough to give observably large product ratios. Obviously, the size of the bulky group (R) should be increased in order to enhance the steric preference for syn vs. anti cyclopropanation products (from TS A in Figure 4.4). So, we have designed a push-pull substituted alkene **4.20**, with more bulky R groups, *gem*-dimethyl, that should electronically prefer one carbene approach path (TS A) over the other (TS B). Steric

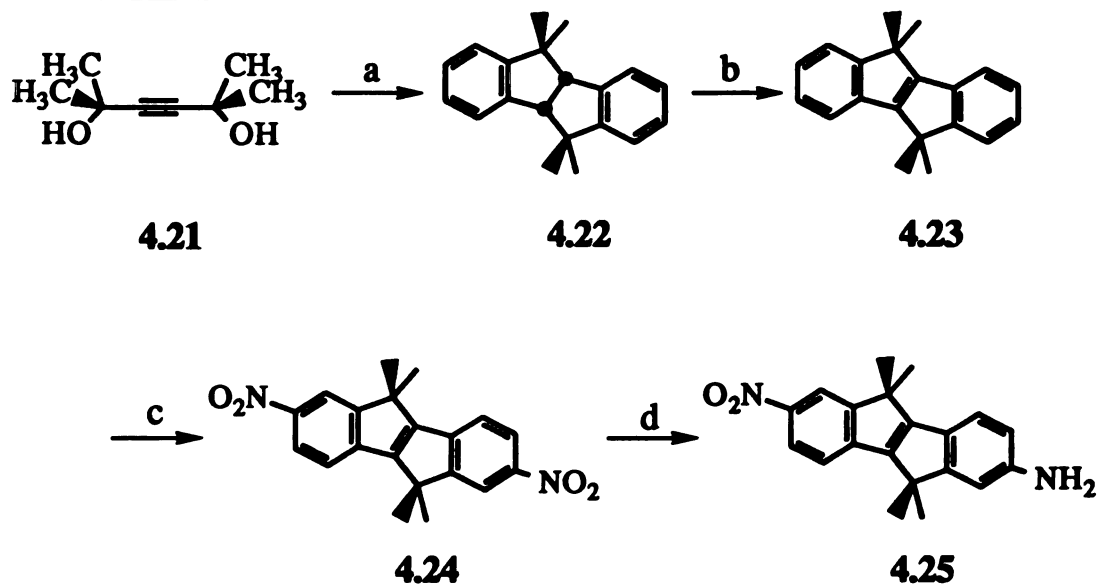


interactions would favor syn-substituted cyclopropane products from the TSs A (as defined in Figure 4.4), so study of the reactions of **4.20** with unsymmetrical carbenes :CXY should reveal the electronic orientation preference in the regiochemistry of the carbene's addition, making a clear distinction between paths. In **4.20**, the donor and acceptor groups are made sterically uniform by being moved away from the olefin center and placed on phenyl ring spacers.

4.6 Results:

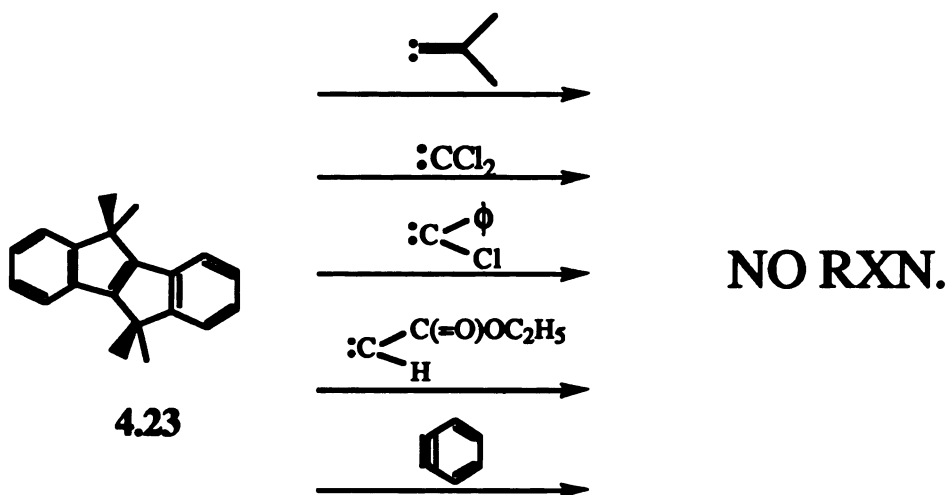
Synthesis of 3-Amino-5,5,10,10-dimethyl-12-Nitro-[2,1,a] Indene (4.25). The desired push-pull disubstituted olefin (4.25) was synthesized from 2,5-dimethyl-3-hexyne-2,5-diol (4.21) in four steps, as shown in Scheme 4.2. Alkene 4.23 was generated by the condensation of 4.21 and benzene in the presence of sulfuric acid to make 4.22, followed by dehydrogenation with DDQ. 4.23, a white solid with a very strong fluorescence, was then treated with nitric acid in acetic acid followed by mono-reduction with Pd/C and cyclohexene in ethanol to afford the push-pull disubstituted olefin 4.25.

Scheme 4.2



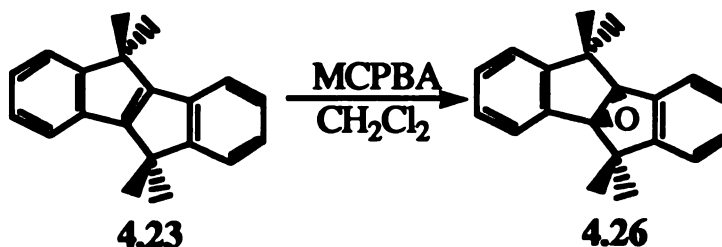
^a H₂SO₄, benzene. ^b DDQ, benzene. ^c AcOH, HNO₃.

^d Pd/C (10 %), cyclohexene, EtOH.

Scheme 4.3**Reaction of 4.23 with Various Carbenes (Scheme 4.3)**

Dimethyl vinylidene was generated from 2,2-dimethylvinyl triflate according to previous literature.¹⁹ Dichlorocarbene was generated from the Seyferth reagent²⁰ and from trichloroacetic acid sodium salt. Phenylchlorocarbene was generated from phenylchlorodiazirine.²¹ Carboethoxycarbene was generated from ethyl diazoacetate by thermolysis in benzene. All reactions of 4.23 with above carbenes were refluxed in dry benzene and products were analyzed either by NMR or GC analysis. Only 4.23 was identified from the reaction mixtures.

Reaction of Benzenediazonium-2-Carboxylate-HCl with 4.23. The benzyne precursor, propylene oxide, and 4.23 were refluxed in bromobenzene for 2 hours, when N₂ ceased coming out from the reaction. After the removal of the solvent, the residue was separated by flash chromatography. No adduct from benzyne addition to 4.23 was isolated.

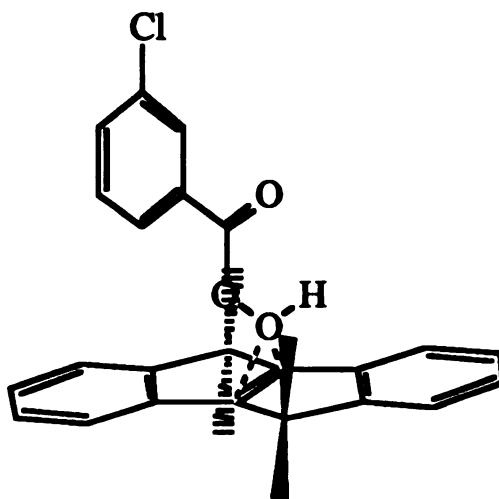
Scheme 4.5

Epoxidation of 4.23. A solution of 4.23 and 3-chloroperbenzoic acid (MCPBA) in methylene chloride was ultrasonicated for 4 hours until no starting material remained, as determined by a TLC. The solution was diluted with hexane, washed with saturated aqueous sodium bicarbonate solution and brine, and dried over magnesium sulfate. After the removal of solvent, a white solid (4.26) was obtained in 82% yield and a reasonable purity without further purification.

4.7 Discussion:

In spite of numerous efforts, the indenoindene (4.23) fails to react with any of the carbenes tried. However, the reaction of the olefin with MCPBA gives a reasonable yield. Since the whole molecule of MCPBA is on the same plane approaching the double bond of 4.23,^{22,23} it may not "feel" the steric hindrance from the *gem*-dimethyl groups next to the double bond. However, those bulky groups are evidently too big to let the carbenes reach the double bond even when sterically "small" such as dimethylvinylidene are examined. So, we have to make some modifications to those bulky groups if this approach is going to reveal the symmetry of the reaction path of a carbene. A variety of synthetic efforts aimed at

building a simplified, less sterically demanding alkene led to no further success.



4.8 Experimental:

General Methods. General experimental procedures are the same as described in Chapter 2.

5,5,10,10-Tetramethyl-4b,5,9b,10-tetrahydroindeno [2,1,a] indene (4.22). The procedure was modified from Hancock's method.²⁴ To a mixture of conc. sulfuric acid (30 mL) and benzene (48 mL) was added slowly 2,5-dimethyl-3-hexyne-2,5-diol (10 g, 70.3 mmol) at 0° C over a period of 40 min. After the reaction mixture was refluxed for 7 h, the reaction mixture was cooled to room temperature and poured slowly onto ice (100 g). The aqueous layer was extracted with hexane (3 x 100 mL) and the combined organic extracts were washed with saturated aqueous sodium bicarbonate solution and brine, dried over magnesium sulfate, and filtered. The organic solvents was removed to give the crude

brown product, which was purified by flash chromatography over silica gel eluting with neat hexane to afford (4.22) (1.7 g, 9%): ^1H NMR (300 MHz, CDCl_3) δ 0.87 (s, 6 H), 1.53 (s, 6 H), 7.17-7.37 (m, 8 H); ^{13}C NMR (75.5 MHz, CDCl_3) δ 28, 46, 61, 123, 126, 127, 128, 142, 154; MS (EI) m/e 77, 91, 247, (M^+) 262.

Dehydrogenation of 5,5,10,10-Tetramethyl-4b,5,9b,10-tetrahydroindeno[2,1,a]indene. A solution of (4.22) (3.8 g, 14.6 mmol), 2,3-dibromo-5,6-dicyano-1,4-benzoquinone (14.0 g, 17.6 mmol) and a few drops of acetic acid in benzene (15 mL) was refluxed for 38 h. The benzene was removed and the residue was purified by flash chromatography eluting with neat hexane to afford a white solid. The white solid was recrystallized from methanol to give (4.23) (1.6 g, 41%): ^1H (300 MHz, acetone- d_6) δ 1.5 (s, 6 H), 7.21 (t, 2 H, $J = 7.5$ Hz), 7.28 (t, 2 H, $J = 7.5$ Hz), 7.48 (m, 4 H); ^{13}C NMR (75.5 MHz, acetone- d_6) δ 159.7, 156.3, 138.5, 127.4, 125.7, 122.7, 120.1, 45.2, 24.2; MS (EI) m/e 260.5 (M^+), 245.4, 230.3, 215.4.

Nitration of 4.23. A suspension of 4.23 (1.0 g, 3.8 mmol) in acetic acid (25 mL) was heated to 50 °C. Concentrated nitric acid (3 mL, 200 mmol) was added dropwise over a period of 15 min and the resulting mixture was then warmed up to 60 - 65 °C and stirred for another 2 h at that temperature. The mixture was allowed to cool down to room temperature and a yellow solid was precipitated. The yellow solid was collected by suction filtration, washed with cold glacial acetic acid (2 x 10 mL) containing potassium acetate (0.25 g) and washed with water several times. The yellow solid was further dried under vacuum over phosphorus pentoxide to afford 4.24 (1.2 g, 81%): ^1H (300 MHz, CDCl_3)

δ 1.6 (s, 12 H), 7.51 (dd, 2 H, $J = 6.9, 2.2$ Hz), 8.26 (dd, 2 H, $J = 7.0, 2.2$ Hz); ^{13}C NMR (75.5 MHz, CDCl_3) δ 159.9, 159.5, 146.2, 142.8, 123.8, 119.9, 117.8, 45.8, 23.9; MS (EI) m/e 350 (M^+), 335, 289, 274, 226.

Reduction of 4.24. A solution of 4.24 (0.762 g, 2.2 mmol) and 10% Pd/C (0.3 g) in absolute ethanol (9 mL) was heated to gentle reflux under argon atmosphere and cyclohexene was then added slowly dropwise. The resulting mixture was refluxed for 12 h. The suspension solution was then filtered hot through a celite pad, and the pad was washed with several portions of ethyl acetate (3 x 10 mL). The filtrate was allowed to cool to room temperature and solvent was under vacuum. The residue was purified by flash chromatography over silica gel eluting with methylene chloride/hexane (30%) to afford a white solid 4.25 (0.49 g, 70%). The white solid was recrystallized from ethanol for further purification: ^1H NMR (300 MHz, CDCl_3) δ 0.97 (s, 6 H), 1.68 (s, 6 H), 7.21 (m, 2 H), 7.30 - 7.60 (m, 5 H); ^{13}C NMR (75.5 MHz, CDCl_3) δ 154.2, 151.6, 135.6, 131.0, 128.2, 125.3, 123.7, 104.9, 48.1, 29.9, 25.2, 25.1; MS (EI) m/e 320 (M^+), 305, 261; HRMS: calcd for M^+ 320.1525, found 320.1525.

Reaction of 2,2-Dimethylvinyl Triflate with Potassium *tert*-Butoxide in Presence of 4.23. Into a 25 mL round-bottom flask equipped with a magnetic stirrer and argon inlet was added dry CH_2Cl_2 (3 mL), 4.23 (0.15 g, 0.57 mmol) and potassium *tert*-butoxide. The mixture was cooled to $-30\text{ }^\circ\text{C}$ and 2,2-dimethyl triflate (0.67 mL) was added slowly. The resulting mixture was allowed to warm up to $0\text{ }^\circ\text{C}$ and stirred for another 3 h. The reaction was quenched by adding water (20 mL) and the aqueous solution was extracted with benzene (3 x

10 mL). The combined organic layer was washed with water and dried with magnesium sulfate. The solvent was removed by vacuum and the residue was directly analyzed by NMR. No addition product was found.

Thermolyses of Trichloroacetic Acid Sodium Salt in Presence of 4.23. A solution of 4.23 (0.26 g, 1.0 mmol) and trichloroacetic acid sodium salt in dry ethyl acetate (15 mL) was refluxed for 2 days under argon atmosphere and at mean time a lot of salt was precipitated out. The mixture was allowed to cool to room temperature, filtered out the white precipitate, and analyzed directly by GC directly.

Reaction of Seyferth Reagent (Phenyl Bromo-dichloromethyl Mercury) in Presence of 4.23. A tube containing 4.23 (50 mg, 0.2 mmol) and phenyl (bromo-dichloromethyl) mercury (0.1 g, 2.3 mmol) in dry benzene (3 mL) was freeze-pump-thawed three times before sealing. The tube was warmed up to 70 °C with a water bath held for another 24 h. After cooling to room temperature, the mixture was diluted with hexane (30 mL) and filtered through a short column of silica gel. The hexane solution was directly analyzed by GC. Only 4.23 was detected.

Thermolyses of Phenylchlorodiazirine in Presence of 4.23. A solution of phenylchlorodiazirine (0.42 g, 2.71 mmol) in dry benzene (25 mL) was added slowly into a refluxing solution of 4.23 (0.31 g, 1.18 mmol) in benzene (5 mL) under a nitrogen atmosphere. After the addition was complete, the mixture was refluxed for another 3 h and then cooled to room temperature. The mixture was concentrated on a rotary evaporator and separated by flash chromatography over silica gel eluting

with hexane. Only 4.23 was recovered. No addition product was obtained.

Thermolyses of Ethyl Diazoacetate in Presence of 4.23. A solution of 4.23 (0.26 g, 4.33 mmol) and ethyl diazoacetate (1.52 g, 1.33 mmol) in benzene (5 mL) was refluxed for 24 h. After the solvent was removed, the residue was purified by flash chromatography over silica gel. Only 4.23 could be detected.

Reaction of Benzenediazonium-2-carboxylate-HCl (Benzyne Precursor) with 4.23. A solution of 4.23 (0.26 g, 1.0 mmol), Benzenediazonium-2-carboxylate•HCl (0.2 g, 1.1 mmol) and propylene oxide (0.4 mL) in bromobenzene (10 mL) was refluxed for 2 h. The solution was cooled down to room temperature and the solvent was removed by vacuum. The residue was purified flash chromatography over silica gel. No addition product was found.

Epoxidation of 4.23. A solution of 4.23 (0.32 g, 1.24 mmol) and *meta*-chloroperoxybenzoic acid (0.32 g, 1.57 mmol) was ultrasonicated for 4 h, and then the solution was diluted with hexane (80 mL), washed with sat. aqueous sodium bicarbonate solution (3 x 20 mL) and brine, and dried with magnesium sulfate. The solvent was removed under vacuum and a white solid was obtained (0.3 g, 83%): ¹H NMR (300 MHz, CDCl₃) δ 1.4 (s, 6 H), 1.67 (s, 6 H), 7.15 - 7.32 (m, 6 H), 7.52 (d, 1 H, *J* = 6.6 Hz); ¹³C NMR (75.5 MHz, CDCl₃) δ 158.3, 137.6, 128.5, 126.3, 125.3, 124.3, 79.8, 43.6, 28.2, 23.3; MS (EI) *m/e* 276 (M⁺), 261, 246, 228, 215, 202.

4.9 References And Notes:

- (1) Moreno, M.; Lluch, J. M.; Oliva, A.; Bertran, J. *J. Mol. Struct., THEOCHEM* **1984**, *107*, 227-232.
- (2) Apeloig, Y.; Karni, M.; Stang, P. J.; Fox, D. P. *J. Am. Chem. Soc.* **1983**, *105*, 4781-1792.
- (3) Bodor, N.; Dewar, M. J. S.; Wasson, J. S. *J. Am. Chem. Soc.* **1972**, *94*, 9095-9102.
- (4) Hoffmann, R. *J. Am. Chem. Soc.* **1968**, *90*, 1475-1485.
- (5) Hoffmann, R.; Hayes, D. M.; Skell, P. S. *J. Phys. Chem.* **1972**, *76*, 664-669.
- (6) Moreno, M.; Lluch, J. M.; Oliva, A.; Bertrán, J. *J. Chem. Soc., Perkin Trans. 2* **1985**, 131-134.
- (7) Rondan, N. G.; Houk, K. N.; Moss, R. A. *J. Am. Chem. Soc.* **1980**, *102*, 1770-1716.
- (8) Rondan, N. G.; Houk, K. N. *Tetrahedron Lett.* **1984**, *25*, 5965-5968.
- (9) Zurawski, B.; Kutzelnigg, W. *J. Am. Chem. Soc.* **1978**, *100*, 2554-2659.
- (10) Fox, D. P.; Stang, P. J.; Apeloig, Y.; Karni, M. *J. Am. Chem. Soc.* **1986**, *108*, 750-756.
- (11) Skell, P. S.; Cholod, M. S. *J. Am. Chem. Soc.* **1969**, *91*, 7131-7137.

- (12) Houk, K. N.; Rondan, N. G.; Mareda, J. *Tetrahedron* **1985**, *41*, 1555-1563.
- (13) Moss, R. A.; Mallon, C. B.; Ho, C.-T. *J. Am. Chem. Soc.* **1977**, *99*, 4105-4110.
- (14) Moss, R. A.; Guo, W.; Krogh-Jespersen, K. *Tetrahedron Lett.* **1982**, *23*, 15-18.
- (15) Fleming, I. *Frontier Orbitals and Organic Chemical Reactions*; Wiley: London, 1976.
- (16) These two compounds should properly be called vinyl alcohol and acrylonitrile, but for the purposes of this discussion, we have elected to name them as substituted ethylenes.
- (17) *Carbene Chemistry*; Kirmse, W., Ed.; Academic Press: New York, 1971; Vol. 2., Chapter 8, Part I and II.
- (18) Moss, R. A. In *Carbenes*; M. J. Jones and R. A. Moss, Ed.; John Wiley & Sons: New York, 1973; Vol. I.; Chapter 2.
- (19) Stang, J. P.; Mangum, M. G.; Haak, P. *J. Am. Chem. Soc.* **1974**, *96*, 4562-4569.
- (20) Seyferth, D.; Burlitch, J. M. *J. Am. Chem. Soc.* **1964**, *86*, 2730-2731.
- (21) Moss, R. A.; Whittle, J. R.; Freidenreich, P. *J. Org. Chem.* **1969**, *34*, 2220-2224.
- (22) Woods, K. W.; Beak, P. *J. Am. Chem. Soc.* **1991**, *113*, 6281-6283.

- (23) Hanzlik, R. P.; Shearer, G. O. *J. Am. Chem. Soc.* **1975**, *97*, 5231-5233.
- (24) Hancock, J. E. H.; Pavia, D. L. *J. Org. Chem.* **1961**, *26*, 4350-4352.